HAL
open science

Caractérisation des comportements physique et mécanique de biocomposites composés d'une matrice de polyéthylène végétale haute densité renforcée par des fibres de bambou : Influence des traitements physiques et chimiques des fibres sur les propriétés locales et globales des composites

Milene Muniz Eloy da Costa

To cite this version:

Milene Muniz Eloy da Costa. Caractérisation des comportements physique et mécanique de biocomposites composés d'une matrice de polyéthylène végétale haute densité renforcée par des fibres de bambou : Influence des traitements physiques et chimiques des fibres sur les propriétés locales et globales des composites. Mechanics of materials [physics.class-ph]. Université Paris Saclay (COmUE); Universidade federal do Ceará, 2019. English. NNT : 2019SACLN032 . tel-03652526

HAL Id: tel-03652526

https://theses.hal.science/tel-03652526v1

Submitted on 26 Apr 2022

HAL is a multi-disciplinary open access archive for the deposit and dissemination of scientific research documents, whether they are published or not. The documents may come from teaching and research institutions in France or abroad, or from public or private research centers.

L'archive ouverte pluridisciplinaire **HAL**, est destinée au dépôt et à la diffusion de documents scientifiques de niveau recherche, publiés ou non, émanant des établissements d'enseignement et de recherche français ou étrangers, des laboratoires publics ou privés.

université PARIS-SACLAY

NNT : 2019SACLN032

Thèse de doctorat

UNIVERSIDADE FEDERAL DO CEARÁ

école normale supérieure paris–saclay

Physical and mechanical behavior of composites made of green polyethylene matrix reinforced by long bamboo fibers: Influence of the physical and chemical treatments of the fibers on the fibers and on the composites

Thèse de doctorat de l'Université Paris-Saclay
préparée à École Normale Supérieure Paris-Saclay

École doctorale n° 579 Sciences mécaniques et énergétiques, matériaux et géosciences - SMEMAG
Spécialité de doctorat: Mécanique des Matériaux

Thèse présentée et soutenue à Fortaleza (Brésil), le 22 Novembre 2019, par

Milene Muniz Eloy da Costa

Composition du Jury :

Ahmed Benallal Professeur, Université Paris-Saclay	Président du jury
Nikolaus Peter Schmitt Professeur, Université Paris-Saclay	Directeur de thèse
Enio Pontes de Deus Professeur, Universidade Federal do Ceará	Co-directeur de thèse
Sandro Campos Amico Professeur, Universidade Federal do Rio Grande do Sul - UFRGS	Rapporteur
José Roberto Moraes D`Almeida Professeur, Pontifícia Universidade Católica do Rio de Janeiro	Rapporteur
Pierre Maurice Christophe Lamary Professeur, Universidade Federal do Ceará	Examinateur

ÉCOLE DOCTORALE
Sciences mécaniques et énergétiques, matériaux et géosciences (SMEMAG)

Titre : Comportement physique et mécanique des composites à matrice polyéthylène verte renforcée par des fibres longues de bambou : Influence des traitements physiques et chimiques des fibres sur les fibres et sur les composites

Mots clés : Fibres de bambou. Polyéthylène vert. Composites polymères. Adhésion fibre/matrice.

Résumé :
La préoccupation environnementale liée à l'utilisation non régulée de ressources non renouvelables, ainsi que l'élimination inadéquate des déchets dans l'environnement, encouragent le développement de solutions alternatives aux composites traditionnels à base polymère, plus respectueuses vis à vis de l'environnement dans les domaines de l'extraction de matières première ou du recyclage des produits usagés. L'utilisation de fibres végétales pour renforcer les matrices polymères est une alternative pour la fabrication de produits industriels dans divers domaines, d'ustensiles ménagers et des emballages aux produits de construction civile. Le choix des fibres de bambou a été motivé par le développement d'un composite à base de fibres longues, de faible coût, de basse densité et offrant une bonne résistance mécanique. En outre, l'utilisation d'une matrice polymérique produite à partir de canne à sucre. Dans ce contexte, l'objectif de cette thèse était de développer un composite entièrement produit à partir de sources renouvelables, en évaluant son applicabilité à travers de la caractérisation et de l'étudier de certaines propriétés morphologiques, physico-chimiques et mécaniques des fibres de bambou, de la matrice de polyéthylène verte et des composites produits, et, surtout, en évaluant l'effet de différents traitements de fibres. La caractérisation des paramètres morphologiques et les propriétés physico-chimiques a révélé une diminution de la masse des fibres après les traitements, ainsi que des variations de densité, de porosité et de taille des pores. Une augmentation de la rugosité de la surface des fibres a également été observée, suggérant la possibilité d'un bon ancrage mécanique de la fibre à la matrice polymère. Pour certains traitements, une augmentation notable des propriétés élastiques et de la résistance en traction des fibres a été constatée. La caractérisation mécanique des composites a montré que les traitements étaient efficaces pour une bonne adhésion entre la fibre et la matrice polymère. Pour conclure, les investigations expérimentales ont montré que les meilleurs traitements étaient la mercérisation et l'acétylation, indiquant que les composites produits sont applicables aux projets où, à un taux de charge élevé, ils supportent une fracture fragile.

Université Paris-Saclay
Espace Technologique / Immeuble Discovery
Route de l'Orme aux Merisiers RD 128 / 91190 Saint-Aubin, France

ÉCOLE DOCTORALE
Sciences mécaniques et énergétiques, matériaux et géosciences (SMEMAG)

Title : Comportement physique et mécanique des composites à matrice polyéthylène verte renforcée par des fibres longues de bambou : Influence des traitements physiques et chimiques des fibres sur les fibres et sur les composites

Keywords : Bamboo fibers. Green polyethylene. Polymeric composites. Fiber/matrix adhesion.

Abstract :
The environmental concern with the unregulated use of non-renewable resources, as well as the inadequate disposal of waste in the environment, encourage the development of awareness measures and technological alternatives. Faced with this problem, there is a need to manufacture products that are less aggressive to the environment, either according to their raw material or according to their post-use. The use of natural fibers applied as reinforcement in polymeric matrices is an alternative for the manufacture of industrial products in various areas, from household utensils and packaging to civil construction products. The choice of bamboo fibers was motivated by the use of a long fiber vegetable source reinforcement, with good mechanical strength, low density and low cost. In addition, the work proposes the use of a polymeric matrix produced from a renewable plant source, sugar cane. In this context, the proposal of this thesis was to develop a composite produced entirely from renewable sources, evaluating its applicability through characterization and investigation of some morphological, physicochemical and mechanical properties of bamboo fibers, green polyethylene matrix and produced composites, and, mainly, evaluating the effect of different treatments performed on fibers on the composites mechanical properties. The morphological and physicochemical characterizations revealed a decrease in fiber mass after treatments, as well as variations in density, porosity and pore size. Also an increase of roughness at the fibers surface was observed, suggesting an improved mechanical anchorage by the polymeric matrix. The tensile tests showed that the mechanical properties (modulus of elasticity and tensile strength) of the fibers were improved with some treatments. The mechanical characterization of the composites highlighted that the treatments were effective for a good adhesion between fiber and polymer matrix. To conclude, the experimental investigations showed that the best treatments were mercerization and acetylation, indicating that the produced composites have applicability for projects which, at a high loading rate, they support fragile fracture.

Université Paris-Saclay
Espace Technologique / Immeuble Discovery
Route de l'Orme aux Merisiers RD 128 / 91190 Saint-Aubin, France

Dados Internacionais de Catalogação na Publicação
Universidade Federal do Ceará
Biblioteca Universitária
Gerada automaticamente pelo módulo Catalog, mediante os dados fornecidos pelo(a) autor(a)

C874p Costa, Milene Muniz Eloy da.
Physical and mechanical behavior of composites made of green polyethylene matrix reinforced by long bamboo fibers : influence of the physical and chemical treatment of the fibers on the fibers and on the composites / Milene Muniz Eloy da Costa. – 2019.
161 f. : il. color.

Tese (doutorado) – Universidade Federal do Ceará, , Fortaleza, 2019.
Orientação: Prof. Dr. Enio Pontes de Deus.
Coorientação: Prof. Dr. Nikolaus Peter Schmitt.

1. Bamboo fibers. 2. Green polyethylene. 3. Polymeric composites. 4. Fiber/matrix adhesion. I. Título.
CDD

UFC PR/PPG	**ATA DA SESSÃO DE DEFESA DE TESE DE DOUTORADO**

Centro/Faculdade Centro de Tecnologia / CT	
Departamento Engenharia Metalúrgica e de Materiais	**Programa de Pós-Graduação** Engenharia e Ciência de Materiais
ATA DA SESSÃO DE DEFESA DA TESE DE DOUTORADO DE **MILENE MUNIZ ELOY DO COSTA**	
REALIZADA NO DIA **22 / 11 / 2019**	

Às **nove horas** do **vigésimo segundo dia do mês de novembro de dois mil e dezenove,** realizou-se a sessão de defesa da tese de doutorado deste Programa de Pós-Graduação, de autoria da discente **MILENE MUNIZ ELOY DO COSTA**. O trabalho tinha como título **"Physical and mechanical behavior of composites made of green polyethylene matrix reinforced by long bamboo fibers: influence of the physical and chemical treatment of the fibers on the fibers and on the composites".** Compunham a banca examinadora os professores doutores **Enio Pontes de Deus**, orientador e presidente da sessão; **Pierre Maurice Christophe Lamary**, membro interno; **Sandro Campos Amico,** membro externo, da Universidade Federal do Rio Grande do Sul; **José Roberto Moraes D'Almeida**, membro externo, da Pontifícia Universidade Católica do Rio de Janeiro, **Ahmed Benallal**, membro externo, da *Université Paris-Saclay*, e **Nikolaus Peter Schmitt**, membro externo, da *Université Paris-Saclay*. A sessão foi aberta pelo Presidente da sessão de defesa, professor **Enio Pontes de Deus**, que apresentou a banca examinadora e a candidata. Após a exposição do trabalho, seguiu-se o processo de arguição da doutoranda. O primeiro examinador foi o professor **Nikolaus Peter Schmitt**. Em seguida, procederam a arguição os professores **Ahmed Benallal, José Roberto Moraes D'Almeida, Sandro Campos Amico, Pierre Maurice Christophe Lamary e Enio Pontes**

de Deus. Logo após, a banca examinadora reuniu-se secretamente, a fim de avaliar o desempenho da doutoranda. A banca examinadora APROVOU o trabalho da aluna, com a ressalva de serem realizadas pelo discente todas as correções e apontamentos indicados pelos examinadores. Nada mais havendo a relatar, a sessão foi encerrada às 12 horas e 34 minutos e eu, **Carlos Henrique de Sousa Vasconcelos**, secretário do Programa de Pós-Graduação em Engenharia e Ciência de Materiais, lavrei a presente ata, que depois de lida e aprovada, será assinada por mim e pelos membros da banca examinadora.

Fortaleza, 22 de novembro de 2019

Carlos Henrique de Sousa Vasconcelos
Secretário

Prof. Dr. Sandro Campos Amico
Examinador

Prof. Dr. Enio Pontes de Deus
Orientador

Prof. Dr. José Roberto Moraes D'Almeida
Examinador

Prof. Dr. Pierre Maurice Christophe Lamary
Examinador

Prof. Dr. Ahmed Benallal
Examinador

Prof. Dr. Nikolaus Peter Schmitt
Examinador

To God.

To my parents, Mário and Cilene.

To me.

ACKNOWLEDGMENT

To God, for my life, for the person I am, for the faith, for the courage and daring to face the world, for offering me the ability to judge what should or should not affect me, for the people who passed/will pass through my life and for the joy of the achievements of my way.

To all my family, Mario, Cilene, Mario Filho e Guilherme, for the immense love and support.

To Higo for the patience and motivation.

To the advisors, Prof. Dr. Enio Pontes de Deus and Prof. Dr. Nicolas Schmitt, for the orientation in this work and in others, for the teachings, for the counsels, and for the faith placed on me.

To the reviewers, Prof. Dr. Sandro Campos Amico and Prof. Dr. José Roberto Moraes D'Almeida, and the participating professors of the panel members, Prof. Dr. Pierre Maurice Christophe Lamary and Prof. Dr. Ahmed Benallal, for the time, for the collaborations and suggestions.

To Prof. Dr. Cleiton Carvalho Silva, as coordinator, for the attention and willingness to always help.

To the colleagues of the postgraduate course, especially Santino Loruan, for the company and the rescue, whenever necessary.

To the students and researches that passed through the Laboratory of Mechanics Fracture and Fatigue (Laboratório de Mecânica da Fratura e Fadiga – LAMEFF), in Federal University of Ceará (Universidade Federal do Ceará – UFC), Eduardo Albuquerque, Joao Victor Miranda, George Pontes de Cunha, Beatriz Mota Brito, Eric Fortunato, Hannah Camurça, Rayane Mendes, Luana Marques, Roberto Abreu, Renardir Maciel, Marcellus Nascimento, Kleiton dos Santos, Saymon Rodrigues, Breno Lucena, Joel Lima and Ana Beatriz Sousa, for the work performed and the friendship.

To the friends of the Department of Metallurgical and Materials Engineering, in Federal University of Ceará, especially the members of the ABM Week Delegation, for moments of support, fun and for providing a boost at the end of this cycle.

To David Freitas, from the Laboratory of the Postgraduate Program in Dentistry (Laboratorio do Programa de Pos-graduaçao em Odontologia – PPGO), in Federal University of Ceará, for the help and support during the characterization of the studied materials.

To the colleagues, especially Alessandra Lie, Flavia de Sá and Nayara Fonseca,

and the employees of the Laboratory of Mechanics and Technology (Laboratoire de Mécanique et Technologie – LMT), in ENS Paris-Saclay, for the attention, help, teaching and good wines during my stay in France.

To Braskem, for the donation of the green polyethylene.

To CAPES, for the financial support with the maintenance of the scholarship, and for the opportunity to experience another daily, academic and professional reality outside the country. This study was financed in part by the Coordenação de Aperfeiçoamento de Pessoal de Nível Superior - Brasil (CAPES) - Finance Code 001.

To thank is not a simple act of kindness, education or obligation. It is a recognition for something another person has done for you, understanding that this person has spent some of his time to give you attention in some way. To thank is to convey the joy of how much a simples gesture had value to you, so thank you very much to all those mentioned.

“[…] - Yes, everywhere in the world there are these two types of people, in any kind of society, race, color, or creed, the big difference is that flexible people as the bamboo do not break easily with the storm. They twitch, sway, twist, bounce, but hardly break, because they have enough flexibility to withstand the inclemencies of life.” Unknown author.

“É preciso muita fibra para chegar às alturas e, ao mesmo tempo, muita flexibilidade para se curvar ao chão.” Unknown author.

RESUMO

A preocupação ambiental com o uso desregrado de recursos não-renováveis, bem como a disposição inadequada de resíduos no meio, incentivam o desenvolvimento de medidas de conscientização e de alternativas tecnológicas. Diante dessa problemática, surge a necessidade de manufatura de produtos menos agressivos ao meio, seja de acordo com sua matéria-prima ou de acordo com sua pós-utilização. O uso de fibras vegetais aplicadas como reforço em matrizes poliméricas apresenta-se como uma alternativa para a fabricação de produtos industriais em diversas áreas, desde utensílios domésticos e embalagens a produtos da construção civil. A escolha das fibras de bambu foi motivada pela utilização de um reforço de fonte vegetal de fibras longas, com boa resistência mecânica, baixa densidade e baixo custo. Além disso, o trabalho propôs a utilização de uma matriz polimérica produzida a partir de uma fonte renovável vegetal, a cana-de-açúcar. Nesse contexto, a proposta dessa tese foi desenvolver um compósito produzido totalmente por fontes renováveis, avaliando sua aplicabilidade através de caracterização e investigação de algumas propriedades morfológicas, físico-químicas e mecânicas das fibras de bambu, da matriz de polietileno verde e dos compósitos produzidos, e, principalmente, avaliando o efeito de diferentes tratamentos realizados nas fibras sobre as propriedades mecânicas dos compósitos. As caracterizações morfológicas e físico-químicas revelaram uma diminuição de massa das fibras após os tratamentos, bem como variações na densidade, porosidade e tamanho de poros. Também foi observado um aumento de rugosidade na superfície das fibras, sugerindo uma melhor ancoragem mecânica pela matriz polimérica. Os testes de tração mostraram que as propriedades mecânicas (modulo de elasticidade e resistência à tração) das fibras foram melhoradas com alguns tratamentos. A caracterização mecânica dos compósitos destacou que os tratamentos foram eficazes para uma boa adesão entre fibra e matriz polimérica. Para concluir, as investigações experimentais mostraram que os melhores tratamentos foram mercerização e acetilação, indicando que os compósitos produzidos apresentam aplicabilidade para projetos em que, a uma alta taxa de carregamento, suportem fratura frágil.

Palavras-chave: Fibras de bambu. Polietileno verde. Compósitos poliméricos. Adesão fibra/ matriz.

ABSTRACT

The environmental concern with the unregulated use of non-renewable resources, as well as the inadequate disposal of waste in the environment, encourage the development of awareness measures and technological alternatives. Faced with this problem, there is a need to manufacture products that are less aggressive to the environment, either according to their raw material or according to their post-use. The use of natural fibers applied as reinforcement in polymeric matrices is an alternative for the manufacture of industrial products in various areas, from household utensils and packaging to civil construction products. The choice of bamboo fibers was motivated by the use of a long fiber vegetable source reinforcement, with good mechanical strength, low density and low cost. In addition, the work proposes the use of a polymeric matrix produced from a renewable plant source, sugar cane. In this context, the proposal of this thesis was to develop a composite produced entirely from renewable sources, evaluating its applicability through characterization and investigation of some morphological, physicochemical and mechanical properties of bamboo fibers, green polyethylene matrix and produced composites, and, mainly, evaluating the effect of different treatments performed on fibers on the composites mechanical properties. The morphological and physicochemical characterizations revealed a decrease in fiber mass after treatments, as well as variations in density, porosity and pore size. Also an increase of roughness at the fibers surface was observed, suggesting an improved mechanical anchorage by the polymeric matrix. The tensile tests showed that the mechanical properties (modulus of elasticity and tensile strength) of the fibers were improved with some treatments. The mechanical characterization of the composites highlighted that the treatments were effective for a good adhesion between fiber and polymer matrix. To conclude, the experimental investigations showed that the best treatments were mercerization and acetylation, indicating that the produced composites have applicability for projects which, at a high loading rate, they support fragile fracture.

Keywords: Bamboo fibers. Green polyethylene. Polymeric composites. Fiber/matrix adhesion.

RÉSUMÉ

La préoccupation environnementale liée à l'utilisation non régulée de ressources non renouvelables, ainsi que l'élimination inadéquate des déchets dans l'environnement, encouragent le développement de solutions alternatives aux composites traditionnels à base polymère, plus respectueuses vis à vis de l'environnement dans les domaines de l'extraction de matières première ou du recyclage des produits usagés. L'utilisation de fibres végétales pour renforcer les matrices polymères est une alternative pour la fabrication de produits industriels dans divers domaines, d'ustensiles ménagers et des emballages aux produits de construction civile. Le choix des fibres de bambou a été motivé par le développement d'un composite à base de fibres longues, de faible coût, de basse densité et offrant une bonne résistance mécanique. En outre, l'utilisation d'une matrice polymérique produite à partir de canne à sucre. Dans ce contexte, l'objectif de cette thèse était de développer un composite entièrement produit à partir de sources renouvelables, en évaluant son applicabilité à travers de la caractérisation et de l'étudier de certaines propriétés morphologiques, physicochimiques et mécaniques des fibres de bambou, de la matrice de polyéthylène verte et des composites produits, et, surtout, en évaluant l'effet de différents traitements de fibres. Le caractérisation des paramètres morphologiques et les propriétés physico-chimiques a révélé une diminution de la masse des fibres après les traitements, ainsi que des variations de densité, de porosité et de taille des pores. Une augmentation de la rugosité de la surface des fibres a également été observée, suggérant la possibilité d'un bon ancrage mécanique de la fibre à la matrice polymère. Pour certains traitements, une augmentation notable des propriétés élastiques et de la résistance en traction des fibres a été constatée. La caractérisation mécanique des composites a montré que les traitements étaient efficaces pour une bonne adhésion entre la fibre et la matrice polymère. Pour conclure, les investigations expérimentales ont montré que les meilleurs traitements étaient la mercerisation et l'acétylation, indiquant que les composites produits sont applicables aux projets où, à un taux de charge élevé, ils supportent une fracture fragile.

Mots-clé : Fibres de bambou. Polyéthylène vert. Composites polymères. Adhésion fibre/matrice.

LIST OF FIGURES

Figure 2.1 – Chemical structure of polyethylene …… 31

Figure 2.2 – Basic structures of the bamboo culm ….....…… 41

Figure 2.3 – Fiber in vascular bundles: A. fiber morphology; B. fibers with one year (thinner wall of less layers); and C. fibers with several years (thicker wall of more layers) ...……. 44

Figure 2.4 – Region of the interface (a) obtained by the application of a thin layer of polymer on the fiber surface (*sizing*); and (b) created from nucleation/crystallization obtained from the chemical and/or physical interaction of the matrix with the fiber surface (usually characterized by a "sheath" around the fiber) …….. 47

Figure 2.5 – Structure of a plant fiber ……. 50

Figure 2.6 – Examples of failure and fracture mechanisms in fiber-reinforced composites …….. 53

Figure 3.1 – Steps for bamboo fibers extraction ……. 59

Figure 3.2 – Flowchart of thermal and chemical treatments applied to bamboo fibers ……... 63

Figure 3.3 – Preparation of the mold for PEg plate: PEg pellets inside the mold …... 64

Figure 3.4 – Compression molding and heating press LabPro TP 1000 from Fontijne Presses …….. 65

Figure 3.5 – Schemes for the BF arrangements according to the fiber direction: (a) U (0°), C; (b) U (45°), C; (c) U (0°), X; (d) R, D; and (e) B, C ……. 69

Figure 3.6 – Illustrative scheme of points in the length of BF where diameters were measured (¼ of the length to D_1, ½ of the length to D_2 and ¾ of the length to D_3) ……... 70

Figure 4.1 – Correlation between circular and elliptical area of (a) BF0110WT, (b) BF0110TA, (c) BF0110TC, and (d) BF0110TD …… 82

Figure 4.2 – Curves of cumulative intrusion volume in relation to pore diameter for thinner fiber (a) BF0110WT, BF0110TC and BF0310TD; (b) BF0110TA and BF0110TB; and for thicker fibers (c) BF1520WT and 85

BF1520TC ……..
Figure 4.3 – Curves of water-absorption index for BF0110WT, BF0110TC and BF0110TD …….. 88
Figure 4.4 – SEM images of BF0310WT (a) magnification 100x; and (b) magnification 500x ……. 90
Figure 4.5 – SEM images of BF0310TB (a) magnification 100x; and (b) magnification 500x ……. 91
Figure 4.6 – SEM images of BF0310TC (a) magnification 100x; and (b) magnification 500x ……. 92
Figure 4.7 – SEM images of BF0310TD (a) magnification 100x; and (b) magnification 500x ……. 93
Figure 4.8 – Influence of the treatments performed in bamboo fibers on some mechanical properties: (a) tensile strength; (b) Young's modulus; and (c) failure strain …….. 95
Figure 4.9 – Weibull distribution of (a) thinner and (b) thicker non and treated bamboo fibers ……. 98
Figure 5.1 – Curves of water-absorption index for PEg matrix …….. 100
Figure 5.2 – Stress-strain curves for compression molded PEg samples deformed until the break at 5 mm/min ……... 101
Figure 6.1 – Curves of water-absorption index for PEg matrix and performed composites of PEg reinforced with BF …….. 106
Figure 6.2 – Diffusion curves fitting plots to determine constants n and k' for the performed composites: (a) PEg/BF0110WT; (b) PEg/BF0110TA; (c) PEg/BF0110TB; (d) PEg/BF0310TC; (e) PEg/BF0110TD; (f) PEg/BF1015WT; (g) PEg/BF1015TC; (h) PEg/BF0110WT%; (i) PEg/ BF0110WTX; (j) PEg/BF0110WTR; and (k) Peg/BF0110WT# ……... 110
Figure 6.3 – Comparison of tensile properties of BF0110 with different treatments, PEg matrix and their composites [U (0°),C] …….. 114
Figure 6.4 – Weibull distribution of PEg/BF0110WT, PEg/BF0110TB, PEg/BF0110TC and Peg/BF0110TD ……. 115
Figure 6.5 – Post tensile test samples of some performed composites, illustrating 116

the non-breaking of the reinforcement: (a) PEg/BF0110WT; (b) PEg/BF0110TB; (c) PEg/BF0110TC; and (d) Peg/BF0110TD …….

Figure 6.6 – Experimental and predicted elastic modulus E_1 of PEg composites reinforced with non and treated BF0110 [U (0°),C] …….. 117

Figure 6.7 – Mechanical parameter of PEg composites reinforced with non and treated BF0110 [U (0°),C]: (a) tensile strength; (b) elastic modulus; and (c) failure strain ……... 118

Figure 6.8 – Illustration of a simplified concept of composite materials with same volume fraction, where $D_L = 2D_T$ ……... 120

Figure 6.9 – Experimental and predicted elastic modulus E1 of PEg composites reinforced with non-treated and mercerized BF1015 [U (0°),C] ……... 121

Figure 6.10 – Comparison of tensile properties of BF0110 without treatment, PEg matrix, PEg/BF0110WT and Peg/BF0110WT% …… 123

Figure 6.11 – Weibull distribution of PEg/BF0110WT%, PEg/BF0110WTX, PEg/BF0110WTR and Peg/BF0110WT# …….. 123

Figure 6.12 – Sample of Peg/BF0110WTX …….. 124

Figure 6.13 – Comparison of tensile properties of BF0110 without treatment, PEg matrix, PEg/BF0110WT and Peg/BF0110WTX …… 124

Figure 6.14 – Comparison of tensile properties of BF0110 without treatment, PEg matrix, PEg/BF0110WT and Peg/BF0110WTR …… 126

Figure 6.15 – Post tensile test samples of Peg/BF0110WT# …… 126

Figure 6.16 – Comparison of tensile properties of BF0110 without treatment, PEg matrix and Peg/BF0110WT# ……. 128

LIST OF TABLES

Table 2.1 – Comparison between conventional PE and the green one …….. 33

Table 2.2 – Physical and mechanical properties of main natural fibers and some of the most used synthetic fibers ……. 39

Table 3.1 – Typical properties for the PEg used (grade SHA7260) …….. 57

Table 3.2 – Conditions for the PEg plate preparation …… 66

Table 3.3 – Data for the composite processing …….. 68

Table 4.1 – Bamboo fiber mass variation after complete treatments …… 79

Table 4.2 – Apparent and bulk densities of bamboo fibers ……... 83

Table 4.3 – Total porosity of bamboo fibers measured by MIP ……. 84

Table 4.4 – Results for mercury porosimeter analysis for bamboo fibers ……. 85

Table 4.5 – Water-absorption index of bamboo fibers ……... 87

Table 4.6 – Average mechanical properties of bamboo fibers in tension …….. 94

Table 4.7 – Comparison of materials efficiencies …….. 99

Table 5.1 – Water-absorption index for PEg matrix …….. 100

Table 5.2 – Mechanical properties of PEg plates …….. 103

Table 6.1 – Water-absorption index for performed composites of PEg reinforced with BF ……... 105

Table 6.2 – Moisture sorption constants and diffusion coefficient of the performed composites …….. 112

Table 6.3 – Mechanical properties of PEg composites reinforced with non and treated BF0110 [U (0°),C] …….. 113

Table 6.4 – Changes in tensile properties of PEg composites reinforced with non and treated BF0110 [U (0°),C] compared to the pure PEg ……. 113

Table 6.5 – Mechanical properties of PEg composites reinforced with non-treated and mercerized BF1015 [U (0°),C] ……. 120

Table 6.6 – Mechanical properties of PEg composites reinforced with non-treated BF0110 in different fiber direction ……. 122

Table 6.7 – Comparative between Young's modulus of PEg/BF0110WT# and calculated Young's modulus using Voigt model (PEg/BF0110WT) and Reuss model (theoretical Peg/BF0110WT_) …….. 127

LIST OF ABBREVIATIONS AND ACRONYMS

B	Bidirectionally orientated (concerning the bamboo fiber orientation in composites)
BF	Bamboo fibers
BF0110TA	Bamboo fibers with diameters between 0.1 to 1.0 mm and with treatment A
BF0110TB	Bamboo fibers with diameters between 0.1 to 1.0 mm and with treatment B
BF0110TC	Bamboo fibers with diameters between 0.1 to 1.0 mm and with treatment C
BF0110TD	Bamboo fibers with diameters between 0.1 to 1.0 mm and with treatment D
BF0110WT	Bamboo fibers with diameters between 0.1 to 1.0 mm and untreated
C	Continuously orientated (concerning the bamboo fiber orientation in composites)
CFRP	Carbon-fiber reinforced polymers
D	Discontinuously orientated (concerning the bamboo fiber orientation in composites)
FEA	Finite element analysis
GFRP	Glass-fiber reinforced polymers
HDPE	High density polyethylene
PEg	Green high density polyethylene
PEg/BF0110TA	Composite of green high density polyethylene reinforced with bamboo fibers with diameters between 0.1 to 1.0 mm, with treatment A and arranged U(0°),C
PEg/BF0110TB	Composite of green high density polyethylene reinforced with bamboo fibers with diameters between 0.1 to 1.0 mm, with treatment B and arranged U(0°),C
PEg/BF0110TC	Composite of green high density polyethylene reinforced with bamboo

	fibers with diameters between 0.1 to 1.0 mm, with treatment C and arranged U(0°),C
PEg/BF0110TD	Composite of green high density polyethylene reinforced with bamboo fibers with diameters between 0.1 to 1.0 mm, with treatment D and arranged U(0°),C
PEg/BF0110WT	Composite of green high density polyethylene reinforced with bamboo fibers with diameters between 0.1 to 1.0 mm, untreated and arranged U(0°),C
PEg/BF0110WT%	Composite of green high density polyethylene reinforced with bamboo fibers with diameters between 0.1 to 1.0 mm, untreated and arranged U(45°),C
PEg/BF0110WT#	Composite of green high density polyethylene reinforced with bamboo fibers with diameters between 0.1 to 1.0 mm, untreated and arranged B,C
PEg/BF0110WTR	Composite of green high density polyethylene reinforced with bamboo fibers with diameters between 0.1 to 1.0 mm, untreated and arranged R,D
PEg/BF0110WTX	Composite of green high density polyethylene reinforced with bamboo fibers with diameters between 0.1 to 1.0 mm, untreated and arranged U(0°),X
PEg/BF0110WT_	Theoretical composite of green high density polyethylene reinforced with bamboo fibers with diameters between 0.1 to 1.0 mm, untreated and arranged U(90°),C
PEg/BF1015TC	Composite of green high density polyethylene reinforced with bamboo fibers with diameters between 1.0 to 1.5 mm, with treatment C and arranged U(0°),C
PEg/BF1015WT	Composite of green high density polyethylene reinforced with bamboo fibers with diameters between 1.0 to 1.5 mm, untreated and arranged U(0°),C
LDPE	Low density polyethylene
LDPEg	Green low density polyethylene

LLDPE	Linear low density polyethylene
LLDPEg	Green linear low density polyethylene
LPG	Liquid petroleum gas
MC	Moisture content
PAN	Polyacrylonitrile
PE	Polyethylene
PEg	Green polyethylene
PHB	Polyhydroxybutyrate
PHBV	Polyhydroxybutyrate-co-valerate
PLA	Polylactic acid
PP	Polypropylene
PVC	Polyvinyl chloride
PVCg	Green polyvinyl chloride
R	Randomly orientated (concerning the bamboo fiber orientation in composites)
SHA7260	Grade of green high density polyethylene from Braskem
U	Unidirectionally orientated (concerning the bamboo fiber orientation in composites)
UHMWPE	Ultra high molecular weight polyethylene
ULDPE	Ultra low density polyethylene
X	In braids orientated (concerning the bamboo fiber orientation in composites)

SUMMARY

1	**INTRODUCTION**	20
1.1	**Overall considerations**	20
1.2	**Objectives**	22
1.3	**Thesis structures**	23
2	**LITERATURE REVIEW**	24
2.1	**Polymeric composites**	24
2.1.1	***Polymeric composites in automotive industry***	27
2.2	**Matrix for polymeric composites**	27
2.2.1	***Eco-friendly polymers***	29
2.2.2	***Green polyethylene***	30
2.3	**Reinforcements for polymeric composites**	34
2.3.1	***Natural fibers: nature, structure and properties***	37
2.3.1.1	*Types of natural fibers*	37
2.3.1.2	*Bamboo fibers*	38
2.4	**Fiber/polymeric composites manufacturing**	43
2.5	**Adhesion between polymeric matrix and natural fibrous reinforcement**	45
2.5.1	***Methods for natural fibers surface modification***	48
2.5.1.1	*Treatments based on physical process*	48
2.5.1.2	*Treatments based on chemical process*	51
2.6	**Failure mechanisms in composites**	52
3	**MATERIALS AND EXPERIMENTAL PROCEDURES**	56
3.1	**Constituents of the green polymeric composites**	56
3.1.1	***Green high desnity polyethylene***	56
3.1.2	***Bamboo fibers***	57
3.1.2.1	*Mechanical operations*	57
3.1.2.2	*Physical and chemical treatments*	58
3.2	**Manufacturing of the composite plates**	62
3.2.1	***Preparation of pure Peg plate***	63
3.2.2	***Processing of composites plates***	66

3.3	**Physicochemical analysis**	70
3.3.1	***Dimensions of bamboo fibers***	70
3.3.2	***Bulk and apparent densities of bamboo fibers***	71
3.3.3	***Porosity and pore size of bamboo fibers***	72
3.3.4	***Water-absorption index of bamboo fibers, Peg plate and performed composites***	73
3.4	**Morphological analysis**	75
3.4.1	***Scanning electronic micrographs of bamboo fibers***	75
3.4.2	***Photographs of PEg plate and composites reinforced with bamboo fibers*** ..	75
3.5	**Mechanical analysis**	75
3.5.1	***Tensile test of bamboo fibers***	75
3.5.2	***Tensile test of PEg plate and composites reinforced with bamboo fibers***	77
4	**PHYSICOCHEMICAL, MORPHOLOGICAL AND MECHANICAL BEHAVIOR OF BAMBOO FIBERS**	79
4.1	**Physicochemical behavior of bamboo fibers**	79
4.1.1	***Mass variation of bamboo fibers***	79
4.1.2	***Cross-section dimensions of bamboo fibers***	81
4.1.3	***Bulk and apparent densities of bamboo fibers***	81
4.1.4	***Porosity and pore size of bamboo fibers***	84
4.1.5	***Water-absorption index of bamboo fibers***	87
4.2	**Morphological behavior of bamboo fibers**	89
4.2.1	***Microstructure of bamboo fibers***	89
4.3	**Mechanical behavior of bamboo fibers**	94
4.3.1	***Tensile behavior and resistance of bamboo fibers***	94
5	**PHYSICOCHEMICAL AND MECHANICAL BEHAVIOR OF PEg MATRIX**	100
5.1	**Physicochemical behavior of PEg matrix**	100
5.1.1	***Water-absorption index of PEg matrix***	100
5.2	**Mechanical behavior of PEg matrix**	101
5.2.1	***Uniaxial tensile behavior of pure PEg***	101
6	**PHYSICOCHEMICAL, MORPHOLOGICAL AND MECHANICAL**	104

BEHAVIOR OF PEg COMPOSITES REINFORCED WITH BAMBOO FIBERS .....

6.1 **Physicochemical behavior of PEg composites reinforced with bamboo fibers** 104

6.1.1 ***Water-absorption index of PEg composites reinforced with bamboo fibers*** 104

6.2 **Mechanical behavior of PEg composites reinforced with bamboo fibers** . 112

6.2.1 ***Uniaxial tensile behavior of PEg composites reinforced with bamboo fibers*** 112

6.2.1.1 *PEg reinforced with long bamboo fibers prepared with different treatments* .. 112

6.2.1.2 *Influence of some morphological aspects of PEg reinforced with bamboo fibers* 119

7 **CONCLUSIONS AND PERSPECTIVES** 129

7.1 **Suggestions for future works** 131

REFERENCES 132

APPENDIX A – GREEN POLYETHYLENE CERTIFICATIONS 150

APPENDIX B – DIMENSIONS OF THE UNTREATED AND TREATED BF 151

APPENDIX C – MECHANICAL PROPERTIES OF PERFORMED COMPOSITES 157

1 INTRODUCTION

1.1 Overall considerations

The constant technological development has contributed for the polymeric industry growth, due to the increased substitution of traditional materials for polymers. Their presence is observed in domestic and professional life, from household utensils and toys to large parts used in construction and transportation industry. In this field of application, the automotive industry is under increasing pressure to meet better efficiency, environmental and performance demands at competitive costs. All plastics and composites in industry, as well as steel, aluminum and magnesium, have been studied to meet the new needs of this area. For decades, advanced plastics and polymer composites have helped improve the appearance, functionality and safety of automobiles, reducing vehicle weight and providing cost-effective customer. In addition, changes in regulations, consumer preferences, and recent technological innovations have encouraged the use of these materials to meet future challenges and opportunities (FENTAHUN & SAVAS, 2018; TODOR & KISS, 2018).

Plastics and polymer composites, which already dominate the interior, exterior, trim and lighting of vehicles, are gaining use in other vehicle systems as lightweight, value-producing materials that can meet increasingly challenging automotive requirements. The many advantages of these materials have allowed them to grow and become a significant part of the materials mix in the automotive industry over the past 40 years. As momentum for light vehicles intensifies, as well as improvements involving mechanical properties, projections indicate that these polymeric materials can and should play an even more substantial role in the automotive industry by 2025 and beyond (PLASTICS DIVISION OF THE AMERICAN CHEMISTRY COUNCIL, 2014; FENTAHUN & SAVAS, 2018).

The world production of plastics is estimated at 311 million tons. The Brazilian participation in the production of thermoplastic resins represents approximately 6.5 million tons (ASSOCIAÇÃO BRASILEIRA DA INDÚSTRIA DE PLÁSTICO, 2015; BELLOLI, 2010; PLASTICS EUROPE, 2015). Of this total, polyethylene (PE) represents approximately 34%, when added the percentages referring to the low density polyethylene (LDPE) with 9.5%, linear low density polyethylene (LLDPE) with 11.4% and high density polyethylene (HDPE) with 13.1% (ASSOCIAÇÃO BRASILEIRA DA INDÚSTRIA DE PLÁSTICO, 2015).

Conventionally, polymers are synthetized from petroleum fractions, which limit

their production due to the depletion of fossil raw materials, providing constant increases of price. These limitations, associated to the increase in the sustainability relevance, as motivating business values and being basis of some development actions, have motivated the search and development of alternative technologies for the production of polymers more sustainable (BELLOLI, 2010). Named as biodegradable polymers, biopolymers and green polymers, these types of polymers present benefits over conventional ones, whether in production, synthesis, processing or degradation, providing less environmental impacts. The growth potential of these is high, supported by current economic development standards based on the use of cleaner products and more improvements for future generations (BRITO *et al.*, 2011; COSTA *et al.*, 2017).

Braskem, a Brazilian multinational company, was the pioneer in the field of plastic development with renewable raw materials, the green polyethylene (PEg). Its main advantage in comparison to conventional PE is the sustainable raw material applied in this process, sugarcane. Its vegetable origin promotes the capture and fixation of carbon dioxide (CO_2) – for every ton of PEg produced, about 2.5 tonnes of CO_2 are captured from the atmosphere. Even synthesized by renewable sources, the PEg does not present biodegradability, keeping the CO_2 fixed throughout its production and lifetime. On the other hand, for each tonne of conventional PE produced, 2.5 tonnes of CO_2 are emitted into the atmosphere. Therefore, the replacement of conventional PE by PEg would stop emitting about 5 tons of CO_2 per tons of polymer produced – a significant benefit in face of the greenhouse problems currently faced (BRASKEM, 201-?a). In addition, as the green polymers exhibit properties and processes similar to the conventional, there is no need for technological changes in the final material processing.

Further extending consideration to environmental concerns, the use of some natural fibers in polymeric composites seeks to mechanically reinforce these green polymers, reducing the amount of polymeric material used and promoting advantages associated with the fibers properties, such as low cost, low density, biodegradability, renewability of raw material, non-toxic nature and lower abrasivety (BLEDZKI & GASSAN, 1999; RIOS, 2015). Besides these properties, the application of these resources helps in the prevention of environmental pollution, which would occur with their inappropriate release at the environment.

The mechanical properties of a fiber reinforced polymeric composite are of great importance in suggesting their end applications. These properties depend on the properties of the matrix, the fibers and the fiber/matrix adhesion. Fibers are the main load bearing

components of a fiber reinforced composites, and their strength generally reflects directly on the strength of them. The adhesion is a critical factor that controls the toughness, transverse mechanical properties and interlaminate shear strength of composite materials. Its improvement increases the tensile and flexural strength of the composite, while lowering the impact strength and toughness (LUO & NETRAVALI, 1999; TSAI & HAHN, 1980). This way, the adhesion is highly important to the mechanical properties of composite materials and one way to improve these is thus to achieve efficient bonding between the polymer matrix and the fiber (ADEKUNLE, 2015; GAMSTEDT *et al.*, 2002). However, this bonding can generally be improved by fiber surface treatment, fiber coating, addition of a coupling agent, or by tailoring the chemical properties of the polymer matrix (ADEKUNLE, 2015; ADEKUNLE, AKESSON & SKRIFVARS, 2010; GAMSTEDT *et al.*, 2002). Physical and chemical methods for natural fibers surface modifications were discussed at the sub-section 2.4.1, being the main subject of this thesis.

According to the reinforcements, in Brazil, there is a large variety of vegetable fibers with different chemical, physical and mechanical properties, being fundamental the knowledge of its composition, structure and characteristics for an appropriate selection. In this context, bamboo fibers are good fillers for composites with polymeric matrix, because they combine high hardness, strength and lightness. Besides that, the bamboo is a fast growing plant (GUIMARÃES Jr., NOVACK & BOTARO, 2010). Bamboo also has superior potential of carbon fixation (when compared to reforestation trees), protects the soil against erosion and can be planted on rough terrain and in inhospitable regions. It also does not require high fertility soil and can be used for the recovery of degraded areas (PEREIRA, 2012).

1.2 Objectives

This study aims to characterize and investigate some physico-chemical, morphological and mechanical properties of the materials used and manufactured on this study: bamboo fibers, green polyethylene and composites involving these materials.

Inside these general objectives, this study aims to investigate the effect of different treatment performed in bamboo fibers surfaces on morphological and mechanical properties, as well as their effect on mechanical properties of the composite.

1.3 Thesis structure

Chapter 2 presents a literature review on polymeric composites, with emphasis on types of matrices and reinforcements used. With respect to the matrices, it presents the benefits in using polymers. Some definitions are inserted in this chapter for polymers from renewable sources and/or biodegradable ones. Among them, the green polyethylene has its production and properties presented. Chapter 2 also presents advantages in using fibers and compares physical and mechanical properties of some synthetic and natural fibers. Within these last ones, the bamboo fibers are studied with greater diligence. Then it presents the importance of having a good adherence between the matrix and the reinforcement, suggesting procedures to optimize the interface/interfase. Finally, the main types of failure mechanisms in composite materials are described.

Chapter 3 focuses first on the materials and compounds used in this research. It summarizes their main properties. Then, it describes the experimental procedures developed to treat the fibers and to prepare the composites. Finally, the characterization techniques and methods employed are described, indicating the equipment used and the places where they were performed.

Chapters 4, 5 and 6 present the results of the physicochemical, morphological and mechanical behavior of bamboo fibers, HDPEg and the performed composites, respectively. According to the characterization of the performed composites, chapter 6 also evaluates the adhesion fiber/matrix.

2 LITERATURE REVIEW

This chapter presents a bibliographic review on the materials used: polymeric composites, green polymer as matrix, natural fibers as reinforcement and adhesion improvement. An emphasis will be given on the natural fiber used – bamboo fibers –, on the possible effects presented by them after physicochemical treatments and on the failure mechanisms after uniaxial loading.

2.1 Polymeric composites

A composite material is a combination of two or more different materials in a macroscopic scale. Depending on the geometric and topologic parameters, several classes of composites can be defined (ASHBY & JONES, 2006). The composite is designed in order to obtain a compound with superior performance and structural properties non-attainable by any of the components itself (ASHBY, 1999). That happens because each material presented in the composite retains its chemical, physical and mechanical properties (CAMPBELL, 2010; BLEDZKI & GASSAN, 1999).

The characteristic length of each phase defines the class of composites. The fibrous ones, such as glass-fiber reinforced polymers (GFRP) and carbon-fiber reinforced polymers (CFRP), have characteristic lengths ranging from several centimeters to several decimeters (ASHBY & JONES, 2006). More conventional composites, such particulate, have characteristic lengths of their microstructure phase ranging from several tenth millimeters to several millimeters (particles with virtually any shape, size or configuration). One well-known example of particulate composites is the concrete (STAAB, 1999). At micron scale, many composites exist, for example metallic alloys. Finally, a new class of composite, namely nanocomposite, are developed in recent years where the reinforcement phases have nanometric lengths. Layered silicates (clay) dispersed as reinforcement in an engineering polymer matrix is one of the most important forms of polymer nanocomposites (BHATTACHARYA, KAMAL & GUPTA, 2007). Others classifications of composites are based on the nature of the matrix phase, on the shape of the reinforcement phase, etc.

Composites can be found in the environment or can be of synthetic origin. Wood is a natural composite material formed from a chemical complex of cellulose, hemicellulose, lignin and extractives. This composite is composed by microfibrils, as the reinforcement, organized and bounded by the complex matrix that together form a stronger component

(SAKA, 1993). Bone is other natural composite, constituted by hydroxyapatite (a hard and brittle material) and by collagen (a soft and flexible substance). On its own, collagen can not sustain the skeleton, but combined with the hydroxyapatite, the composite presents the necessary properties to support the body (THE ROYAL SOCIETY OF CHEMISTRY, 20-?). Examples of man-made composites can be found since several thousands of years: in 3400 B.C., the ancient Egyptians and Mesopotamians performed the plywood by making up of an uneven number of thin layers of wood called veneer, at different angles, joined together by an adhesive; between 2181 to 2055 B.C., the Egyptians used linen soaked in plaster to prepar death masks; around 1500 B.C., the ancient builders and artisans used mud bricks, pottery and boats reinforced with straw (ZAKRZEWSKI, SHORTLAND & ROWLAND, 2016; MAR-BAL INCORPORATED, 201-?).

Regarding their structural composition, composites presents a continuous phase, called matrix. Its principal functions are to bind the reinforcements (fillers, fibers, particles) in an orderly array, to transfer load between them and to protect them from abrasion, preventing attack from moisture, chemicals and oxidation. It also provides shear, transverse tensile and compression properties to the composite, and governs the behavior of the composite under applied temperatures (THOMAS *et al.*, 2012; CLARKE, 1996). The matrix can be polymer, metal or ceramic, depending what is the final properties desired. Their nature is motivated by particular properties: polymers have low strength and stiffness; metals have intermediate or high strength, stiffness and high ductility; and ceramics have high strength and stiffness but is brittle (CAMPBELL, 2010). The reinforcing (or dispersed) phase is embedded in the matrix in a discontinuous form. This phase is generally made of short or long fibers or of particulates that are harder, stronger and stiffer than the matrix. It provides the final strength and stiffness of the composite (THOMAS *et al.*, 2012; CAMPBELL, 2010).

Composites have been extensively used due to their advantages: low weight, optimum strength and stiffness variability, improved fatigue strength, high corrosion resistance and relatively satisfier performance requirements (JAIN & LEE, 2012; THOMAS *et al.*, 2012). But these materials also have certain disadvantages: high costs of certain raw materials and of fabrication and assembly process; sensitivity to some physico-chemical effects (temperature, moisture, molecular interaction); some non-viable applications due to a complex load applied (lugs, fittings); susceptibility to impact damage and delamination or ply separation; greater difficulty in reparation (comparing to metallic structures) and in recycling (comparing to polymeric materials) (CAMPBELL, 2010).

The initial use of polymeric composites as structural materials has started during

the Second World War, in the 1940s, with the manufacture of military vehicles, such as airplanes, helicopters and rockets. This happened because the necessity of light-weight equipments (more cargo could be carry) aligned with high-strength materials started to be advantageous. As example, the British aircraft company De Havillan designed a military plane largely out of plywood, the *Mosquito*. The design of an advanced fiber composite structure and the use of adhesives in composite structural design provided the great number of its production and use (HULT, 1994). After the war, the technology was rapidly commercialized and new demands started to emerge from the military space programs, resulting in the research for other higher modulus fibers: carbon, boron and aramid (Kevlar) fibers (MAR-BAL INCORPORATED, 2015; PALUCKA & BENSAUDE-VINCENT, 2002). The US Airforce fighter plane *F-111* was the first to use boron fibers composites and the European fighter planes – Saab *Gripen*, Dassault *Rafale* and Eurofighter Consortium *EFA* –, started to use carbon fiber composites in the wings, in the tail fin and also in the front fuselage (HULT, 1994).

Associated with this, the industry of polymer was growing and it was necessary to make some adaptations for expanding the market to a large number of variety. Therefore, researchers started to study solutions to increase the mechanical properties of the plastics (PALUCKA & BENSAUDE-VINCENT, 2002; HOLLAWAY, 1993). At that time, certain materials – such as fine threads of glass held by some resin (epoxy or polyester), or glass fibers – were appearing with an extremely high theoretical strength (THE ROYAL SOCIETY OF CHEMISTRY, 20-?; HOLLAWAY, 1993). Using this new product as reinforcement, military engineers started to develop another composite made of a polymeric matrix. The result was a stronger, stiffer and lighter-weight product (PALUCKA & BENSAUDE-VINCENT, 2002).

By the mid 1990's, the polymeric composites hit mainstream manufacturing and engineering industry, replacing lots of traditional materials performed with metal (MAR-BAL INCORPORATED, 2015). Associated with this and with the advantages cited before, the increased attention towards a sustainable environment pressed engineers to connect energy and resources consumption with social factors, financial constraints and final product performance. These factors accelerated the development of high performance resins, new types of reinforcements, such carbon nanotubes and nanoparticles, and treatments to promote better interaction between the phases (JAIN & LEE, 2012). As a result, nowadays, polymeric composites are used in almost every type of engineering structure, ranging from airspace to automobiles and navigation vehicles equipment's, passing from sportive and domestic goods,

from industrial equipments and civil infrastructure, until biomedical devices (MASUELLI, 2013).

2.1.1 Polymeric composites in automotive industry

In addition to the requirements of light weight and lower cost, materials used in automotive applications should also meet safety requirements and be able to absorb impact energy in what is referred to as crashworthiness. Inserted in this context, polymeric composites have been replacing metal components due to their reduced weight, improving fuel consumption, their durability and their crashworthiness (HALLAL *et al.*, 2013).

The use of natural fibers as reinforcement in polymeric composites emerges as a class of new materials that have various applications in the automotive industry. The raw material most used by automakers is composed by polypropylene resin, natural fibers and recyclable materials, being applied in the manufacture of door and package medallions, door holders and interior coverings, rearview body, headrests, among others (PENNAFORT Jr., 2015).

Major automakers, such as Volkswagen, General Motors, Ford, Fiat, Honda, Toyota, Renault, Peugeot, Scania and Mercedes Benz are currently investing in the development of parts with natural fibers, which have ensured sound-absorbent properties of polymer composites, contributing to the smaller internal noise level. Other features of the product are the low weight of the part, the flexibility of applications, the shortest time required to make the production tools, the best visual appearance and the mechanical strength (PENNAFORT Jr., 2015).

However, the introduction of the natural fiber-reinforced polymeric composites in this automotive sector has been driven by price and commercialization rather than technical requirements. In addition, they are an important source of income for agricultural societies, with positive social impacts. Brazil has great potential for vegetable fibers production, which can be found natively or cultivated, all of them with commercial applications, becoming a source of income for many local communities (PENNAFORT Jr., 2015; ALVES *et al.*, 2011).

2.2 Matrix for polymeric composites

The word polymer is originated from greek: poly (many) and mere (repeating units). That is, polymer is a macromolecule composed of the repetition of ten thousands of

small and simple chemical units called meres. Such units are generally equivalent or nearly equivalent to the monomer or the starting material from which the polymer is formed (BARBOSA, 2011; CANEVALORO Jr, 2004). In other words, polymers are made up of organic macromolecules, that can be natural or synthetic. Polyethylene (PE) and epoxy resin are examples of synthetic polymers, while leather, silk, cotton, wool and natural rubber consist of natural organic macromolecules (PADILHA, 2000; NASCIMENTO, 2009).

Polymers are distinct from other structural materials as metals and ceramics because of their macromolecular nature. The long chain structure covalently bonded gives it a high molecular weight and this determines the mechanical strength and benefits properties like strain-to-break, impact resistance, wear, and others (MASUELLI, 2013; CLARKE, 1996). It also stands out for its weight, in general they are lightweigth materials (compared to metals), besides being electrical and thermal insulators, they are flexible and have good corrosion resistance (PADILHA, 2000).

Many different polymers can work as matrices, depending on the application and on the final properties desired. They are classified as thermorigids (thermosets) or thermoplastics, being the main difference between them identified by their behavior when heated.

The thermosets are chemically cross-linked with a heat treatment. As the name suggests, these polymers can be molded once, because, after cure polymerization, the chemical reaction irreversibly sets the material to a given form, making it impossible for these polymers to be fluid. Consequently, another applied temperature or pressure will not change any physical characteristics. Its stiffness is caused by the formation of covalent crosslinks between the adjacent chains during the initial heat treatment. They are low molecular weight and insolubles, infusibles and non-recyclables (CAMPBELL, 2010; CANTWELL & MORTON, 1991). They exhibit high hardness and greater brittleness when compared to thermoplastics. Typical thermosets used are bakelite, epoxy, polyester, among others (BARBOSA, 2011; MANO, 2000).

In contrast, thermoplastics are not chemically cross-linked. They have high molecular weight and, under temperature and pressure effects, they can be melted and be molded. Their polymerization do not promote cross-linking of the monomers, this way the polymer can be re-heated subsequently and easily re-molded (CAMPBELL, 2010). However, with each increase in temperature, the strength of the secondary connections decreases, so a weakening occurs and the movement of adjacent chains occurs more easily with some applied load. That is, the polymer weakens and decreases its useful life or, in other words, the

degradation process starts. In general, they are soft and ductile polymers. Thermoplastics are made up of most linear polymers and of some branches with chain flexibility. The most widely used thermoplastics in the industry are polyethylene (PE), polypropylene (PP) and polyvinyl chloride (PVC) (BARBOSA, 2011; MANO, 2000).

Factors such as high cost in the development of new polymers, specific applications of composites and alloys, properties improvement and cost reduction through the combination of expensive with cheaper materials, present themselves as motivators for the current trend of using polymeric alloys, blends and composites (AQUINO, 2003). In sum, with the limitations observed for the polymer produced from petroleum and with the increasing of sustainability relevance as a business guideline, researches and industries are seeking alternatives and improving technologies to develop more environmental friendly polymers.

2.2.1 Eco-friendly polymers

The durable characteristic of the polyolefins, due to the resistance to oxidation, water and microorganisms, make them the most used polymer in general industry. However, the dwindling fossil resources, the increasing energy demand, the global warming and the enormous waste generation (when they are not reused), encouraged the production of bio-based and/or renewable polymers. Besides that, these productions stimulate other sustainable actions, such as the use of biomass residue as energy and the promotion of carbon fixation during the polymerization (MÜLHAUPT, 2013; COSTA, 2012). In this way, variations as biodegradable polymers, biopolymers and green polymers appear as alternatives to conventional polymers due to their technical and economic viability, presenting high potential for expansion (COSTA, 2012; BRITO *et al.*, 2011). In order to avoid any erroneous comparisons, it is worth noting the difference between the above mentioned polymers.

Every polymer degrades on a certain time-scale depending on environmental conditions, resulting in the decrease of molecular weight through chain scission in the backbone and, this way, resulting in end products with low molecular weight compounds and biomass (IMRE & PUKANSZKY, 2013). However, for biodegradable polymers, the chain scission is caused by cell activity (human, animal, fungi, etc.), thus it is an enzymatic process, being usually accompanied and promoted by physicochemical phenomena as well. In favorable conditions, the degradation occurs in just few weeks or months (ASTM D6400-04; IMRE & PUKANSZKY, 2013). These polymers may come from renewable sources (starch,

cellulose, surgarcane), be synthesized by bacteria, yielding materials such as polyhydroxybutyrate (PHB) and polyhydroxybutyrate-co-valerate (PHBV), or be derived from animal sources such as chitin, chitosan or proteins. Besides these, they can also be obtained from fossil sources (petroleum or mixture between organic matter and petroleum). The best known biodegradable polymers from this source are polycaprolactones, polyesteramides, aliphatic copolyesters and aromatic copolyesters (COSTA, 2012; BRITO *et al.*, 2011).

In its turn, biopolymers are all the polymers produced from renewable sources (cellulose, sugar cane, corn), by bacteria, by animal or by fossil sources (petroleum or mixture with organic matter and petroleum) (COSTA, 2012; BRITO *et al.*, 2011). The most common are starch, polyhydroxybutyrate (PHB), chitin and chitosan, polycaprolactones, polyesteramides, and others.

Biopolymers are polymers or copolymers produced from raw materials from renewable sources, biomass in general, presenting great potential for conventional polymers replacement in certain applications (COSTA, 2012; NBR 15448-1). Biodegradability, on the other hand, is independent of the source used in biopolymer production. Thus, biodegradation is not an obvious characteristic of this polymer category (IMRE & PUKANSZKY, 2013). Disadvantages in relation to the use of biopolymers are due to some technical limitations that make it difficult to process and use as final product, being necessary studies aiming at modifications in their structures (COSTA, 2012). The most used are starch, polylactates, polyhydroxyalkanoates and xanthan.

Green polymers are polymers that during their synthesis, processing or degradation produce less environmental impacts than polymers from unsustainable raw materials. Normally, these are polymers that were previously produced by fossil sources and which, after technological advances, are now also synthesized by renewable sources (COSTA, 2012; BRITO *et al.*, 2011). They present the same properties as the conventional polymers and they are not biodegradable. However, they can be called as biopolymers, differentiating only because they have a similar conventional polymer. The most known green polymers are green polyethylene (PEg) and green polyvinyl chloride (PVCg).

2.2.2 Green polyethylene

Among the thermoplastics available in the market, polyethylene (PE) is the most produced and popular polymer commodity used in common and daily products. This versatile

plastic is used in a wide range of applications from grocery bags, bottles and toys, until bulletproof vests and materials for civil construction (BRITISH PLASTICS FEDERATION, 201-?; POLYMER SCENCE LEARNING CENTER, 2003-2017).

Polyethylenes cover a density range of 0.917 to 0.965 g/cm^3, with high density polyethylene (HDPE) being the most used polyethylene (PE) type in manufacture of fiber-reinforced composites. This is a highly linear polymer and its compact structure gives it a high density. On the other hand, low density polyethylene (LDPE) and low linear density polyethylene (LLDPE) have a higher degree of branching in their chains, which gives them a lower degree of crystallinity (GABRIEL, 2010; ARAUJO, 2009). In general, LDPE is intended for applications that require flexibility and transparency, whereas HDPE is better for applications requiring rigidity, mechanical strength and good chemical resistance (ARAUJO, 2009; COUTINHO, MELLO & SANTA MARIA, 2003). Also, the HDPE is a nontoxic material, impermeable to liquids and gases, with almost zero moisture absorption, excellent resistance and chemical properties, besides low friction coefficient (INCOMPLAST, 1977).

PE molecular structure consists of long backbone chain of covalently linked carbon atoms with a pair of hydrogen (H) atoms attached to each carbon (C) and with the chain ends finalized by methyl (CH3) groups (Figure 2.1). It consists chemically in alkanes, formula $C_{2n}H_{4n+2}$, with *n* being the number of ethylene monomers polymerized to form the polymeric chain (degree of polymerization) (PEACOCK, 2000).

Its wide range of applications is due to the possibility to process this polymer into soft and flexible as well as into tough, hard, strong, chemically inert and electrically resistant products. It can also be processed to shape parts in all kind of dimensions and sizes (from the simplest to the most complex shapes) that is combined with its low cost (PLASTICS EUROPE, 201-?; PEACOCK, 2000).

Figure 2.1 – Chemical structure of polyethylene

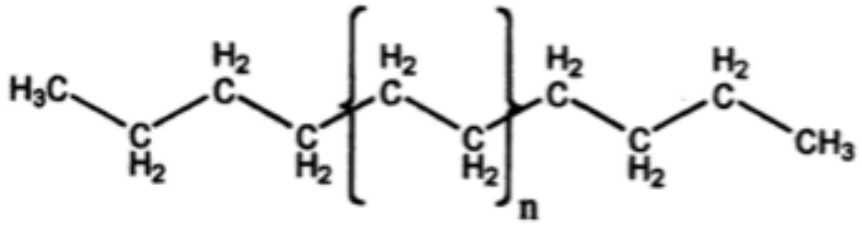

Source: PEACOCK (2000).

The ethylene or ethene (C_2H_4) monomers are the starting point for the production

of different grades of PE and other bulk and base chemicals (MOHSENZADEH, ZAMANI & TAHERZADE, 2017; ZUMMERMANN & WALZE, 2012). In chemical industries, this compound is produced by pyrolysis of saturated hydrocarbons and uses a moderate variety of raw materials, such as naphtha, ethane (natural gas), liquid petroleum gas (LPG), condensates, gas oils and ethanol (MARINHO & ANTUNES, 2007). Since 1980, the increased production of bioethanol from sugarcane, molasses, corn grains or lignocellulosic materials opened up the reverse process of production of biobased ethylene with the same characteristics as the conventional ethylene ones (MOHSENZADEH, ZAMANI & TAHERZADE, 2017; BROEREN, 2013; MORSCHBACKER, 2009).

According to recent studies, 0.3% of the global capacity of ethylene is produced from bioethanol. The principal commercial facilities are located in Brazil and India, besides other plants that are under construction and planned in China (MOHSENZADEH, ZAMANI & TAHERZADE, 2017; BROEREN, 2013).

After years doing research and development, Braskem's biobased ethylene (green ethylene) plant was fully functional in September 2010. This marked the beginning of the *I'm green*™ polyethylene (PE) production on a commercial scale (BRASKEM, 201-?a). The Dow Chemical Company, one of the PE global supplier, also tried to construct a polymer based sugarcane complex in Brasil. It makes first some partnerships without success, with Crystalsev – one of the greatest sugar and alcohol trading. Later, Dow Chemical Company developed partnerships with Mitsui & Co. LTDA – a Japanese company that started with the bioethanol production by sugarcane through the operation of the plant Santa Vitoria Açúcar e Álcool (SVAA) (NOVA CANA, 2017; DOW CHEMICAL, 2016; THE CORPORATE SOCIAL RESPONSIBILITY NEWSWIRE, 2007).

Sugarcane has its origin in the Southeast Asia and started to be cultivated in Brazil in the 16th century, with the purpose of producing sugar to be used in the food industry. Brazil has vast and fertile lands, with climate and ideal soil for sugarcane cultivation, making it the world's largest producer of this vegetable. Furthermore, Brazilian sugarcane is a source of a renewable energy which combines sustainable and low-cost characteristics. Its plantation helps to capture CO_2 from the atmosphere during its natural photosynthesis process, keeping that compound fixed throughout its processing and for all product life cycle (BRASKEM, 201-? a). Nowadays, about 1% of the arable lands is dedicated to sugarcane production, with 0.02% for the development of the bioethanol used for polymerization (BRASKEM, 201-?a). This ends the myth of direct competition between the growing areas for bioethanol or food and its consequently collaboration to raise the food market prices.

The green prolyethylene (PEg) is a thermoplastic polymer, presenting the same performances and characteristics as the ones made from non-renewable raw material, resulting in economy for the plastics manufacturers that do not have to invest in new equipment and can use the conventional process conditions and productivity rates. Also, after the consumption, the compounds produced from this green polymer can be recycled in the same conventional PE recycling structures (BRASKEM, 201-?b). In relation to the market, although identical to conventional PE, PEg presents a very different market dynamics, as it can be seen in Table 2.1 (BELLOLI, 2010; BRASKEM, 201-?a).

Table 2.1 – Comparison between conventional PE and the green one

Fossil PE	**Green PE**
Sold, for the most part, for plastics transformers	Sold, mostly, for companies with end direct consumer
Purchased by companies looking for a standard product	Purchased by companies seeking differentiation
Large number of customers (small, medium and large companies)	Limited number of customers with sustainability guidelines
Demand influenced by macroeconomic trends, such as Chinese growth	Demand influenced by own initiatives and/or specific regulations
Large number of producers and suppliers	Low availability and only a few production company in the world

Source: BELLOLI (2010); BRASKEM (201-?a); COUTINHO, MELLO & DE SANTA MARIA (2003).

Green polymers are generally classified as market segments whose particular needs are few explored or nonexistent (niche market), with features built around sustainable issues and benefits they bring to the environment. In contrast, the conventional PE presents itself as a commodity, material of great global consumption and vast number of producers, customers and different product types. In relation to its commercial value, the sustainable characteristic presented by the PEg is a differential that adds value to the final product. The measurement of this value is essential for its success, since economic viability is part of every business and industrial project (BELLOLI, 2010). In this context, despite its added value, PEg has an advantage, since it is based on ethanol from sugarcane and offers no extra costs to the buyer to adapt any equipment and process, making its final value competitive in the market.

2.3 Reinforcements for polymeric composites

Reinforcements dominate the composite properties, providing the strength and stiffness, being harder, stronger and stiffer than the matrix. Usually, the reinforcement is a particulate or a fiber (CAMPBELL, 2010). Their selection is a critical point for the design of the composite material, since it is defined in a way that a large portion of the load applied to the composite is transmitted by the reinforcements (ASHBY, 1999).

Particulate composites have dimensions that are approximately equal in all directions. The reinforcements may be spherical, platelets or present any other geometry. Particulate composites tend to be weaker and less stiff than continuous-fiber composites, but they present usually much less incorporated value. Another difference compared to the fiber reinforcement is associated with the quantity of material used: particulate reinforced composites usually contains less reinforcement (up to 40 to 50 % v/v) due to processing difficulties and brittleness (CAMPBELL, 2010).

Fibers produce high-strength composites because of their small diameter, presenting fewer defects (normally surface defects) compared to the material produced in bulk. As a general rule, the smaller is the diameter of the fibers, the higher is its strength, but also the higher is the cost associated to the performed composites. In addition, these fibers have greater flexibility and are more amenable to fabrication processes (CAMPBELL, 2010). This way, the appropriate reinforcement choice, as well as the chemical nature, the shape and the orientation distribution of the fibers, help to design composite parts with high strength to weight ratios. Also, the characteristics of the final products define the choice of the fiber to be introduced in the composite. That happens because the final mechanical properties are influenced by the type of fiber and by the surface chemical activity undergone between them, or even by their surface topography (LEVY NETO & PARDINI, 2006). The most common types of fiber as reinforcements are glass, carbon, Aramid (Kevlar), UHMWPE, boron, particulates (ceramic, metallic) and whiskers (GOTRO, 2016; MALLICK, 2007; LEVY NETO & PARDINI, 2006).

Glass fibers are the most used for reinforcing polymeric matrix because they are low cost materials, are chemically inert, present high tensile strength and excellent insulating properties. However, they have low elasticity modulus, high density (among the commercial fibers), are self-abrasiveness during handling (frequently reducing its tensile strength), present low fatigue resistance, and high hardness (wearing the molding dies and the cutting tools) (TARANU *et al.*, 2016; MALLICK, 2007; LEVY NETO & PARDINI, 2006).

Carbon fibers have different morphologies and specific characteristics. The most common precursors are polyacrylonitrile (PAN), cellulose (viscose, cotton), petroleum pitch and coal tar (LEVY NETO & PARDINI, 2006). As carbon fibers, they can also be classified according to the elasticity modulus, 207 GPa (30 x 10^6 psi) to 1035 GPa (150 x 10^6 psi); to the mechanical strength (directly influenced by the previous property, i.e., smaller is the elasticity modulus, higher are the tensile and compressive strengths and the tensile strains-to-failure); and to the heat treatment temperature (temperatures above 2000 °C are associated with fibers of high elasticity modulus, around 1500 °C are associated with fibers of high resistance and less than 1000 °C are linked to low elasticity and low resistance) (LEVY NETO & PARDINI, 2006; DONNET & BANSAL, 1998). Some disadvantages associated with this type of fiber are their low strain to failure, low impact resistance, high electrical conductivity and high cost (MALLICK, 2007).

Polymeric fibers are polymers whose chains are stretched in a straight line, or almost straight, and aligned side by side along the same axis, presenting strong inter-atomic covalent bonds. According to its intense reinforcing utility, the most widely used polymeric fibers are aramid and UHMWPE (LEVY NETO & PARDINI, 2006; CHODAK, 1998). Aramid fibers, known in the market as Kevlar 49, present highly crystalline aromatic polyamide fibers with low density and high tensile strength-to-weight ratio among the current reinforcing fibers. Some disadvantages are associated with: i) the negative coefficient of thermal expansion in the longitudinal direction, like carbon fibers; ii) the low compressive strengths; and iii) the difficulty in cutting or machining. The PE fibers, known under the commercially name Spectra, have the highest strength-to-weigth ratio of all commercial fibers available. They present low moisture absorption, high abrasion and provide high impact resistance. Their disadvantages are associated with: i) the low manufacturing temperature about 125 °C (they exhibit a significant and fast reduction in strength and an increase in thermal shrinkage above this temperature); and ii) their poor adhesion to the continuous phase (the adhesion can be partially improved by some surface modifications) (MALLICK, 2007).

Natural fibers, besides the objective of intensify the mechanical properties of the composites, present a wide variety of species and availability and are used to adjust environmental, social and economic issues. Thus, these fibers are very interesting and effective reinforcements in our current reality, being better detailed below.

According to the fiber orientation and to the possibility of incorporate a large number of fibers into a thin layer of matrix, forming a lamina (ply), the final properties of the composite can be estimated (MELO, 2016; MALLICK, 2007):

- If long fibers are arranged continuously and along one direction, the composite material presents the highest strength and stiffness in the longitudinal direction of the fibers and the lowest ones in the transverse direction;
- If long fibers are arranged bidirectionally (fibers oriented in two directions), usually perpendicular to each other, the composite material presents a varied strength and stiffness in different orientations, according to the different amount of fibers in the longitudinal and transverse direction;
- If long fibers are arranged multi-directionally (fibers in more than two directions), the composite material will also present a varied strength and stiffness depending to the amount of fibers in direction of the applied load;
- If short fibers are arranged discontinuously and unidirectionally, for the same reinforcement mass content in the composite, the final product exhibits lower strength and stiffness than the composite with long fibers;
- If the short fibers are arranged discontinuously and randomly, it is possible to obtain isotropic mechanical and physical properties in the plane of the composite.

To increase the mechanical properties (stiffness and strength to in plane loading or flexural loading) of a composite plate, several laminas can be stacked in varied sequence, forming various laminates arrangements (all in one direction or in different directions). It is also possible to combine different types of fibers to form an interply (different kinds of fibers in different laminas) or an intraply (two or more different kinds of fibers interspersed in the same lamina) hybrid laminate. It is even possible to combine some of the performed laminas cited before with thin layer of aluminum or other metallic sheets (MALLICK, 2007).

According to the length, long fiber combines high levels of stiffness, strength and toughness together in a single material. When used as reinforcement, long fiber composites present a high mechanical performance characteristics, being often selected as substitutes for metals, as a replacement for under-performing plastics, or as alternatives to higher cost engineering polymers through up-engineering of lower cost plastics (PLASTICOMP, 201-?a).

Stiffness is the extent to which an object resists deformation in response to an applied force (BAUMGART, 2000). The increasing of fiber length included in the composite contributes to increased stiffness. Utilizing composites that offer more stiffness increases load carrying ability or allows designing with thinner wall sections to decrease material use and lower cost. Stiffness gains through fiber reinforcement also translate into increased performance at elevated temperatures (PlastiComp, 201-?a). Strength of materials is focused

on analyzing stresses and deflections in materials under load. Longer length, or higher aspect ratio (length/diameter), of reinforcing fibers provides composites with increased strength, which translates into the ability to resist deformation or creep under loads and higher fatigue endurance with minimal compression. More fiber filament surface area provides the polymer with more ability to grab onto and transfer stress to the stronger internal fiber skeleton (PLASTICOMP, 201-?a; PLASTICOMP, 201-?b).

Typically, stiffer plastics are more brittle. However, using fiber as reinforcement, long lengths promote a tougher composite, I.e., a composite that absorbs more energy and plastically deforms without fracturing. This is caused by the higher aspect ratio of the fiber, that facilitates a more efficient energy transfer between the polymer and fiber filaments. In case of using a long fiber intertwined network as reinforcement, it aids in dissipating those forces throughout the composite structure instead of keeping them localized in one area. The inclusion of long fiber helps composites resist cracking and impedes crack propagation. Longer fiber length also minimizes material fragmentation during failure and promotes to composites a considerable durability at low and elevated temperatures, making them desirable for devices exposed to varying climates (PLASTICOMP, 201-?a; PLASTICOMP, 201-?b).

2.3.1 Natural fibers: nature, structure and properties

2.3.1.1 Types of natural fibers

Natural fibers may have vegetable, mineral or animal origin, but, for application as reinforcements in composites, the focus will be centered on the first one (FRANK, 2005). These fibers comes from elongated structures of hollowed and rounded cross-section distributed throughout the plant (thallus, leaves, wood and surface) (BARBOSA, 2011). These fibers, commonly called lignocellulosic fibers, are naturally occurring composites composed of cellulose microfibrils (60-80 wt%) incorporated in an amorphous matrix of lignin and hemicellulose (MALLICK, 2007; SATYANARAYANA *et al.*, 1990). They are also composed of pectin, inorganic salts, nitrogenous substances, natural dyes and moisture (about 20 %wt) (BARBOSA, 2011; MALLICK, 2007).

Examples of vegetable with lignocellulosic compounds are jute, flax, hemp, sisal, coconut (coir), banana (abaca), wood, bamboo, etc. These vegetables grow as agricultural plants in many parts of the world especially in rural and underdeveloped areas, contributing to their economic and social development (RIOS, 2015; FRANK, 2005). The use of vegetable

fibers in composites is influenced by some factors, such as: their low cost (much less expensive than glass and carbon fibers), varying with the region and with the obtaining method; lower weight; renewable raw material and biodegradability; high modulus-weight ratio greater than the glass fibers, being very useful in stiffness-critical designs; high acoustic damping (when in composites); high availability; non-abrasiveness characteristics; low energy consumption during their production; fixation of carbon dioxide (CO_2) during their photosynthesis; and stimulation of works in rural areas (RIOS, 2015; BARBOSA, 2011; MONTEIRO *et al.,* 2011; MALLICK, 2007; LEVY NETO & PARDINI, 2006). Some disadvantages of using these fibers are associated with some limitations, like the low values for tensile strength, compared to values for glass fiber and aramid fiber for example (see Table 2.4 above). Others limitations are the low processing temperatures, about 200 °C, tolerated during their consolidation inside the matrix; high sensitivity to environmental effects, such as moisture; high influence of the planting and cultivation process on the final properties; and lack of standard in relation to mechanical properties, geometric structure and dimensional stability (LEVY NETO & PARDINI, 2006).

Some physical and mechanical properties of some natural and synthetic fibers can be observed and compared in Table 2.2. According to the fibers elasticity, the composites based natural fibers can be classified in two groups, determining their applications: high-modulus fibers, improving strength of the composite; and low-modulus fibers, proportionating better impact strengths and enabling the final material to be manipulated in the post-cracked stage, controlling the cracks opening and propagation, which, when applied adequate fibers percentages, increases their tenacity (BARBOSA, 2011; CAETANO *et al.*, 2004).

Frequently, performance is maximized by selecting the subset of materials with the greatest value of a grouping of materials properties. For example, considering natural fibers, a minimum weight design of strong beams is observed for materials with high value of $\sigma^{2/3}/\rho = C$ (ASHBY, 1999).

2.3.1.2 Bamboo fibers

Bamboo fiber is a vegetable fiber that still little used as engineering material. However, this lignocellulosic fiber, often known as natural glass fiber due to its high strength with respect to its microfibrils longitudinally aligned, has presented interesting benefits that should be better evaluated (RASSIAH & AHMAD, 2013; MONTEIRO *et al.*, 2011; OKUBO, FUJII & YAMAMOTO, 2004).

Table 2.2 – Physical and mechanical properties of main natural fibers and some of the most used synthetic fibers

Fiber types		Density (g/cm^3)	Elongation (%)	Young's Modulus (GPa)	Tensile strength (MPa)	Maximum $\sigma^{2/3}/\rho$ ($MPa^{2/3}.cm^3/g$)	Ref
Plant fiber	Abaca	1.5	3.-10.	12	400	36.2	[1-3]
	Bagasse	0.3-.3	1.1	15-27	135-512	213.3	[1-4]
	Bamboo	0.6-1.2		11-17	106-230	62.6	[1-4]
	Banana	0.7-1.5	2.5-5.9	12-32	700-1194	160.8	[1,3,4]
	Coir	1.2-1.5	15.0-51.4	4-10	95-220	30.4	[1-5]
	Cotton	1.5-1.6	3.0-10.0	5.5-12.6	287-800	57.5	[1,3-6]
	Flax	1.3-.5	2.7-3.2	26-80	344-1035	78.7	[1,3-6]
	Hemp	1.1-1.5	1.6	35-70	389-900	84.7	[1,3-6]
	Jute	1.3-1.5	1.5-1.8	10-55	393-800	66.3	[1,3-6]
	Kenaf	-	1.6	53	930	-	[1-3]
	Oil palm	0.7-1.6	25	3.2	248	56.4	[1-3]
	Piassava	1.1-1.5	21.9	1-6	109-1750	132.0	[1,4]
	Ramie	1.5	1.2-3.8	25-128	400-1620	92.0	[1,3-6]
	Sisal	1.3-1.5	2.0-5.1	9-28	287-913	72.4	[1,3-6]
Petroleum fiber	E-glass	2.5-2.6	2.5	70-73	2000-3500	92.2	[3-5]
	Aramide	1.4	3.3-3.7	63-131	3000-4100	183.0	[3-5]
	Carbon	1.4-1.8	1.4-1.8	230-400	2500-6350	244.9	[3-5]

Source: [1] JONH & ANANDJIWALA (2008); [2] FARUK *et al.* (2012); [3] VERMA *et al.* (2016); [4] MONTEIRO *et al.* (2011); [5] BLEDZKI & GASSAN (1999); [6] CHEUNG *et al.* (2009).

Bamboo is a plant with a wide variety of species around the world, estimated that there are approximately 1500 species sub-distributed in 115 generas, scattered in all continents of the Earth, except in Antarctica and Europe, where there are not any native species (SILVA, 2015). In a world scale, the largest producers of bamboo are China, some Southeast Asian countries and India (SALAM & PONGEN, 2008). Brazil is the country with the highest diversity of bamboo species among the countries of America, with about 250 native species (not all formally described) distributed in approximately 34 genera (18 ligneous and 16 herbaceous) (GENEROSO *et al.*, 2016; GUIMARÃES Jr., NOVACK & BOTARO, 2010). More than 20 species have been introduced in Brazil, mainly during the colonial period

and later by Japanese immigrants (SILVA, PEREIRA & SILVA, 2011). Ligneous bamboos present high height and their morphologies are structured by roots, culm, branches and leaves. Herbaceous bamboos are inferior in height, quite similar to shrubs, being constantly used as ornamental plants (SOUZA, 2014).

Inserted in the category of ligneous bamboo, the production of *Bambusa vulgaris* in Brazil has been encouraged due to its high potential for manufacturing long fibers, which are widely used for cellulose synthesis (SILVA, 2007). At the beginning of 2015, the Brazilian production of pulp from bamboo was around 150 thousand tons (11,3% of the total production registered in the same period in the world) (Indústria Brasileira de Árvores, 2015; SANTI, 2015). Some Brazilian industries have sought to invest in the use of bamboo as biomass for the generation of renewable energy in boilers, due to its low cost in operation and in implantation. With this, the Brazilian Northeast gained a bamboo energetic forest and has developed a sustainable bamboo industry to stimulate the economic sector of this region. The large forests masses with bamboo for commercial use in pulp production and biomass are located in Maranhão, Piauí, Pernambuco, Paraíba and Bahia (SANTI, 2015).

Bamboo presents essential elements for its application in composites, contains long and aligned cellulosic fibers immersed in a matrix with high content of holocellulose (α-cellulose and hemicellulose) and low lignin content (less energy for purification of cellulose), and its microstructure results in good mechanical and dimensional properties (GUIMARÃES Jr *et al.*, 2015; SANTI, 2015). Thus, in order to understand the advantages and disadvantages about the use of bamboo, it is imperative to know its plant structure and chemical composition.

In general, the bamboo macrostructure is composed of two parts, an aerial one, consisting of lateral branches and culms with ligneous tissues, generally hollow and with fibers arranged in the form of bundles (mainly at the outermost region); and another subterranean one, constituted by rhizome and roots (SOUZA, 2014).

The culms, also defined as stems, are constituted by nodes, internodes and diaphragms (Figure 2.2). They are cylindrical and hollow, extremely compact and their constituents are lined longitudinally in the axis direction. The culm tissue is made of usually 50% of parenchyma cells, 40% of fiber bundles and 10% of conductive tissues (vascular bundles) (SPOLIDORO, 2008). Theirs nodes have internal diaphragms that, despite being points of tension accumulation, are extremely important to avoid buckling of the tube. The internodes are long, have variable wall thickness and are located between different sets of nodes and diaphragms. These are the ones that explain the significant variations in bamboo

properties, both in the vertical and transverse directions (MISKALO, 2009). Thus, the culms may have different wall thicknesses, heights, diameters (usually regular up to 75% of its height, with later narrowing until the top), growth forms, colors and even odor, varying according to their species (CORREIA, 2014).

Figure 2.2 – Basic structures of the bamboo culm

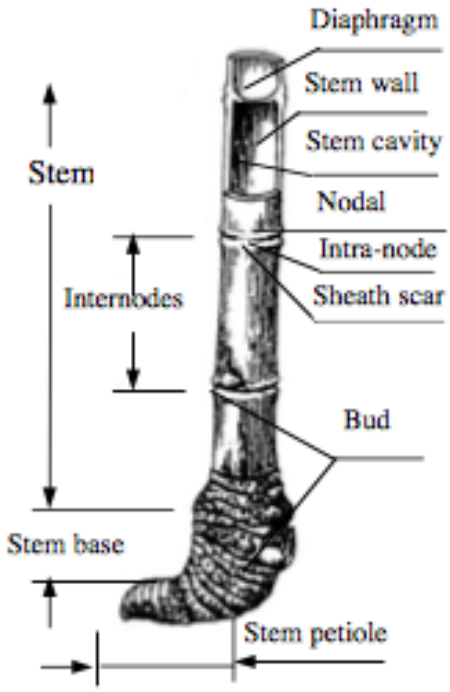

Source: QISHENG, SHENXUE & YONGEJU (2002).

When in adult age, the *Bambusa vulgaris* presents height between 8 to 20 m and external diameter between 5 to 10 cm (MELO, 2016; WAHAB *et al.*, 2012). Studies have shown variations on its characteristics and physical properties according to its age and along the height of the culms. In relation to the physical characteristics, the culms will tapering discreetly and slightly from the middle of the bamboo to the top, decreasing the diameter, the circumference and the thickness of the culm wall (WAHAB *et al.*, 2010; WAHAB *et al.*, 2009). The diameter variations are more expressive with the increment of bamboo age. However, the observed changes in wall thickness from the base to the top are more apparent in the younger bamboos (this thickness along the bamboo tends to equate with the increasing age) (MARINHO, NISGOSKI & MUNIZ, 2014; WAHAB *et al.*, 2010; WAHAB *et al.*, 2009). The internodes length also varies with the height of the culm, increasing from the base to the middle and decreasing from there to the top. With the advancement of the age, maturation

tissues develop and change their density, varying their resistance (MARINHO, NISGOSKI & MUNIZ, 2014; WAHAB *et al.*, 2010).

Bambusa vulgaris presents the highest moisture content (MC), varying with age, height and relative position in the thickness of the culm wall. MC decreases with age, from the base to the ridge and from inside to outside of the culm walls. These variations are related to the anatomical structure (distributions of vascular bundles and parenchymal cells) and the chemical composition presented by the culms with different ages and vertical positions (MARINHO, NISGOSKI & MUNIZ, 2014; WAHAB *et al.*, 2010). Similarly, the basic density of bamboo increases considerably in relation to age and to extension, then remaining constant, with the increase of the internodes position in the culm.

In relation to age, this indicates a greater maturation with the aging of the bamboo; i.e., an increase of fibers and parenchymal cells number, causing, consequently, a higher components concentration by volume (density) and an increase in the average thickness of the culms. Chemically, it can be explained by the deposition of starch and the lignification process that occur in bamboo culms with their maturation (MARINHO, NISGOSKI & MUNIZ, 2014; WAHAB *et al.*, 2010). Starch is the main form of plants energy storage, especially in times of dormancy and germination. The higher concentration of this polysaccharide is probably related to the growth cycle of the plant, since this is its initial energy reserve. The vegetable, when it obtains photosynthetic foliage (during the development), starts to have a new source of energy and the starch is stored, indicating maturation (ALVIN & MURPHY, 1988).

In relation to lignin, a significant statistical variation is usually more evident in the first year of maturation. The various stages of this process are related to the growth stages of the plant, which starts at the base and follows to the top of the culm. This process is different only in relation to the lignin observed in the internodes: lignification occurs from top to bottom and from inside to outside (MARINHO *et al.*, 2012; PEREIRA & BERALDO, 2007).

Concerning the vertical position of the internodes, this density varies because the maturation process begins in the higher internodes, passing to the lower ones. Although maintaining a relatively constant distribution, the density variation can be explained by the higher concentration of fibers. Associated with the decreasing of diameter, circumference and thickness of the culm walls, a higher fiber concentration per space increases the culm density (MARINHO, NISGOSKI & MUNIZ, 2014; WAHAB *et al.*, 2010).

According to previous studies, *Bambusa vulgaris* is considered with a reasonable maturation when it presents age between 2 and 4 years, being considered too young up to 2

years.

In relation to microstructure, bamboo is basically formed by cells and tissues. These elements compose the surface system (epidermis, sub-cutis, cortex), fundamental system (fundamental tissues, medullary rings, medulla) and vascular system. In a general way, the bark (skin) is the surface system of the bamboo, located at the outermost part of the stem, while the medullary rings and medulla, from fundamental systems, are located in the innermost part. Together, those systems form the protective layers of the fundamental tissues and vascular system. Vascular bundles are distributed in wood (green and yellow bamboo), in an inhomogeneous form, among the fundamental tissues (QISHENG, SHENXUE & YONGEJU, 2002).

Fibers are part of the vascular system, together with: i) xylem, which transports water and inorganic salts upwards; ii) phloem, which transports the photosynthesis products down; and iii) parenchymal cells, which perform the photosynthesis. The fibers are elongated and have both pointed ends. Their walls thicken according to the age and present rounded pores (QISHENG, SHENXUE & YONGEJU, 2002). The microstructure of the bamboo fibers can be observed in Figure 2.3.

As it was said before, these fibers are often called natural glass fibers because of their relative high mechanical strength and their low density, as well as raw material cost, making them as good reinforcements subject to stress applications and economically viable (RASSIAH & AHMAD, 2013).

2.4 Fiber/polymeric composites manufacturing

Plastic extrusion and plastic injection processes of fabrication are widely used for the production of many polymeric pieces. For composites, length and distribution of the fibers present a great impact while developing thermoplastic composites using these techniques. Extrusion compounding and injection molding processes are frequently employed to particulate or short fiber reinforced composites (FU, HU & YUE, 1999). This happens because these techniques may reduce significantly the fiber length through breakage, leading in a decrease of the composite strength, modulus and fracture toughness (FU, LAUKE & MAI, 2009).

Figure 2.3 – Fiber in vascular bundles: A. fiber morphology; B. fibers with one year (thinner wall of less layers); C. fibers with several years (thicker wall of more layers)

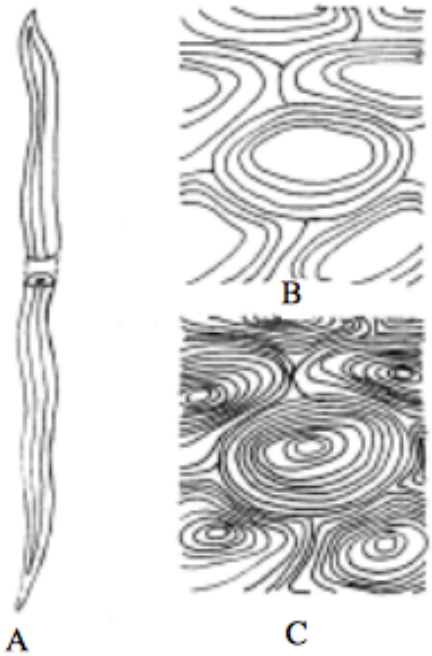

Source: QISHENG, SHENXUE & YONGEJU (2002).

Compression molding is another common technique for manufacturing plastic and polymeric composite products. In this process, the polymeric matrix is placed between two stationary and movable molds, heated to a high temperature coupled with high pressure. Often, preheating time is required to reduce the holding time during the process. The composite subsequently is cooled down to ambient temperature either via rapid cooling (water quenching) or slow cooling (air cooled or naturally) to achieve a solid form. This technique enables the polymeric matrix with loose short fibers, mat or long fibers in random or aligned orientation. The fiber is sandwiched together between the matrix sheet before the heat and pressure is applied. The viscosity of the matrix needs to be properly controlled to ensure that fiber is fully impregnated by the melting matrix (SAPUAN, ISMAIL & ZAINUDIN, 2018). As it was cited, one of its advantages is that the content and type of the fiber can be easily controlled to yield a wide variety of mechanical and physical properties, being considered as an optimal manufacturing option for long and natural fibers composites (PARK & LEE, 2012).

As presented before, there is a great benefit to use long fibers instead of short fibers in thermoplastic composite. Also concerting the techniques cited, extrusion

compounding and injection molding are not appropriated for the fabrication of samples with some controlled microstructures and some orientation of the long fibers – the characterization of fiber/matrix adhesion is one of the objective of this study. Thus, the compression molding appears as the more indicated process for manufacturing the polymeric composite reinforced with natural and long fibers.

2.5 Adhesion between polymeric matrix and natural fibrous reinforcement

One of the remaining challenges for the composites manufacture is to develop the structure-property relationships between fiber/matrix adhesion and composite mechanical properties. It has been known that imperfections of the behavior of composite systems can be associated with imperfect adhesion between materials phases. In other words, poor adhesion usually means also poor composite properties (MADHUKAR & DRZAL, 1991; SIH *et al.*, 1973).

Some works has extended the concept of the fiber-matrix interface, which exists as a two-dimensional boundary between the two surfaces, into a fiber-matrix interphase, that exists in three dimensions region between the two phases (OKHUYSEN *et al.*, 1993; DRZAL, RICH & LLOYD, 1983).

In Finite Element Analysis (FEA), interface is typically modeled in zero dimensional terms, but in practice it is not easy to define the point at which the matrix ceases and the fiber reinforcement begins (JESSON & WATTS, 2012). In this context, the interface may be described as the boundary (contact surface) between two layers of different chemistry and/or microstructure, in this case fiber and matrix. Often, the physical and chemical interactions at the interface provide a structural gradient, providing the adhesion. The presence of a third phase immediately involving the fibers, presenting different properties and/or microstructure in relation to the core of the matrix, is described as interphase (NOHARA *et al.*, 2007; DRZAL, RICH & LLOYD, 1983). This term is widely used to indicate the presence of a chemically or mechanically altered zone between adjacent phases. An interphase zone leads to a gradation of properties from one phase to another, instead of the abrupt change suggested by a two-dimensional interface (JESSON & WATTS, 2012).

Focusing on relatively simple model systems, the properties elucidation of the interface existing between two phases is more efficient when embracing an interlayer or interfacial zone. Generally, the extensive property X of a system, consisting of the phases A and B, can be expressed by Equation 2.1, where A/B is the interphase of the system. The

thickness, and the correspondent amount of X, is a function of where the boundaries are positioned, including all the area that is influenced by the interface (GECKELER, RUPP & GEIS-GERSTORFER, 1997).

$$X = X_A + X_B + X_{A/B}$$ **Equation 2.1**

As observed, an interface might be viewed, in a mathematical sense, as a geometric line in a cross-section, especially when macroscopically viewed. But in most cases, this is not represent the real spatial extension of the transition zone between two phases and the locally occurring phenomena. In order to make the situation more real, it is necessary to examine the interfaces microscopically, which allows a better differentiation between the interphase and the interface. Thus, in cross-section, an expansion from one- to two-dimensional system is required to deal with the change from two to three dimensions in reality (GECKELER, RUPP & GEIS-GERSTORFER, 1997).

This way, the interphase region can be intentionally formed by application or formation of a thin layer of polymer (generally at concentrations less than 1% of the total composite mass), also called as *coating* or *sizing*; or can be spontaneously developed by interactions between the polymeric matrix and the fibers (NOHARA *et al.*, 2007). Figure 2.4 illustrates the interphase region obtained from sizing and the same region created from physical and/or chemical interaction.

Fibers in general (mainly the natural ones) may have morphological variations near the fiber surface which are not present in the bulk of the fiber, including the presence of pores or cracks. For using natural vegetable fibers as reinforcement agent in thermoplastics composites, it is necessary to perform some treatments that can change chemically the fiber surface (DRZAL, RICH & LLOYD, 1983). This way, with a chemically and structurally different region, it is possible to create a compatibility between the fiber and the matrix, so that the interfaces can transmit the part of the applied load from the composite to the fibers (MELO, 2016; JAHAN *et al.*, 2012). When this transfer between the polymeric matrix and the fibrous reinforcement is not effective, the fibers can peel off the matrix easily, may causing the behaving of this continuous phase as a composite defect (MELO, 2016).

Figure 2.4 – Region of the interface (a) obtained by the application of a thin layer of polymer on the fiber surface (*sizing*); and (b) created from nucleation/crystallization obtained from the chemical and/or physical interaction of the matrix with the fiber surface (usually characterized by a "sheath" around the fiber)

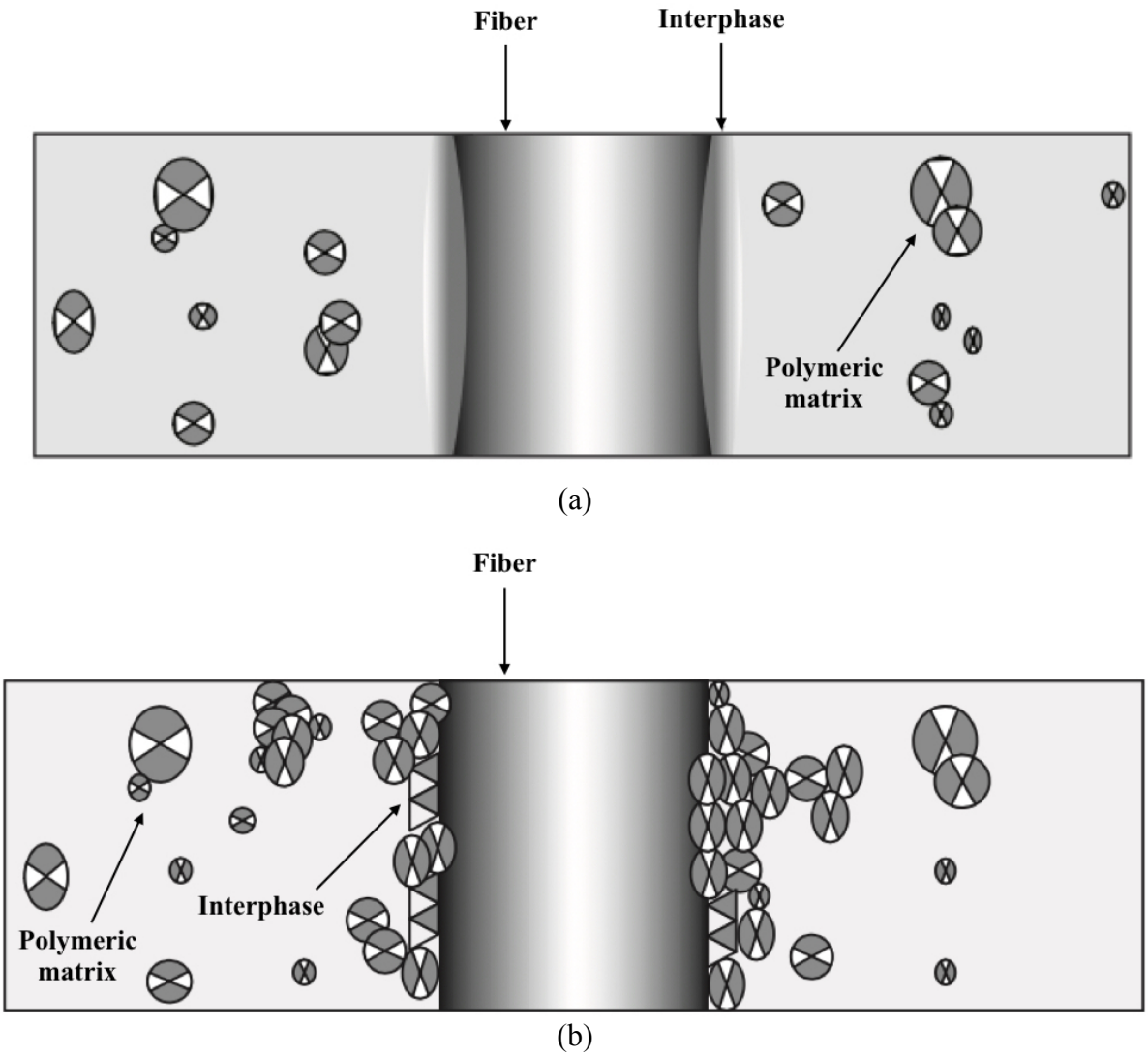

Source: NOHARA *et al.* (2007).

Natural fibers present an inherent surface roughness that was supposed to favor the mechanical interlocking to the wall of the polymeric resin. However, because of their inherently polar and hydrophilic nature, they present a facility in absorbing moisture (in a normal ambient condition, the moisture content of natural fibers can vary between 5 to 10%) (MONTEIRO *et al.*, 2011; JOHN & ANANDJIWALA, 2008; NABI SAHEB, 1999). This can leads to dimensional variations and bad adhesion, resulting in poor mechanical properties and

reducing dimensional stability. Another restriction to perform a durable composite is the low microbial resistance and the rotting susceptibility, which provide problems during shipping, storage and processing (JOHN & ANANDJIWALA, 2008).

Some techniques permit to improve the matrix/fibers adhesion, such as drying the fibers before incorporating them in the matrix. This process can carried out directly, by heating, or indirectly, by solvent exchange method (methanol-benzene) (RAY, CHAKRAVARTY & BANDYOPADHYAY, 1976). Taking out the water of the fiber surface avoids that this acts as a separating agent in contact with the hydrophobic polymer matrix and preserves the molecular organization of the fiber, making it more pliable and hence more suitable for technological processing. Besides that, dried fibers avoid also that the water evaporates from the composite (during its processing), creating unwanted voids in the matrix (JOHN & ANANDJIWALA, 2008; BLEDZKI & GASSAN, 1999; RAY, CHAKRAVARTY & BANDYOPADHYAY, 1976).

Other solution to create a better adhesion is to pretreat the fibers to clean, extract and functionalize the macrostructure of the fibers surface. Some physical and chemical methods can be applied as surface modifiers, resulting in different efficiency in fiber/matrix adhesion (JAHAN *et al.*, 2012; JOHN & ANANDJIWALA, 2008; BLEDZKI & GASSAN, 1999).

2.5.1 Methods for natural fibers surface modification

Modification in natural fibers structures can be made within the core of the fiber or only on its surface, depending on the process applied (type and intensity). However, to maintain the original mechanical properties of the fibers is important to keep the internal fiber structure absent from modifications. This way, it is necessary to define the most efficient treatment (including concentration of solutions, treatment time and temperature) appropriated for each case of study, depending on fiber, matrix and final composite desired properties.

2.5.1.1 Treatments based on physical process

Some treatments, as stretching, calandering, thermotreatment and hybrid yarns production, do not change the chemical composition of the fibers (BLEDZKI & GASSAN, 1999; BLEDZKI, REIHMANE & GASSAN, 1996). Another example is the electric discharge (corona, cold plasma). Corona treatment changes the surface energy of the cellulose fibers and

can increase the amount of aldehyde groups, in case of wood surface activation. Cold plasma treatment promotes the same previous effects. Depending on the type and nature of the gases used, different surface modifications are obtained (introduction of crosslinkings or increase/decrease of energy or production of reactive free radicals and groups) (BLEDZKI & GASSAN, 1999; BLEDZKI, REIHMANE & GASSAN, 1996).

The most important and old physical process of natural fiber modification is mercerization. This alkali treatment leads to fibrillation, reducing the fiber diameter, developing a rough surface topography, increasing the number of possible reactive sites and allowing better balance of adhesion and cohesive forces (KAKROODI *et al.*, 2015; KALIA, KAITH & KAUR, 2009; SREEKALA *et al.*, 2000). Reaction 2.1 presents a general chemical scheme of the natural fibers mercerization.

$$\text{Fiber-OH} + \text{NaOH} \rightarrow \text{Fiber-O}^{-}\text{Na}^{+} + H_2O \qquad \textbf{Reaction 2.1}$$

Mercerization has also an effect on the chemical composition of the fibers, removing hemicellulose and part of lignin, which affects their tensile characteristics. When the hemicellulose is removed, the inter-fibrillar region becomes less dense and less rigid, making the fibrils more capable to rearrange themselves along the direction of tensile deformation by forming new hydrogen bonds. When stretched, such fibrils rearrangements would result in higher stress development in the fiber. Furthermore, the softening of the inter-fibrillar material negatively affects the stress transfer between the fibril and, this way, all the stress development in the fiber under tensile deformation. Further, some authors reported an increase in the percentage crystallinity index of alkali treated natural fibers, as coir, flax, jute and cotton (GASSAN & BLEDZKI, 1999; SREENIVASAN, BHAMA IYER & KRISHNA IYER, 1996; SHARMA *et al.*, 1995; VARMA, VARMA & VARMA, 1984; SHELAT, RADHAKRISHNAN & IYER, 1960; ROY, 1953). This happens because natural fibers derived from plants mainly consist of cellulose, hemicellulose, lignin, pectin and other waxy substances, as shown in Figure 2.5. The outermost part of the fiber is formed for lignin/pectin and hemicellulose (the cementing part) that are partially or completely removed after the mercerization. This leads to a better packing of cellulose chains – the highly crystalline structure which contains as much as 80% of crystalline regions (BHATTCHARYYA, SUBASINGHI & KIM, 2015; BLEDZKI & GASSAN, 1999; GASSAN & BLEDZKI, 1999).

Figure 2.5 – Structure of a plant fiber

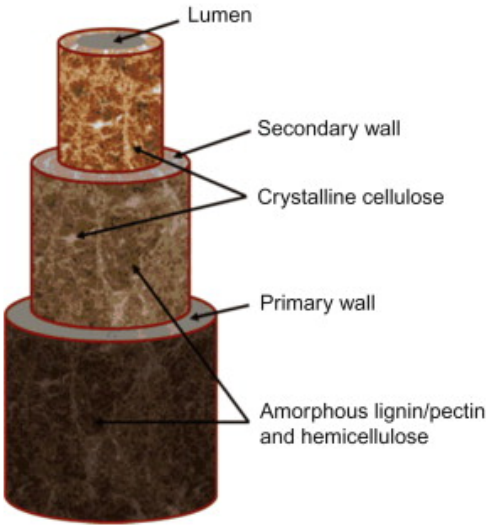

Source: FRIEDRICH & BREUER (2015).

Some studies evaluated the type of the alkali solution concentration, the soaking time for natural fibers and the treatment temperature. The effect of NaOH concentration (0.5 to 30% w/v) revealed that maximum strength resulted from 4 to 5% w/v NaOH treatment (MELO, 2016; VENKATACHALAM *et al.*, 2016; MOHD YUHAZRI *et al.*, 2011; KALIA, KAITH & KAUR, 2009; RODRIGUEZ, STEFANI & VAZQUEZ, 2007; MISHRA *et al.*, 2002; RAY *et* al., 2001; MORRISON *et al.*, 2000; SREEKALA *et* al., 2000). This is due to the fact that, for small concentrations of alkali, the diameter of the hydrated ions is too large to penetrate into the macromolecular structure of vegetable fibers. As the concentration increases, the number of water molecules available for the formation of hydrates decreases and, thus, hydrated ion pairs are capable to penetrate into the fiber structure of cellulose, forming hydrogen bonds with the molecular chains of cellulose (KARMAKAR, 1999). That is, low concentrations allow the alkaline solution to act only on the fiber surface.

According to the soaking time, its prolongation period can increase the weight loss, resulting in the damage of fiber surface, indicated by the removal of inter and intracellular non-cellulosic substances. Additionally, the mercerization leads to a decrease in spiral angle (closer to fiber axis) and in molecular orientation – a fair amount of randomness is introduced on the orientation of the crystallites due to the removal of non-cellulosic matter. These factors can confer greater flexibility on the elements, allowing for the increase of slippage and readjustment that could enhance fiber elongation (SREENIVASAN, IYER & IYER, 1996). As a way to spend less time in solution, approximately 1 h, it is suggested that

the solution in 4 to 5 % w/v NaOH solution occurs with light heating, around 60 to 65 °C (MELO, 2016; RODRIGUEZ, STEFANI & VAZQUEZ, 2007; RAY *et* al., 2001; MORRISON *et al.*, 2000; SREEKALA *et* al., 2000).

2.5.1.2 Treatments based on chemical process

As observed before, natural fibers are amenable to chemical modifications as they present hydroxyl groups from their constituents – strongly polarized cellulose fibers. These groups are involved in the hydrogen bonding within the cellulose molecules thereby reducing the adhesion towards the hydrophobic polymeric matrix (SREEKALA *et al.*, 2000; BLEDZKI & GASSAN, 1999). Chemical modifications can activate the hydroxyl groups or introduce a third compound, with intermediate properties, that facilitate the connection between fibers and matrix without stress concentration at the interface (JOHN & ANANDJIWALA, 2008; SREEKALA *et al.*, 2000; BLEDZKI & GASSAN, 1999; BLEDZKI, REIHMANE & GASSAN, 1996). The most common examples of chemical treatments for fibers modification are acrylation, acetylation, etherification, benzoylation and silane reaction (MONTEIRO *et al.*, 2011; KALIA, KAITH & KAUR, 2009; LI, TABIL & PANIGRAHI, 2007).

Among these, the acetylation is a well-known esterification method causing plasticization of cellulosic fibers. The reaction is originally applied to wood cellulose to stabilize the cell walls against the moisture, improving dimensional stability and environmental degradation. The modification with acetic acid and acetic anhydride substitutes the hydroxyl groups of the cell wall with acetyl groups, modifying the properties of the fibers, becoming hydrophobic (HILL, ABDUL KHALIL & HALE, 1998). The acetic anhydride is more reactive and give better yields of product than acetic acid. The function of this acid is to swell the fiber, since acetic anhydride is not a good swelling agent for cellulose. In other words, the use of acetic acid is to facilitate the accessibility of the fiber hydroxyl groups to the acetylating agents, and to dissolve the acetylated products, allowing the progress of the reaction (ONYLKWERE, IGBOANUGO & ADELEKE, 2019; DIHARJO *et al.*, 2017; JOHN & ANANDJIWALA, 2008). The individual acetylation reaction can be observed using acetic acid and acetic anhydride in Reactions 2.2 and 2.3, respectively.

$$\text{Fiber-OH} + CH_3\text{-C(=O)-OH} \rightarrow \text{Fiber-OCO}CH_3 + H_2O \qquad \textbf{Reaction 2.2}$$

$$\text{Fiber-OH} + CH_3\text{-C(=O)-O-C(=O)-}CH_3 \rightarrow \text{Fiber-OCO}CH_3 + CH_3COOH \qquad \textbf{Reaction 2.3}$$

The complete procedure includes an alkaline treatment initially, followed by acetylation. This solution is suggested to be prepared with the both cited reagents, catalyzed by some drops of sulphuric acid, and the reaction presented efficiency at 100 °C for 1 h (MELO, 2016; KALIA, KAITH & KAUR, 2009; BLEDZKI & GASSA, 1999; HILL, KHALIL & HALE, 1998).

2.6 Failure mechanisms in composites

During the utilization of a composite material, it can be subjected to various types of stresses, giving rise to complex mechanisms which reduce the stiffness and the strength of the material, and determine its lifetime with various types of fracture (REIFSNIDER, 1982). The failure mechanisms start at plastic micro deformations. In a polymeric material, this process initiates with the breaking of bonds that composes the molecular chains and continues with the formation and propagation of cracks, intrinsic discontinuities, residual stresses, and formation and propagation of crazes (RIOS, 2015).

Conventional fracture mechanics methodology assumes a dominant crack that grows in a self-similar aspect, increasing in size (stable or unstable growth) but maintaining its shape and orientation. However, a fiber-matrix composite fracture is often controlled by numerous microcraks distributed throughout the material (ANDERSON, 2005). The type and form of fiber-matrix composite failure can be influenced by accumulation of defects in a certain area or due to stress concentrations, such as porosity, geometry changes, inclusions, etc; or by some others factors, such as type and direction of the applied load, physical, chemical and mechanical properties of the fibers and the matrix, manufacturing process, composite material configuration, fiber percentage, absorbed moisture, working temperature and obtained interface/interphase (RIOS, 2015; BARROS, 2006).

Due to the wide variety of factors it is extremely difficult to predict where and how a failure is formed as well as how it is propagated in a composite material. Studies show that even varying only one of the factors mentioned above, there will be significant variations on the formation and propagation of the failure (BARROS, 2006; HULL & CLYNE, 1987). Even so, comparing with materials in general, one advantage of composite materials is that fracture seldom occurs catastrophically without warning, but tends to be progressive, dispersing subcritical failure through the material (ANDERSON, 2005).

Figure 2.6 illustrates various failure mechanisms in general fiber-reinforced composites. In plane, tensile loadings can produce fiber pull-out, fiber bridging, fiber/matrix

debonding, fiber rupture and matrix cracking (ANDERSON, 2005).

Figure 2.6 – Examples of failure and fracture mechanisms in fiber-reinforced composites

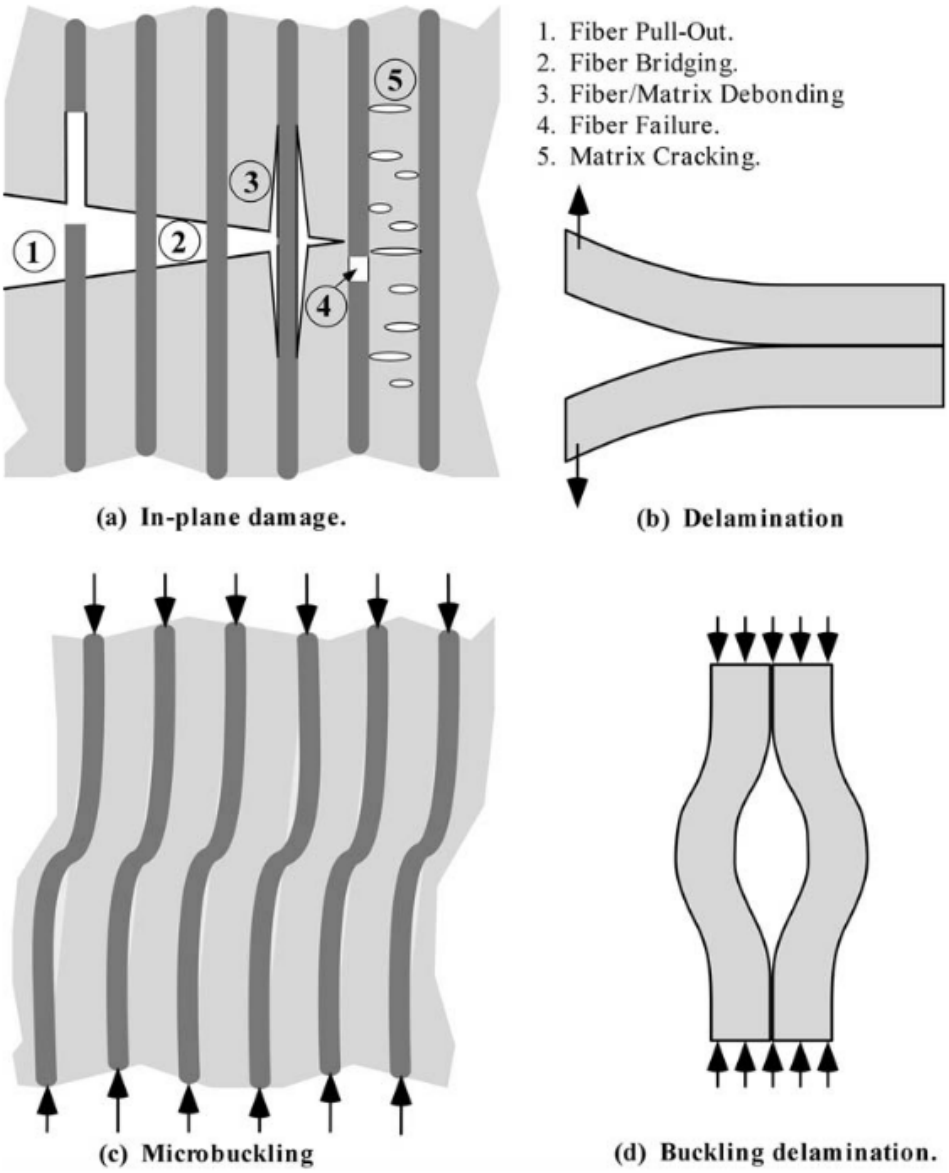

Source: ANDERSON (2005).

The fiber pull-out (1) occurs when fragile fibers or discontinuous fibers are embedded in a high strength matrix or also when the performed interface/interphase are not so good, maybe because of the inefficient fiber treatment or the absence of roughness (GOMES, 2015; BARROS, 2006; ANDERSON, 2005). The fibers fracture results in a local stress concentration where the fiber has been broken. This stress concentration can be relieved, since the release of the fiber to matrix occurs, preventing it from breaking. At this situation, the

fibers are pulled-out from within the matrix (GOMES, 2015; AGARWAL, BROUTMAN & CHANDRASHEKHARA, 2006).

The formation of fiber bridging (2) is a type of debonding between fiber and matrix, but in some way can contribute to improve the matrix resistance – in some instances, the crack grows around a fiber, which then bridges the crack faces and adds resistance to further crack growth (AGARWAL, BROUTMAN & CHANDRASHEKHARA, 2006; BARROS, 2006; ANDERSON, 2005).

The fiber/matrix debonding (3) occurs when the crack in the matrix is unable to propagate through the fiber, without an extensive deformation of the matrix. This debonding is possible caused by an adhesive fracture, suggesting a bad interface/interphase formation between fiber and matrix (GOMES, 2015; AGARWAL, BROUTMAN & CHANDRASHEKHARA, 2006; BARROS, 2006; ANDERSON, 2005).

The fibers failure (4) – Figure 2.6a – occurs when the crack propagates in the normal direction of the fibers, eventually promoting the transverse or longitudinal rupture of the fiber (fiber cohesive fracture), without necessarily forming cracks on the matrix (GOMES, 2015; AGARWAL, BROUTMAN & CHANDRASHEKHARA, 2006; BARROS, 2006; ANDERSON, 2005). This occurs over tensile loading, when the maximum allowable stress or deformation of the fiber is exceeded. Although the fibers are responsible for the mechanical strength of the composite, the fiber fracture represents a very low energy percentage to the amount of energy absorbed by the composite material. However, the presence of the fibers influences the flow mode of the composite and, consequently, the total energy absorbed after impact (GOMES, 2015; AGARWAL, BROUTMAN & CHANDRASHEKHARA, 2006).

In matrix cracking (5) – Figure 2.6a –, one or more cracks occur in the dispersed phase of the composite material (matrix cohesive fracture) (BARROS, 2006; ANDERSON, 2005). The cracks nucleation occurs in a highly stressed region of the composite, either by the effect of a temporary overload or by the presence of stress concentrators such as inclusions, porosity, notches or surface defects from processing. After reaching a certain size, the crack is oriented perpendicularly to the direction of the load. As a consequence of stress concentration, a plastic zone is formed at the crack tip vicinity. This causes a small crack opening and, consequently, its propagation (SPILLER, 2012).

The propagation of a crack by a matrix can stop when it reaches fibers of an adjacent layer. Because of the high shear stresses adjacent to the crack crest, the crack can be split and propagate parallel to the plane of layers. These out of plane cracks are called delamination cracks (Figure 2.6b). This often occurs when laminates are flexed (GOMES,

2015; AGARWAL, BROUTMAN & CHANDRASHEKHARA, 2006; ANDERSON, 2005).

Compressive loading can produce the microbuckling of fibers (Figure 2.6c) – the polymer matrix is soft compared to the fibers, being these ones unstable in compression. If the material contains a preexisting delaminated region, compressive load can also lead to macroscopic delamination bucking (ANDERSON, 2005).

3 MATERIALS AND EXPERIMENTAL PROCEDURES

This chapter presents a description of the materials used at this study and the experimental procedures performed. The processes of obtaining, treating and characterizing physico-chemically, morphologically and mechanically the natural fibers were carried out at laboratories of *Universidade Federal do Cear* (Brazil) and of *École Normale Supérieure de Cachan – Université Paris-Saclay* (France). The manufacture of the composites and their characterization also were carried out at laboratories of the previous cited universities.

Manufacturing and testing procedures followed international standards or successful literature references, providing repeatability and reproducibility.

3.1 Constituents of the green polymeric composites

3.1.1 Green high density polyethylene

The choice of the polymer matrix of the composite is a crucial point for the development of a new product. Considering the informations about the types of PE and concerning the green polymers, the material used at this work was the green high density polyethylene, just called here as PEg. This thermoplastic is produced at Triunfo's Petrochemical Pole by Braskem S.A., in Rio Grande do Sul (RS)/Brazil, in a plant with a capacity for product 200 thousands tons per year. The grade used was SHA7260 and some typical properties are given in Table 3.1. It has been certified by renowned laboratories and international organizations (see Appendix A) with the *I'm green*™ label, which guarantees the use of the ethanol sugarcane as raw material for its production.

This resin presents a good flowability, is easy processed and has a high productivity, stiffness, strength and hardness. Its narrow distribution of molar mass results in a low bending tendency. This grade has a minimum renewable source content of 94% as determined by ASTM D6866 – *Standard Test Methods for Determining the Biobased Content of Solid, Liquid, and Gaseous Samples Using Radiocarbon Analysis.*

3.1.2 Bamboo fibers

The bamboo plants were cultivated at a bamboo plantation in *Campus do Pici* at the *Universidade Federal do Cear* , located in Fortaleza/Ceará (CE)/Brazil (Figure 3.1a). The bamboo used was *Bambusa vulgaris*, a significant example from tropical and subtropical climates. For the fibers production, the bamboo sticks were picked up at maturity with age between 3 and 6 years, because in this period they reach high resistance due to the complete lignification process.

Table 3.1 – Typical properties for the PEg used (grade SHA7260)

Typical properties	SHA7260
Flow rate (190 °C/2.16 kg) (g/10 min)	20
Density (g/cm^3)	0.955
Yield stress (MPa)	29
Rupture stress (MPa)	25
Flexural modulus (MPa)	1150
Toughness (Shore D)	60
Softening temperature Vicat (°C)	121
Thermal deflection temperature (0.45 MPa) (°C)	67

Source: BRASKEM, 201-?a.

The fibers are obtained from culms (or stems) of the bamboo after several manufacturing and treating steps. These can be divided in two main steps, namely i) mechanical based operations in order to extract fibers from the stem, and ii) physical and chemical treatments to stabilize the microstructure and to obtain the desired properties.

3.1.2.1 Mechanical operations

1. Cutting: After the plant harvest and the elimination of the leafs, the stems were cut in several parts between the nodes (Figure 3.1b). The internode rods obtained presented almost the same height and a regular diameter (the stem usually has a regular diameter up to 75% of its height, narrowing until the top). Their walls were laminated manually and in the longitudinal direction, removing their barks (skin) (Figure 3.1c, at the left part). From each internode, a cross longitudinal cut was made to facilitate the next

steps. Then, each smaller piece was manually and longitudinally cut at the outermost part (Figure 3.1c, at the right part), to obtain thinner laminas containing lots of fibers.

2. Defibration: This process was carried out manually and in the longitudinal direction, with the aid of a household knife. The defibration was performed on the peeled part, where it presented a greater amount of visible fibers (Figure 3.1d).
3. Sizing and separation: With the previous steps, the fibers showed a great cross section variation. As fibers have small dimensions, any variations in cross section present significant changes in their microstructures. Smaller cross sections present lower density of defects/flaws/irregularities, both in the surface and inside the volume of the fibers, tending to be more homogeneous than thicker ones (MONTEIRO *et al.,* 2010). Thus, to separate fibers having nearly the same thickness, the fibers were passed through circular holes of different sizes and ranged in three groups: fibers crossing holes between 0.3 and 1.0 mm (BF0110), 1.0 and 1.5 mm (BF1015), and 1.5 and 2.0 mm (BF1520), respectively. As these materials present small dimensions, little variations tend to result in significant variation in their properties.

3.1.2.2 Physical and chemical treatments

After sizing and separation processes, the fibers passed through some treatments in order to make its surface more propitious to adhesion with the polymeric matrix.

Reagents used

Different reagents were used in analytical grade and had not passed for any previous purification, being used directly as purchased.

1. Sodium hydroxide (NaOH), also known as caustic soda, is a strong base common used in the textile industry, giving to cotton yarns and fabrics, a shiny and silky appearance, greater color absorption and strength. The mercerization removes the surface lignin through cleavage of alkaline ether bonds which may be accompanied by condensation reactions. It was shown that the rate of the lignin to be removed is directly proportional to the concentration of the alkaline solution (MELO, 2016; KALIA, KAITH & KAUR, 2009; BECKERMANN & PICKERING, 2008; HUDA *et al.*, 2008);

Figure 3.1 – Steps for bamboo fibers extraction

(a) (b)

(c) (d)

Source: Author; MELO, 2016.

2. Ethanoic anhydride ($C_4H_6O_3$), better known as acetic anhydride, is one of the simplest acid anhydrides and is widely used as a reagent in organic synthesis. It is widely used as dehydration and acetylation agent in the synthesis of organic products for the chemical and pharmaceutical industry (NATIONAL CENTER FOR BIOTECHNOLOGY INFORMATION, 201-?a);
3. Ethanoic acid (CH_3COOH), more popular known as acetic acid, is a saturated and open-chain weak carboxylic acid. It is corrosive with vapors that causes eye irritation, burning of the nose and throat, and pulmonary congestion (NATIONAL CENTER FOR BIOTECHNOLOGY INFORMATION, 201-?b). Along with the acetic anhydride, it is used to prepare the acetylation solution. This one stabilizes the cell

walls against moisture, improving dimensional stability and reducing the environmental degradation (KALIA, KAITH & KAUR, 2009).

4. Sulfuric acid (H_2SO_4) is a viscous and liquid acid, colorless, odorless and soluble in water, producing a highly exothermic reaction (National Center of Biotechnology Information, 201-?c). This acid used in a variety of processes in the chemical industry, is used even as catalyst. Thus, it increases the reaction speed and decreases the activation energy. The reactions should be conducted at a moderately elevated temperature, increasing the reaction rate (KALIA, KAITH & KAUR, 2009). The acetylation process is based on the reaction of cell wall hydroxyl groups of lignocellulosic materials, but without the use of a good catalyst, as H_2SO_4, only the easily accessible hydroxyl groups react (BLEDZKI & GASSAN, 1999).

Treatments of bamboo fibers

Figure 3.2 illustrates a flowchart of the treatments performed on the rough fibers obtained after the mechanical operations and their conditions are detailed below according to the resulting fibers.

The fibers were weighed before and after complete treatment in order to evaluate any mass loss. To determine the mass variation, the following expression was used:

$$m_{variation}(\%) = \frac{m_i - m_f}{m_i}.100 \qquad \textbf{Equation 3.1}$$

Where m_i is the initial BF mass; and m_f is the mass of the wet BF immediately after treatment.

The procedures were carried out at Laboratory of Mechanics of Fracture and Fatigue – *Laboratório de Mecânica da Fratura e Fadiga* (LAMEFF) – from *Universidade Federal do Cear* (Brazil).

a) Without treatment (WT)

The fibers were used in the form that they were obtained, without washing and/or drying. These bamboo fibers without treatment (BF_WT) were used as reference fibers to be compared with the other treatments performed.

For both untreated and treated fibers, the empty space at the nomenclature refers to the dimensions of the fibers used (0.1 to 1.0, 1.0 to 1.5 and 1.5 to 2.0 cm).

b) Treatment A (TA)

The bamboo fibers were completely immersed in water and dried. This treatment, called Treatment A, was performed to do an initial and a superficial cleaning of the fibers, removing some contaminants and adhering dirt (VENKATACHALAM *et al.*, 2016). As it was explained, natural fibers presents an inherently polar and hydrophilic nature, presenting a facility in absorbing moisture. In order to solubilize the part of the fiber that stores water (pectin, some polysaccharides, as starch, and any other polar residue), the first part of the treatment consisted in immersing the fibers in water at room temperature (~ 25 °C) for 2 hours. This period was defined according to some studies to guarantee a water absorption of more than 50 %. Bamboo fibers presented water absorption of about 73.2 % after 2 h (MELO, 2016). This way, by removing, in the second part of the treatment, the water-absorbing compounds, it was possible to reduce a few the sensitivity of the fibers to moisture.

The nomenclature for the BF after this treatment was BF_TA.

c) Treatment B (TB)

The bamboo fibers were immersed in water, than boiled and dried. This treatment, although more intense than the previous one, was performed only for a superficial cleaning, melting the wax present in the fiber (VENKATACHALAM *et al.*, 2016). The treatment started with the prior procedure (immersion of the fibers in water at room temperature), followed by the fibers immersion in boiling water at 100 °C for 1 hour. Then, they were dried at the same conditions used before (100 °C for 40 min).

The nomenclature for the BF after this treatment was BF_TB.

d) Treatment C (TC)

The previous treatment was performed until the boiled step. Posteriorly, the fibers were immersed in a 5% w/v NaOH solution, ensuring a sufficient volume for a complete fibers immersion (maximum of 20 g for 100 mL). This step was accomplished at 60 - 65 °C for 1 hour. These conditions were adopted considering the best parameters, including soaking

time, temperature and concentration according the subsection 2.4.1.1. After the mercerization, the fibers were soaked in water for 15 min with – at least – four water changes, in order to ensure the complete removal of the alkaline solution. Then, they were dried at the same conditions used before (100 °C for 40 min).

The nomenclature for the BF after this treatment was BF_TC.

e) Treatment D (TD)

The aforementioned steps were carried out until removal of the alkaline solution. After this, an acetylation solution was prepared: $C_4H_6O_3$ and CH_3COOH (3:2 in volume) with 7 drops of H_2SO_4 for each 250 mL of solution. The fibers were completely immersed at 100 °C for 1 hour (maximum of 10 g for 100 mL). These conditions were adopted on the basis of the subsection 2.4.1.2. After the acetylation, the fibers were soaked in water for 15 min with, at least, 4 water changes in order to ensure the complete removal of the acid solution. Then, they were dried at the same conditions used before (100 °C for 40 min).

The nomenclature for the BF after this treatment was BF_TD.

3.2 Manufacturing of the composite plates

The confection process used in this study was compression molding, with controlled pressure and temperature.

A specific mold has been designed to shape composite plates. The mold was made of two parts. The bottom part was made of a plate with grooves on which bars were screwed to obtain a cavity. The grooves permitted a good alignment of the bars and a good sealing to avoid the molten and high pressed matrix to scape. The upper part was a top cover plate that was partially inserted in the previous part to create the slab of the mold. It was equipped with positioning screws to insure a controlled thickness of the plate shaped during the compression molding and high parallelisms between both sides of the plate. This means that if, initially, a given pressure was applied to the molt, depending on the content of the raw material, a part of the load was transmitted by the screw if there was some matrix leak between the two parts.

The size of the sample plates (x = 180 mm, y = 210 mm) was designed knowing the maximum force of the press, the space available in the press frame and the maximum pressure to apply to the sample. The thickness range of the plate that can be shaped was, approximately, 2 to 4 mm.

Figure 3.2 – Flowchart of thermal and chemical treatments applied to bamboo fibers

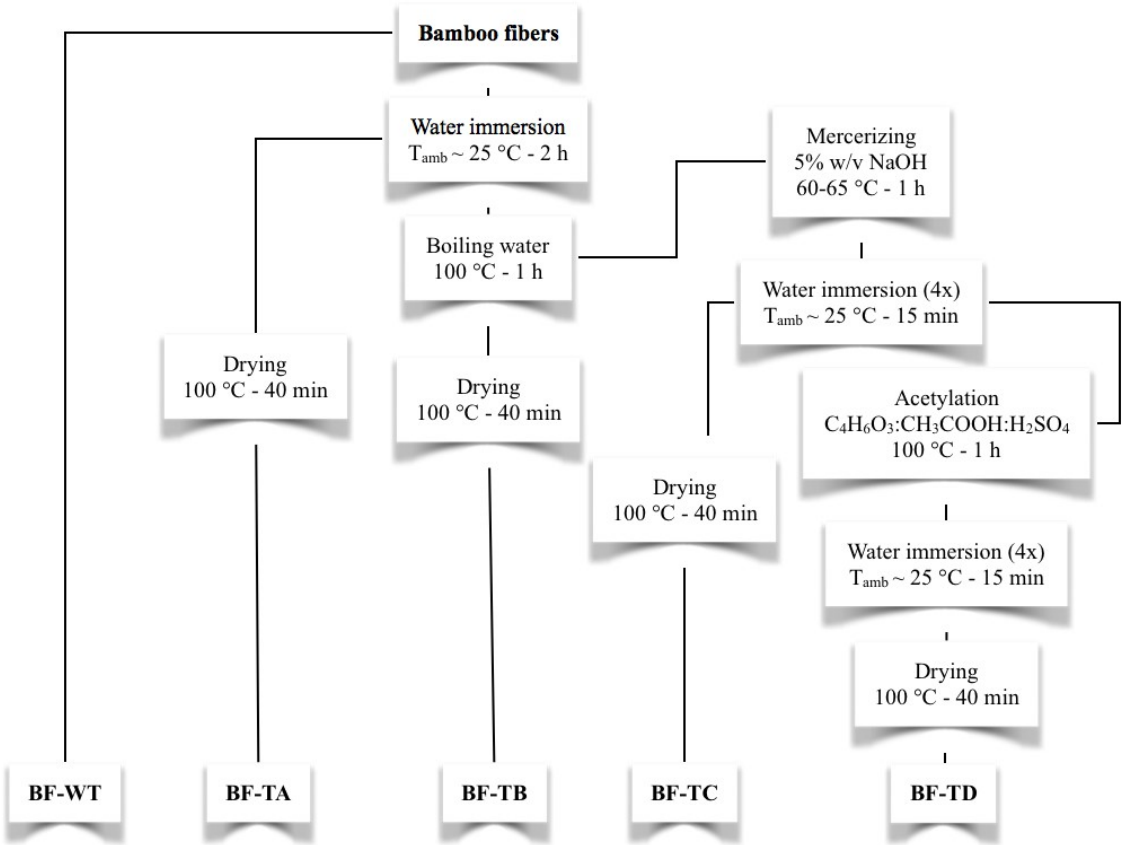

Source: Author.

3.2.1 Preparation of pure PEg plate

Knowing the bulk density of the resin, ρ_{PEg} = 0.955 g/cm^3 (Table 3.2), and the useful volume of the mold for a plate sample of 4-mm size, V_{mold} = 151.2 cm^3, the mass of green high density polyethylene (PEg) used to prepare the PEg plate was calculated to be 144.40 g.

The preparation of the mold started with the coating of the bottom and top surfaces of the mold, using an adhesive film that do not adhere to the polymer during the melting. After this, the elements of the bottom part were assembled and the PEg, in format of pellets, was spread out into the cavity, Figure 3.3. Finally, the mold was closed with the top cover plate.

The heating and pressing operations were made in a compression molding and heating press LabPro TP 1000 from Fontijne Presses (old Fontune Presses) – Figure 3.4. This press was made of 2 columns press frame. The upper platen (500 x 500 mm) was fixed and the lower platen was movable allowing to apply a force between 30 and 1000 kN. Both platen

can be heated up to 300 °C with a controlled heating rate. The temperature distribution was uniform over the full surface of the platens when they were in contact. A digital controller allows to program a complex history of both force and temperature allowing to reproduce the manufacturing process. For each increment of temperature, a dwell time was define so that the temperature inside the mold could be equated to its surface temperature. The manufacturer ensure a precise force and temperature distribution, over the full platen surface.

Figure 3.3 – Preparation of the mold for PEg plate: PEg pellets inside the mold

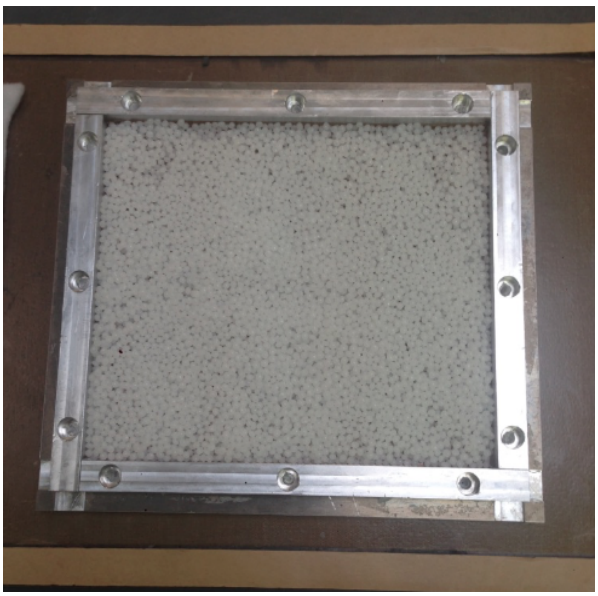

Source: Author.

The polymeric plates were produced in several steps:

- The first step consisted to apply a load of 30 kN at room temperature (~ 25 °C) and a load of 30 kN on the mold, corresponding to a pressure of 0.12 MPa. That was the minimum load applicable to guarantee a good and uniform contact between the mold and the platen and a pre-pressure to the components introduced in the mold cavity;
- The second step consisted in heating the mold/sample. The final temperature to reach in the material was 160 °C. First the apparatus was heated in 10 min from room temperature to 125 °C (temperature defined by the thermocouple of the press fixed on one platen). After a dwell time of 10 min, the temperature in the material was considered as uniform and constant. Then the temperature was raised up to in a period of 5 min and maintained at this temperature for 15 min;
- The third step begin with the unloading and followed by a heat dissipation process of

the mold/sample for 30 to 40 min – the apparatus was maintained inside the press to guarantee a slow cooling, with application of artificial cooling using running water, at approximately 20 °C, as the press coolant;

- The fourth step consisted in remove the cooler mold from the press and allow it, in a suitable place, for cooling to room temperature. This process occurred for another 30 to 40 min until the extraction of the produced piece.

Figure 3.4 – Compression molding and heating press LabPro TP 1000 from Fontijne Presses

Source: Author.

According to values observed in studies for PEg differential scanning calorimetry (DSC) analysis, for the SHA7260 grade, the melting temperature starts at, approximately, 126 °C, presenting the peak of crystalline melting temperature (T_m) at 136 °C and the peak of crystallization temperature (T_c) at 115 °C (ARAUJO *et al.*, 2016; OLIVEIRA, 2015). One of the studies also presented that the temperature increase of consecutive material processing (10 in total) had few influence on melting and crystallization temperature (processing at 180 °C presented T_m =133 °C and T_c =114 °C and processing at 220 °C had T_m =136 °C and T_c = 114 °C) (ARAUJO *et al.*, 2016). This way, it can be ensured that there was sufficient time for plasticization of the piece produced prior to its extraction. Table 3.2 shows a resume of the process steps performed.

Table 3.2 – Conditions for the PEg plate preparation

Step	Process	Conditions
0	Preparation	t_0 = 0 min T_0 = 25 °C (ambient) P_0 = 0 kN
1	Heating ($Tset_1$ = 125 °C) and pressuring	t_1 = 0 min T_1 = 25 °C (ambient) P_1 = 30 kN
2		t_2 = 5 min T_2 = 80 to 110 °C P_2 = 30 kN
3		t_3 = 10 min T_3 = 120 to 130 °C P_3 = 30 kN
4		t_4 = 20 min T_4 = 125 °C P_4 = 30 kN
5	Heating ($Tset_2$ = 160 °C) and pressuring	t_5 = 25 min T_5 = 140 to 165 °C P_5 = 30 kN
6		t_6 = 40 min T_6 = 160 °C P_6 = 30 kN
7	Cooling, without pressure	t_7 = 80 min T_7 = 60 to 70 °C P_7 = 0 kN
8	Extraction	t_8 = 120 min T_8 = 25 °C (ambient) P_8 = 0 kN

Source: Author.

The produced plate was named PEg. During the compression molding of the plate, material was lost as the resin is highly flowable and the seal at high temperature difficult to guarantee. The final thickness of the plate was 2.5 mm (e_{PEg} = 2.5 mm).

This procedure was carried out at Laboratory of Mechanics and Technology – *Laboratoire de Mécanique et Technologie* (LMT) – from Paris-Saclay University (France).

3.2.2 Processing of composites plates

The manufacture of homogeneous plates of composites faces some difficulties. One problem is to ensure that each fiber is embedded in the polymer matrix. This condition is satisfied in the core of the plate. But close to the interface plate/mold, it is not the case as revealed by the preliminary tests. Consequently, it was decided to deposit the BF between two

thin plates of pure PEg, so that, during the melting, the fibers are entirely embedded by resin. This technique can be used as the properties of the resin is not modified by the second heating of the matter, as cited in previous subsection.

The objective was to manufacture BF reinforcing PEg with content of fibers between 10 to 15% in volume and different alignments. The volume fraction was defined according to previous experiences between both materials in order to keep the fibers preferably within the matrix. This amount of fibers was defined to provide efficient reinforcement to the composite and to avoid its presence on the surface. Being completely surrounded by the polymeric matrix, the fibers are protected from moisture, not affecting the properties of the composite as well as the useful life of the final product.

To facilitate the production process, the procedure was divided in different steps:

- Preparation of pure PEg plates with approximately 1 mm thick;
- Preparation of a thin layer of BF impregnated with PEg in order to promote a better align of the fibers (the weight of the fibers is chosen depending on the volumetric content desired);
- Assembly of the composites constituents by layering the impregnated fibers layer between the two PEg plates;
- Temperature and pressure treatment to obtain the composite (parameters similar for the production plates).

Taking into account the desired thickness of the composite, the useful volume of the mold, the density of the polymer (Table 3.2), the density of the fiber (Table 2.3) and the required percentage of reinforcement, the mass of PEg and the mass of BF required to produce the polymeric composite can be calculated.

Attention was paid to the fact that during the pressing at high temperature some resin was lost due to the leakage. This was estimated by measuring the weight of the plate after shaping and comparing with the weight of the components (mass of the two PEg plates and mass of the impregnated BF layer).

Several types of composites were manufactured changing the treatments, fiber dimensions and alignments in order to determine the best parameters. The fibers were arranged according above informations:

- Unidirectional and continuously (0 or 45°), with long fibers oriented in same direction of a mechanical request (0°) or with 45° deviation of the same request. For reinforcement in 0°, the nomenclature for this composite is formed by PEg/BF_ _,

being the first empty space referred to the fibers dimensions (0.1 to 1.0 and 1.0 to 1.5 cm) and the second one referred to the performed treatment (WT, TA, TB, TC and TD). In case of the composite with reinforcement in 45°, this information is aded at the nomenclature, PEg/BF0110WT%;

- Bidirectional and continuously (0 and 90°), with long fibers oriented in direction of a mechanical request (0°) and in perpendicular direction of the same request (90°). The nomenclature for this composite is PEg/BF0110WT#;
- Random and discontinuously, with short fibers cut to 5 mm and arranged without orientation. The nomenclature for this composite is PEg/BF0110WTR;
- Unidirectional and continuously in braids (0°), with braided long fibers bundles (3 or 4 fibers per strand) and oriented in same direction of a mechanical request (0°). The nomenclature for this composite is PEg/BF0110WTX.

After this, the preparation of the composite consisted in put one of the plates into the mold cavity, followed by impregnated fibers and, finally, by the second plate. Another informations about the polymeric composites performed can be observed at Table 3.3 and Figure 3.5.

Table 3.3 – Data for the composite processing

Composite	$m_{PEgplate1}$	$m_{PEgplate2}$	$m_{PEglaminate}$	m_{fiber}	$\%_{fibers}$ (v/v)	$e_{composite_real}$	Fiber direction
PEg/BF0110WT	36.13 g	36.72 g	14.10 g	6.22 g	10.3%	2.88 mm	U (0°),C
PEg/BF0110TA	38.59 g	38.14 g	14.10 g	6.09 g	9.8%	3.00 mm	U (0°),C
PEg/BF0110TB	38.67 g	38.06 g	15.82 g	6.04 g	9.2%	2.67 mm	U (0°),C
PEg/BF0110TC	38.35 g	37.62 g	14.74 g	5.89 g	9.4%	2.51 mm	U (0°),C
PEg/BF0110TD	37.61 g	37.18 g	14.12 g	6.00 g	10.0%	2.40 mm	U (0°),C
PEg/BF1015WT	38.38 g	33.93 g	14.03 g	6.07 g	10.6%	3.20 mm	U (0°),C
PEg/BF1015TC	38.61 g	38.19 g	14.05 g	6.07 g	10.7%	2.68 mm	U (0°),C
PEg/BF0110WT%	34.37 g	33.82 g	14.04 g	6.10 g	10.8%	2.68 mm	U (45°),C
PEg/BF0110WTX	34.78 g	34.92 g	14.19 g	6.06 g	11.6%	2.58 mm	U (0°),X
PEg/BF0110WTR	35.25 g	33.95 g	14.03 g	6.14 g	11.1%	3.00 mm	R,D
PEg/BF0110WT#	37.42 g	36.99 g	14.19 g	6.26 g	10.5%	2.50 mm	B,C

U: unidirectionally (0 or 45 or 90°); B: bidirectionally (0 and 90°); R: randomly; C: continuously; D: discontinuously; X: in braids.
Source: Author.

Figure 3.5 – Schemes for the BF arrangement according to the fiber direction: (a) U (0°), C; (b) U (45°), C; (c) U (0°), X; (d) R, D; and (e) B, C

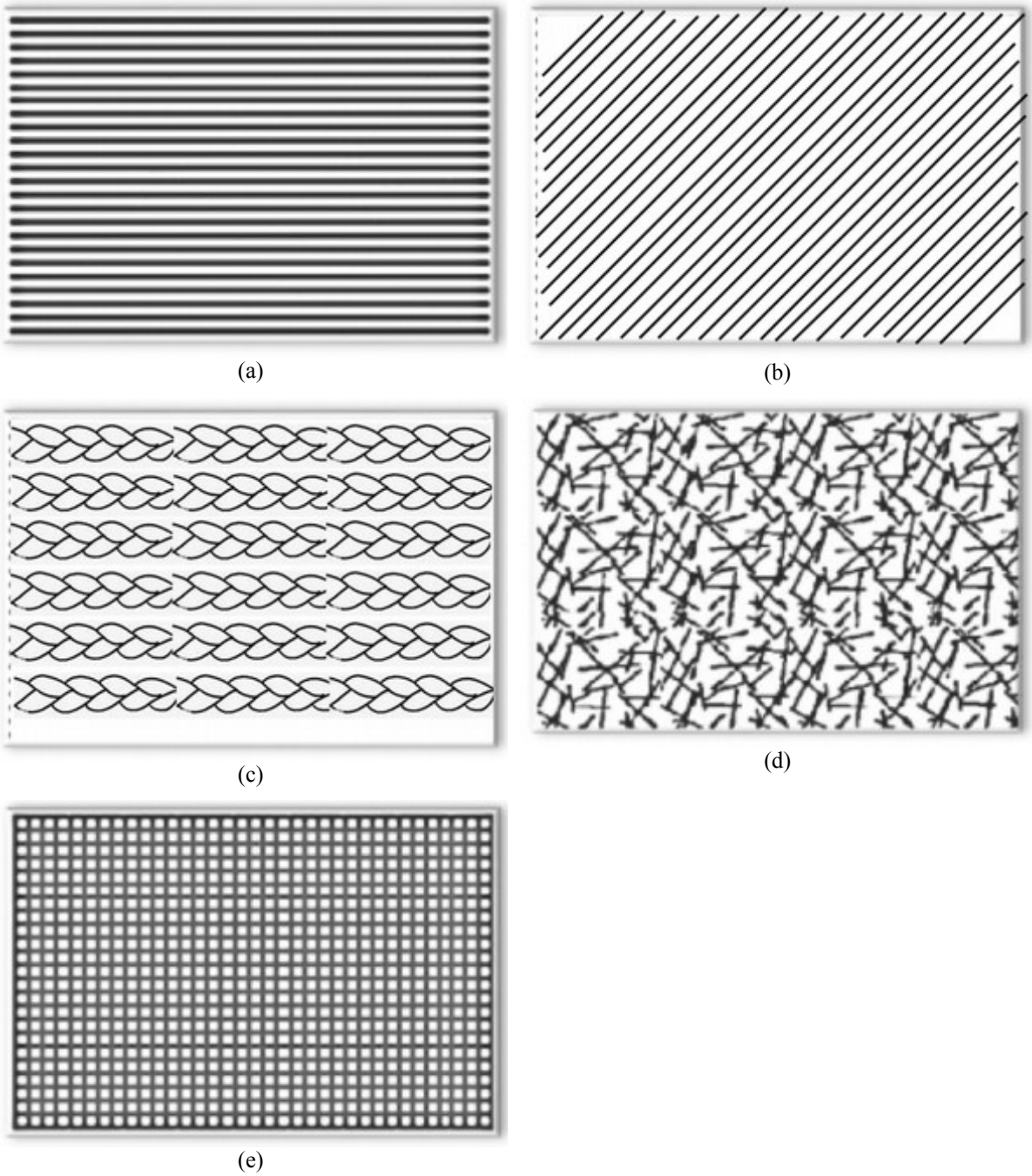

Source: Author; MELO (2016).

According to the processing parameters, the polymeric composite production occurred in three parts: 2x heating, pressing and cooling for the PEg plates preparation (1st part); 1x heating, pressing and cooling for the laminate preparation (2nd part); and 1x heating, pressing and cooling for the final composite preparation (3rd part). Every processing part occurs similarly quoted in the previous session.

These procedures were carried out at Laboratory of Mechanics and Technology – *Laboratoire de Mécanique et Technologie* (LMT) – from Paris-Saclay University (France).

3.3 Physicochemical analysis

3.3.1 Dimensions of bamboo fibers

The dimensions (length and cross-sections dimensions) of natural fibers are geometric parameters that are very scattered. An optical microscopy (OM) and the software Image J were used to observe the geometric trend of BF and to measure their cross-sections. The average dimensions of 50 fibers, size category 0310, was calculated, for each one, according to three largest and thinnest cross-section dimensions measured along the fiber length: one quarter (D_1), middle (D_2) and three quarter (D_3), illustrated at Figure 3.6.

To calculate the circular areas, the largest values for obtained cross-sections dimensions were used, according to Equations 3.2 and 3.3. To the elliptical areas, the both largest and thinnest values were used, according to the Equations 3.4 and 3.5.

Figure 3.6 – Illustrative scheme of points in the length of BF where diameters were measured (¼ of the length to D_1, ½ of the length to D_2 and ¾ of the length to D_3)

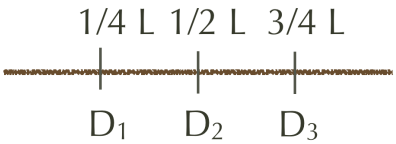

Source: Author.

$$\underline{D}_L = \frac{D_{L1} + D_{L2} + D_{L3}}{3} mm$$ **Equation 3.2**

$$A_C = \frac{\pi \cdot \underline{D}_L^2}{4} mm^2$$ **Equation 3.3**

$$\underline{D}_T = \frac{D_{T1} + D_{T2} + D_{T3}}{3} mm$$ **Equation 3.4**

$$A_E = \frac{\pi \cdot \underline{D}_L \cdot \underline{D}_T}{4} mm^2$$ **Equation 3.5**

Where D_{Li} is referred to the largest cross-section dimension measured at the corresponding point (i = 1, 2 or 3); $\underline{D_L}$ is referred to the largest average cross-section dimension; A_C is referred to the circular area; D_{Ti} is referred to the thinnest cross-section dimension measured at the corresponding point (i = 1, 2 or 3); $\underline{D_T}$ is referred to the thinnest average cross-section dimension; and A_S is referred to the elliptical area.

The measurements were conducted in an OM, model VHX-2000 Keyence, at Laboratory of Mechanics and Technology – *Laboratoire de Mécanique et Technologie* (LMT) – from Paris-Saclay University (France).

3.3.2 Bulk and apparent densities of bamboo fibers

The apparent density ($\rho_{apparent}$) considers the structural (skeletal) volume of the sample subtracted from the total volume of intruded mercury (compact solid material and of closed pores). Thus, the apparent density depends only on the density of the particles, excluding the voids in the material. The bulk density (ρ_{bulk}) considers the total volume with all the open pores (voids), including the air voids between the agglomerates, and inside them. The bulk volume is the volume that would be obtained if the sample was wrapped in thin film.

The determination of the apparent and bulk densities of BF were carried out by mercury intrusion method. The popularity of this method makes mercury intrusion porosimetry (MIP) widely used in the analysis of pore size distribution and specific surface area of the porous material.

Due to the presence of surface tension, the mercury is nonwetting to most solids and the contact angle (θ) between mercury and solid is more than 90°, so it is necessary to apply a pressure to force the mercury into the solid pores. Under equilibrium conditions, the applied force equals the force due to the surface tension (γ), which tends to keep the mercury out of the pore. That is, a force of the same magnitude and in opposite direction must be made on the mercury to penetrate the pore (MOURA & FIGUEIREDO, 2002). That affirmation can be explained by the Equation 3.6.

$$F_{applied} = F_{surface\,tension} \qquad \textbf{Equation 3.6}$$

Where $F_{applied}$ is the force applied to introduce the mercury inside the pore; and $F_{surfacetension}$ is the force due to the surface tension.

This equation shows that with increasing pressure, mercury is intruded into successively smaller pores. In practice, for each value of pressure, a correspondent intruded mercury volume is recorded. From the resulting curve of the cumulative volume of mercury for successive pressure increases (intrusion curve), information about size and distribution of the pores can be extracted.

The analysis consisted of two stages at low and high pressure. The process used a mercury surface tension of 485 dyn/cm and a known contact angle of 130 degrees. The parameters established for low pressure analysis were: evacuation pressure of 50 µmHg, evacuation time of 5 mins, mercury filling pressure of 0.003 MPa and equilibration time of 10 s. For high pressure analysis, an equilibrium time of 10 s and a maximum intrusion volume of 0.77 mL/g were used.

All the non- and treated fibers with diameter varying between 0.1 to 1.0 mm (nomenclature: 0110) were analyzed (approximately the same amount for each type), as well as the non-treated and the mercerized fibers (treatment C) with the biggest diameter, between 1.5 to 2.0 mm (nomenclature: 1520).

The procedure was conducted for BF in a mercury porosimeter Micromeritics AutoPore IV 9500, using the program Win 9500, at Laboratory of Soils, Structures and Materials Mechanics – *Laboratoire de Mécanique des Sols, Structures et Matériaux* (LMSSMat) – from Paris-Saclay University (France).

3.3.3 Porosity and pore size of bamboo fibers

The determination of porosity and pore size of BF were also carried out by mercury intrusion method.

After the analysis, the amount of aggregates present in the specimens tested was determined. The porosity results were expressed in bulk density in relation to apparent density, according to Equation 3.7.

$$\varepsilon = 1 - \frac{\rho_{apparent}}{\rho_{bulk}}$$ **Equation 3.7**

Where ε is the porosity; $\rho_{apparent}$ is the apparent density; and ρ_{bulk} is the bulk density.

The parameters were calculated by the software of the equipment and curves representing the inversely proportional relationship between pressure and pore sizes could be prepared.

The procedure was conducted for BF in same parameters and conditions mentioned in the previous item.

3.3.4 Water absorption index of bamboo fibers, Peg plate and performed composites

The water absorption index (WAI) reflects the water absorption capacity of lignocellulosic fibers and the polymeric matrix, by it self and as unit. Equally important, it indicates the efficiency of the fiber-matrix interface interactions.

Moisture absorption into the composite materials is drove by three major mechanisms: (i) diffusion of water molecules inside the microgaps between polymer chains; (ii) capillary transport of water molecules into the gaps and flaws at the interface between fibers and polymer due to the incomplete wetability and impregnation; and (iii) transport of water molecules by micro cracks in the matrix, formed during the compounding process. Though all three mechanisms are active, the overall effect can be modeled conveniently considering the diffusion mechanism.

Water diffusion mechanism in natural fiber reinforcing plastics follows Fickian law, in which the rate of diffusion is much less than that of the polymer segment mobility. Also, apart from diffusion, two other minor mechanisms are active in moisture exposure of composite materials. One of them is the capillary mechanism, which involves the flow of water molecules along the fiber/matrix interface. It becomes particularly important when the initial interfacial adhesion is weak or when debonding of fibers has started. The other mechanism is the transport by microcraks, which includes the flow and storage of water in the cracks, pores or small channels in the composite structure. These imperfections can be originated during the material processing or due to environmental and service effects (KUSHWAHA & KUMAR, 2010).

For the tests, the natural and modified BF were cut to a length of 50 mm, while the PEg plate and the performed composites were cut to a circular area of, approximately, 254 mm^2. Samples were placed in an oven at 100 °C for 2 h in order to remove any presented moisture. After the defined period, the samples were weighed on an analytical balance, with accurate to 0.0001 g. Then, the samples were placed in appropriate apparatus and covered with distilled water. During defined periods, the swollen materials were removed from the

apparatus and the excess surface water was dried with some wipes. The materials were weighed, determining, at each period, the percentage of water absorption and placed again in the apparatus with distilled water. This cycle was repeated until the reach of water absorption equilibrium.

The percentage of gravimetric water absorption was calculated using Equation 3.8.

$$\%_{water_absorption} = \frac{m_i - m_{dry}}{m_{dry}} \qquad \textbf{Equation 3.8}$$

Where $\%_{water_absorption}$ is the percentage of gravimetric water absorption; m_{dry} is the mass of composite after the remove of moisture; and m_i is the mass of sample after different periods (for BF, i = 0.5 h, 2 h, 18 h and 24 h; and for PEg and performed composites, i = 0.5 h, 1 h, 2.5 h, 4 h, 5.5 h, 24 h, 168 h and 312 h).

The analysis of the diffusion mechanism and kinetics was performed based on the Fick's theory. The mechanism of water uptake and hence the study of the kinetic parameters n and k where analyzed by adjusting the experimental values to the following equations:

$$\frac{M_t}{M_s} = k.t^n \qquad \textbf{Equation 3.9}$$

$$\log\left(\frac{M_t}{M_s}\right) = \log(k) + n.\log(t) \qquad \textbf{Equation 3.10}$$

Where M_t is the mass gain at time t; M_s is the mass gain at the equilibrium ($t \rightarrow \infty$); k is a constant characteristic of the sample which indicates the interaction between the sample and water; and n is a constant that indicates the mechanism of sorption.

The diffusion coefficient (D) is the most important parameter of Ficks's model, which shows the ability of the water molecules to penetrate inside the composites. This parameter was calculated using the Equation 3.11 from the initial slope of the plot of M_t/M_s versus $(\text{time})^{1/2}$.

$$\frac{M_t}{M_s} = \frac{4}{h}.\left(\frac{D}{\pi}\right)^{1/2}.t^{1/2} \qquad \textbf{Equation 3.11}$$

Where h is the composite thickness; and D is the diffusion coefficient.

These procedures were carried out at Laboratory of Mechanics of Fracture and Fatigue – *Laboratório de Mecânica da Fratura e Fadiga* (LAMEFF); at Laboratory of Ceramic Materials Development – Laboratório *de Desenvolvimento de Materiais Cerâmicos*; and at Laboratory of Research in Corrosion – *Laboratório de Pesquisa em Corrosão (LPC)* – from Federal University of Ceará (Brazil).

3.4 Morphological analysis

3.4.1 Scanning electronic micrographs of bamboo fibers

For evaluating the morphology of the microstructure and observing the effect of surface modifications provided by the treatments, some scanning microscope observations were taken from BF.

This analysis were conducted for the non- and treated BF in a scanning electron microscope (SEM), model S-3400N Hitachi with a vacuum of 15.0 kV, at Laboratory of Mechanics and Technology – *Laboratoire de Mécanique et Technologie* (LMT) – from Paris-Saclay University (France). Samples were metalized before the observations.

3.4.2 Photographs of PEg plate and composites reinforced with bamboo fibers

For evaluate the morphology of the macrostructure, observing the alignment and dispersion of the fibers inside the matrix, the visual defects in the composites and the formation of cohesive zones, some photographs were taken using a camera and an apparatus equipped with special lighting for observation through the materials.

These procedures were carried out at Laboratory of Mechanics of Fracture and Fatigue – *Laboratório de Mecânica da Fratura e Fadiga* (LAMEFF) – from Federal University of Ceará (Brazil).

3.5 Mechanical analysis

3.5.1 Tensile test of bamboo fibers

To analyze the mechanical behavior of BF, some tensile tests were performed.

Between 10 to 15 fibers of each mentioned fiber diameter and type of treatment were evaluated.

The testing procedure was performed according to the standard ASTM 3379 – *Standard Test Method for Tensile Strength and Young's Modulus for High Modulus Single-Filament Materials*. Pieces of cardboard were glued to the ends of the fibers samples, with total length of 80 mm, to avoid direct contact of the fibers surface to the grip. This procedure prevents slippage without damaging the fiber. The distance between grips was 40 mm, being the same fiber length evaluated. During the test, the grips moved in opposite directions, imposing a displacement rate of 0.5 mm/min.

The nominal stress was defined as the load (F) divided by the average value of the initial cross-section area (A_0) of the fiber. The section was considered as circular, with the dimension D being the average value of three cross-sections dimensions taken before the tensile test and measured along the length of the fibers (D_1, D_2 and D_3), as explained before. The nominal strain was determined by the ratio length change (ΔL) to the initial length between the grips (L_i = 40 mm). The length change was measured using the Linear Variable Differential Transformer (LVDT) transducer of the testing machine. The maximum tensile strength (σ) of the fiber was determined as the maximum stress before the rupture, and its associated strain is called the failure strain (ε). Young's modulus (E), or elastic modulus, was determined in the elastic linear phase of the stress-strain curve.

The application of Weibull distribution of fiber tensile strength is described by several authors (FIDELIS, 2014; DEFOIRDT *et al.*, 2010; SILVA *et al.*, 2008; CHAWLA *et al.*, 2005; TRIPATHY *et al.*, 2000). Here, it was used the representation presented by FIDELIS, 2014 and SILVA *et al.*, 2008. Weibull statistics were used to rank fiber relative strength versus fiber failure probability to obtain a measure of variability according to fiber treatment. According to the Weibull analysis, the probability of survival of a fiber at a stress is given by Equation 3.12.

$$P(\sigma) = \exp\left[-\left(\frac{\sigma}{\sigma_0}\right)^m\right] \qquad \textbf{Equation 3.12}$$

Where σ is the fiber strength for a given probability of survival; σ_0 is the characteristic strength, which corresponds to $P(\sigma) = 1/e = 0.37$; and m is the Weibull modulus.

The higher the value of m, the lower the variability in strength. Ranking of the fiber strengths is performed by using an estimator given by Equation 3.13.

$$P(\sigma)_i = 1 - \frac{i}{N+1}$$ **Equation 3.13**

Where $P(\sigma)_i$ is the probability of survival corresponding to the *i*th strength value and N is the total number of fibers tested. Substituting Equation 3.13 into 3.12 yields

$$\ln\ln\left[\frac{N+1}{N+1-i}\right] = m\ln\left(\frac{\sigma}{\sigma_0}\right)$$ **Equation 3.14**

Thus, a plot of ln ln [(N + 1)/(N + 1 – I)] versus ln (σ/σ_0) yields a straight line with slope m.

The fiber flexibility can be expressed in terms of moment (M), Equation 3.15, required to bend a fiber with a circular cross-section to a given curvature (K), the reciprocal of the radius of curvature.

$$M = \frac{\pi . E . K . D^4}{64}$$ **Equation 3.15**

The flexibility, defined as K/M, is dominated by D but also depends on E.

Tensile tests were conducted in an Instron testing machine (3345 series), with a load-cell of 500 N, at Laboratory of Post-graduated Program in Dentistry – *Laboratório do Programa de Pós-graduação em Odontologia* – from Federal University of Ceará (Brazil). The testing temperature was 25 °C and the relative humidity of the air was between 70 and 80%.

3.5.2 Tensile test of PEg plate and composites reinforced with bamboo fibers

To observe the mechanical behavior of PEg plate and composites reinforced some tensile tests were performed. About 3 to 5 specimens of each performed material were selected.

The test procedure involved requirements of two standards, ASTM D638 – *Standard Test Method for Tensile Properties of Plastics* and ASTM D3039 – *Standard Test Method for Tensile Properties of Polymer Matrix Composite Materials*. According to the first one, it was defined that the material under study belongs to Type I, presenting thickness of 7 mm or under. However, the geometry recommendations for the second standard are more tolerant. This way, the specimens were defined to be rectangular with a total length of 165 mm and a width of 20 mm. The use of not dumbbell-shaped sample was defined in order to provide the alignment of reinforcement throughout all the specimen. The material thickness presented variations between 2 to 4 mm (D3039 recommends specimen thickness up to 2.5 mm, while D638 is applicable for materials up to 14 mm thick, which is the main reason for using the test speed recommendation by this standard). The grips of the test equipment were placed at a distance of 115 mm, which was the effective test length. Prior to the loading, to eliminate any effect caused by bending on the specimens, a 5 N preload was applied at a rate of 0.1 mm/min. After this step, according to recommended test speeds, the test started at 5 mm/min with progressive increase of load until rupture, which was expected to occur in ½ to 5 min.

The cross-sectional area of the specimen at any time can be calculated by Equation 3.16, resulting in Equations 3.17 and 3.18.

$$A = w.e$$ **Equation 3.16**

$$\exp(\varepsilon_w) = \frac{w}{w_i} \Rightarrow w = w_i.\exp(\varepsilon_w)$$ **Equation 3.17**

$$\exp(\varepsilon_e) = \frac{e}{e_i} \Rightarrow e = e_i.\exp(\varepsilon_e)$$ **Equation 3.18**

Where w and e are, respectively, the width and thickness at any time during the test; w_i and e_i are, respectively, the initial width and initial thickness of the sample; and ε is the strain at maximum load.

Tensile tests were conducted in an Instron testing machine (3345 series), with a load-cell of 5 KN, at Laboratory of Post-graduated Program in Dentistry – *Laboratório do Programa de Pós-graduação em Odontologia* – from Federal University of Ceará (Brazil). The testing temperature was 25 °C and the relative humidity of the air was between 70 and 80%.

4 PHYSICOCHEMICAL, MORPHOLOGICAL AND MECHANICAL BEHAVIOR OF BAMBOO FIBERS

At this chapter, some evaluated properties of bamboo fibers are presented, including mass variation after treatments, correlation between circular and elliptical areas, changes in porosity and pore size according to the treatments, apparent and bulk densities, water-absorption index, morphological observation by scanning electronic microscopy (SEM) and mechanical analysis by tensile tests.

4.1 Physicochemical behavior of bamboo fibers

4.1.1 Mass variation of bamboo fibers

The mass variation of the fibers after the treatments represents a qualitative index qualifying the removal or the addition of substances at the surface or at the core of the fibers. The results of measurements are reported in Table 4.1.

Table 4.1 – Bamboo fiber mass variation after complete treatments

BF	Mass variation after TA (%)	Mass variation after TB (%)	Mass variation after TC (%)	Mass variation after TD (%)
BF0110	9.87 ± 0.24	21.07 ± 0.59	37.56 ± 1.47	60.42 ± 4.66
BF1015	6.16 ± 0.44	14.64 ± 0.26	30.40 ± 1.46	46.01 ± 5.76
BF1520	6.99 ± 0.58	14.95 ± 0.05	31.17 ± 2.23	55.13 ± 3.72

Source: Author.

Treatment A: Water immersion

As it was reported previously, the components of natural fibers include cellulose, hemicellulose, lignin, pectin, waxes and water soluble substances. Hemicellulose consists of highly hydrophilic polysaccharide chains, the main contributor to water-absorption by BF (FROLLINI *et al.*, 2004). In studies carried out with water-absorption of BF (*Bambusa vulgaris*), these fibers absorbed about 73.2 ± 0.01 % of water after 2 hours (time used to perform Treatment A). This way, for this treatment, water partly solubilizes the hemicellulose

and superficial soluble impurities, causing a little mass loss for all the range of dimensions analyzed.

Treatment B: Hot water extraction (HWE)

The Treatment B is a type of hot water extraction (HWE) without pressure and powerful vacuum. According to the increased values for mass variation, this treatment allows for the partial or complete selective removal of hemicellulose (CHANG *et al.*, 2015; PELAEZ-SAMANIEGO *et al.*, 2013; AMIDON *et al.*, 2008). The mass variations measured are compatible with some studies that used a process better controlled, with an application of high pressure, an inert atmosphere and a controlled temperature rate (CHANG *et al.*, 2015). Associated with the partial extraction of hemicellulose, this treatment can also readily degrade starch, source of food for some fungi and insects, providing the control of possible contaminations and, this way, preserving the quality of the BF (WELLS & PAYNE, 1980).

Treatment C: Mercerization

The mercerization removes completely any residual superficial hemicellulose, making the inter-fibrillar region less dense (more soft). This treatment also removes partially the lignin, which promotes the gradual microvoids elimination. With the cement part (hemicellulose and lignin) partially removed, the mercerized BF presented an increased mass loss for all the range of dimensions analyzed. If the period of alkali treatment would intensified, also intracellular non-cellulosic substances could be solubilized, intensifying the performed procedure (SREENIVASAN, IYER & IYER, 1996).

Treatment D: Acetylation

As it was said before, the acetylation method (Treatment D) is a reaction that substitutes the hydroxyl groups of the cell walls for some acetyl groups (esterification). The literature reports that the reactivity of this reaction decreases as follows: lignin > hemicellulose > cellulose (TSERKI *et al.*, 2005). This way, the acetylation has a directly influence on the quantity of fibers content, extracting the lignin and some extractibles and, after, also promoting a slow decrease of the cellulose content. This is motivated by its degradation and by acetylated cellulose deposition on the surface (BLEDZKI *et al.*, 2008;

TSERKI *et al.*, 2005). With the initial mass loss, caused by the treatments until mercerization, and with the removal of others components, increased by the temperature used (100 °C), the mass variation after the acetylation was the highest.

In general, according to Table 4.1, for the thinner BF cross-section and according to the treatment, the mass variations were more intense, indicating that these fibers are more susceptible, suggesting the presence of further macropores at the surface, i.e., the treatment can be performed deeper.

4.1.2 Cross-section dimensions of bamboo fibers

For the smaller dimensions, varying between 0.1 to 1.0 mm, the average dimensions of the largest cross-section ($\underline{D_L}$) of the fibers and the respective circular area (A_C) measured of the non- and treated BF with 5 cm length can be observed in Appendix B – Table B.1. The average dimensions of the largest ($\underline{D_L}$) and the smallest ($\underline{D_S}$) cross-section of the fibers, as well as the elliptical area (A_E) calculated from them, can also be observed in Appendix B – Table B.1.

Figure 4.1 shows the correlation between the circular and the elliptical areas calculated for non- and treated BF. As can be seen, the values of the areas are similar (correlation factor varying from 1.32 to 1.53). The fibers presented many variations in their dimensions, possibly explained by the observation of some fibers with one of the cross-section measurement very higher than the other one and motivated by the natural origin. Even so, because it represents the thinner cross-section measurements, 0.1 to 1.0 mm, closest to the trend line, the non-circular effects of BF were neglected at this research.

4.1.3 Bulk and apparent densities of bamboo fibers

For non- and treated BF with dimensions varying between 0.1 to 1.0 mm and also for non- and treated BF (only treatment C) with dimensions varying between 1.5 to 2.0 mm, the apparent and bulk densities were obtained by mercury intrusion porosimetry (MIP).

Figure 4.1 – Correlation between circular and elliptical area of (a) BF0110WT, (b) BF0110TA, (c) BF0110TB, (d) BF0110TC, and (e) BF0110TD

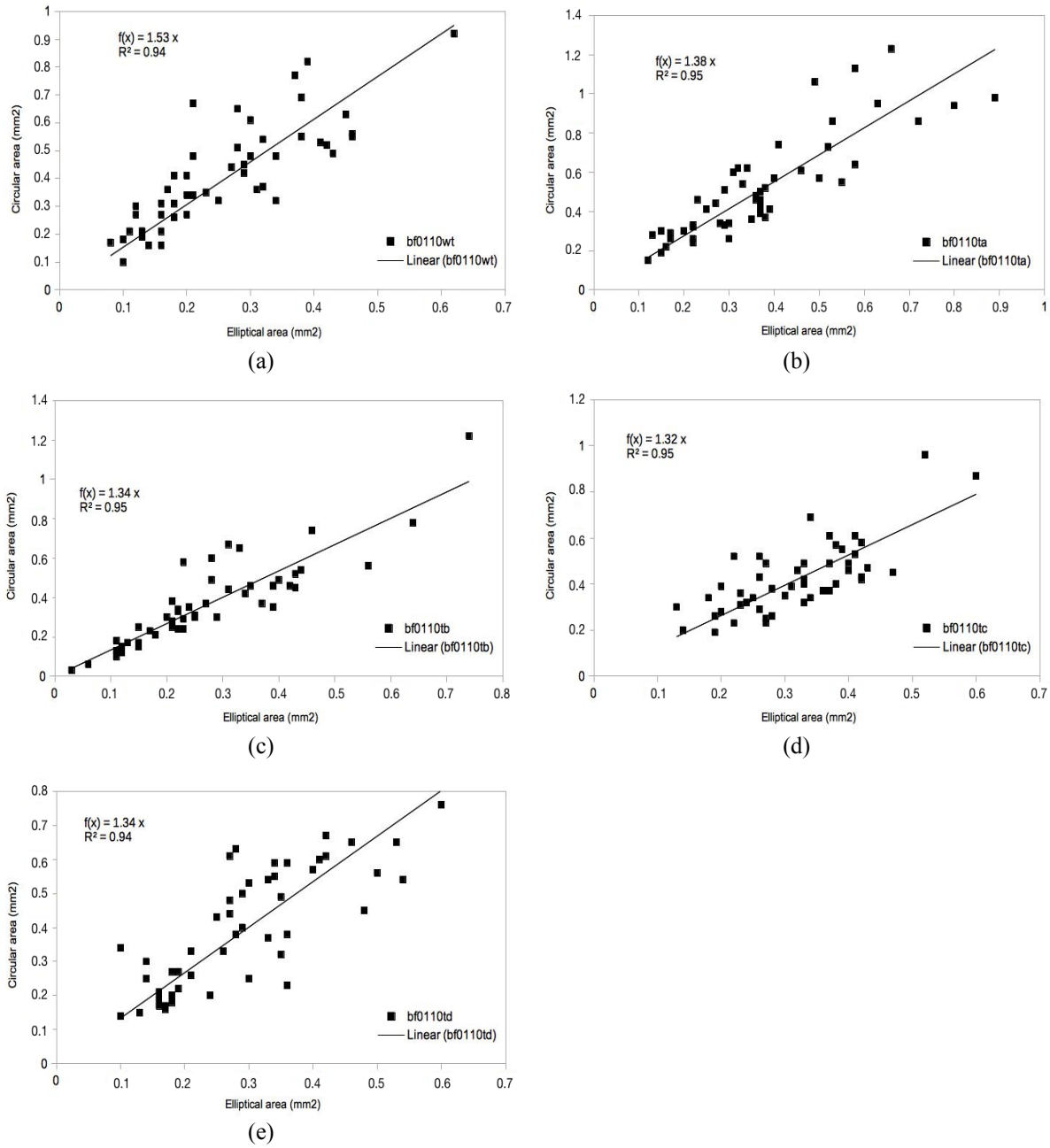

Source: Author.

According to Table 4.2, the increases of the bulk densities observed with the aggressiveness of performed treatment are due to the mass and volume variations. As observed before, the treatments promote a considerably mass reduction associated with the remove of constituents. Associated with this, some studies indicated that the chemical treatments cause fiber defibrillation, i.e., break-up of fiber bundles (ANDRADES & PEREIRA, 2015; MISHRA *et al.*, 2002; BISANDA & ANSELL, 1991). Moreover, causes a

reduction in the fiber size cross-section (ZHANG, WANG & KEER, 2015). Also, as the innermost part of the fibers are more compacted, any mass loss occurs on its surface, resulting in decrease of its dimension. Thus, the decrease in the fiber cross-section size results in an even greater reduction of their volumes (volume is squarely influenced by the diameter). Therefore, even if the masses of the treated fibers also decrease, their volumes decrease even more, resulting in higher densities according to the aggressiveness of the treatments.

Table 4.2 – Apparent and bulk densities of bamboo fibers

BF	ρ_{bulk} (g/cm^3)	$\rho_{apparent}$ (g/cm^3)
BF0110WT	1.03	0.40
BF0110TA	1.09	0.51
BF0110TB	0.98	0.56
BF0110TC	1.20	0.13
BF0110TD	1.51	0.13
BF1520WT	0.94	0.25
BF1520TC	1.52	0.41

Source: Author.

For BF just treated with water (Treatment A and B), the apparent density ($\rho_{apparent}$) increased. This is caused by a slight decrease in the fiber cross-section and thus a decrease in its volume. Even though it loses mass with the surface cleaning, the volume variation is more expressive, resulting in higher apparent density values than untreated BF. The bulk density (ρ_{bulk}) did not change much due to, as observed later, the higher integrity of parenchymal cells (the bulk volume changes proportionally with the mass loss) and the presence of some impurities embedded on its surface, resulting in a material with less roughness, i.e., higher components concentration per volume.

For mercerized and acetylated BF, the bulk density increased as a consequence of the collapse of their cellular structure (DAI & FAN, 2014). Associated with these results, the increased porosity, according to the following section, resulted in decreased values for apparent densities.

The thicker fibers also presented increased bulk densities associated with the mass and volume variation. Comparing the both mercerized BF (Treatment C), the apparent density of BF1520 is higher than BF0110. As observed in Table 4.1, the mass variation for thinner and thicker mercerized BF are almost the same (37.56 ± 1.47 and 31.17 ± 2.23, respectively),

resulting in a higher bulk density for thicker fibers as they present almost same mass but with more voids. The apparent density values are compatible with the results presented for bulk densities and porosity.

4.1.4 Porosity and pore size of bamboo fibers

In relation to the porosity, measured by intruding mercury in the fibers, it was observed that, for thinner fibers and higher the aggressiveness content of the treatments, higher is the porosity observed, confirming that they increase the voids. The BF0110TA and BF0110TB presented a porosity decrease, indicating that water just clean the surface, without opening or increasing any voids at the parenchymal cells. The results are presented in Table 4.3. It can be also observe that, for non-treated fibers, the increase of the diameter promotes an increase of porosity. Again, this indicates that thinner fibers are more compact and have fewer inter-most voids.

Table 4.3 – Total porosity of bamboo fibers measured by MIP

BF	ε (%)
BF0110WT	61.45
BF0110TA	53.09
BF0110TB	42.70
BF0110TC	89.39
BF0110TD	91.47
BF1520WT	73.11
BF1520TC	73.06

Source: Author.

In relation to the pore size distribution, the experimental data obtained after the analysis are presented at Table 4.4. The most basic porosimetry graph is the mercury intrusion volume as a function of the cross-section dimension. The change in the curve inclination gives a view of how the porosity is distributed, how the filling occurred, if the structure collapsed and indicates if the BF had been compressed with the high pressure application.

Table 4.4 – Results for mercury porosimeter analysis for bamboo fibers

BF	Intrusion volume			Total pore area (m^2/g)
	Total (mL/g)	Mesopores (%)	Macropores (%)	
BF0110WT	0.5994	16.68	83.32	23.814
BF0110TA	0.4873	17.30	82.70	13.666
BF0110TB	0.4358	20.28	79.72	12.527
BF0110TC	0.7474	32.98	67.02	14.465
BF0110TD	0.6072	7.86	92.14	13.456
BF1520WT	0.7742	14.76	85.24	22.870
BF1520TC	0.4819	24.59	75.41	17.322

Micropore: $< 2.10^{-3}$ µm; mesopore: 2.10^{-3} to 50.10^{-3} µm; macropore: $> 50.10^{-3}$ µm, as defined by MCCUSKER (2005).

Source: Author.

Figure 4.2 illustrates the intrusion curves as a function of the pore diameter for non- and treated BF in two different cross-sections sizes.

Figure 4.2 – Curves of cumulative intrusion volume in relation to pore diameter for thinner fiber (a) BF0110WT, BF0110TC and BF0110TD; (b) BF0110TA and BF0110TB; and for thicker fibers (c) BF1520WT and BF1520TC

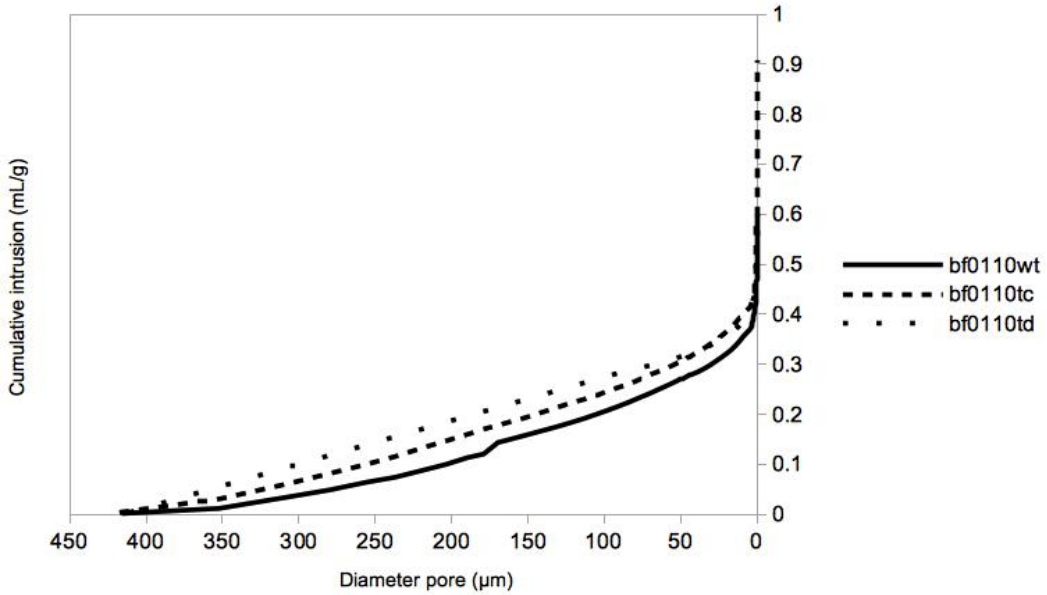

(a)

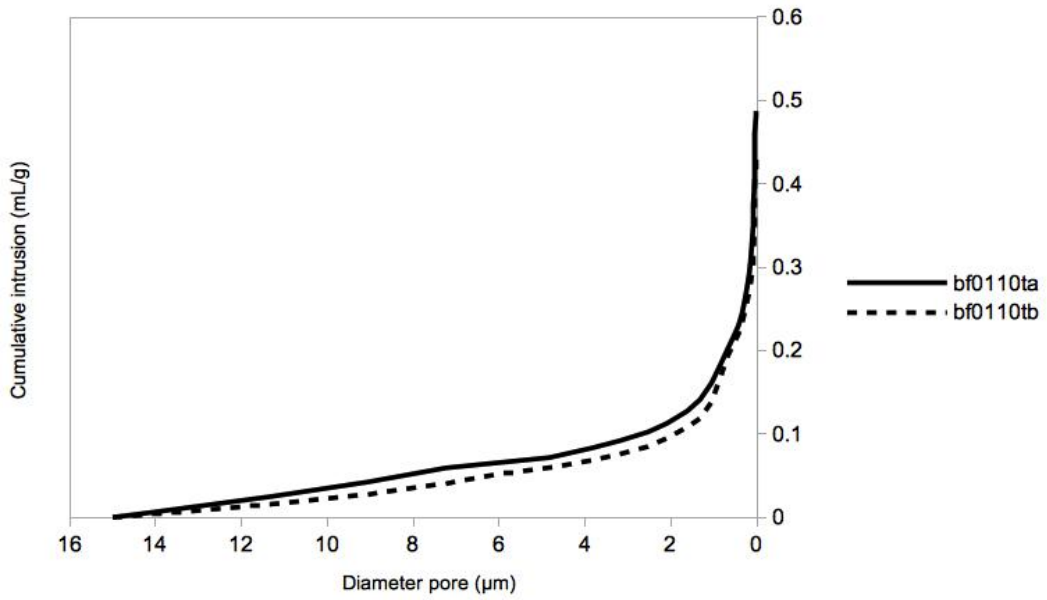

(b)

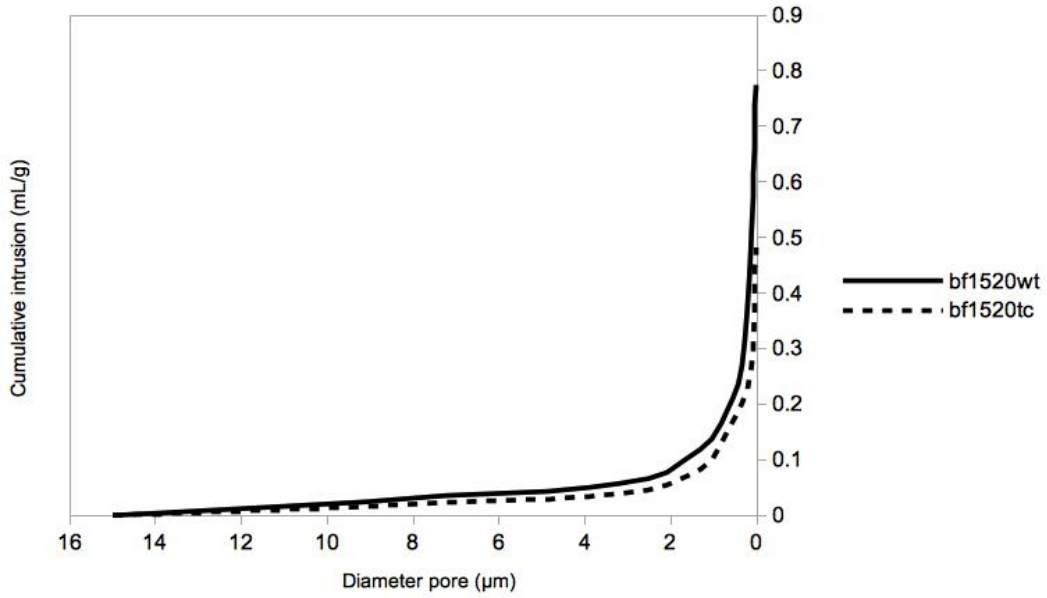

(c)

Source: Author.

The mercury intrusion occurred in a discrete way. The initial intrusion occurred at low pressures due to mercury penetration into inter-particular spaces of the samples. It is possible to observe that the treatments influenced the pores structure. The thinner fibers presented pores with large and small diameters (specifically between 0.01 to 416.02 µm) and the thicker ones presented just pores with small diameters (specifically between 0.03 to 15.00 µm). That is, although the pore areas been practically the same, the thinner fibers present an

inter-most part more compact (more dense, less mesopore volume) and a surface more roughness (more macropore volume); while the thicker fibers present a soften structure.

For Treatments A and B, as explained before, the water solubilizes partly the hemicellulose (amorphous material, which explains the higher porosity of the untreated BF when compared with BF0110TA and BF0110TB) and some impurities (pectin and others), resulting in a cell wall (primary wall) composed in most part by lignin. Which, during the maturation of the vegetable, polymerizes into the spaces in the existing wall, lowering its porosity and creating a rigid water-impermeable cell-wall barrier (SHIMIZY, 2018; DAVISON *et* al., 2013).

With the complete removal of hemicellulose and part of lignin (Treatment C), the BF0110TC becomes less dense and less rigid. It is believed that this mechanism involves the intermolecular saponification of ester bonds between hemicelluloses and lignin, increasing the percentage of mesopores and, this way, increasing the porosity of the material (SHIMIZY, 2018). As BF1520TC presents a soften structure, the treatment did not rise much the pore size, presenting a little increase in percentage of mesopores.

Treatment D promotes directly influence on the quantity of fibers content, extracting the lignin and also a few cellulose content (SHIMIZY, 2018; MIRANDA *et al.*, 2015). This loss occurs mainly on its crystalline fraction, maintaining the amorphous part and, this way, the material is spongier, increasing the percentage of macropores.

4.1.5 Water-absorption index of bamboo fibers

Table 4.5 and Figure 4.3 presents the changes of water-absorption indexes versus time for the bamboo fibers without and treated. Measurements were made in triplicate.

Table 4.5 – Water-absorption index of bamboo fibers

Material	**Absorption (%) after**			
	0.5 h	**2 h**	**18 h**	**24 h**
BF0110WT	67.0 ± 0.23	73.2 ± 0.31	76.5 ± 0.25	77.4 ± 0.38
BF0110TC	95.2 ± 0.10	96.4 ± 0.07	102.4 ± 0.26	103,3 ± 0.39
BF0110TD	47.2 ± 0.29	51.0 ± 0.18	51.2 ± 0.53	37.3 ± 0.29

Source: Author.

Figure 4.3 – Curves of water-absorption index for BF0110WT, BF0110TC and BF0110TD

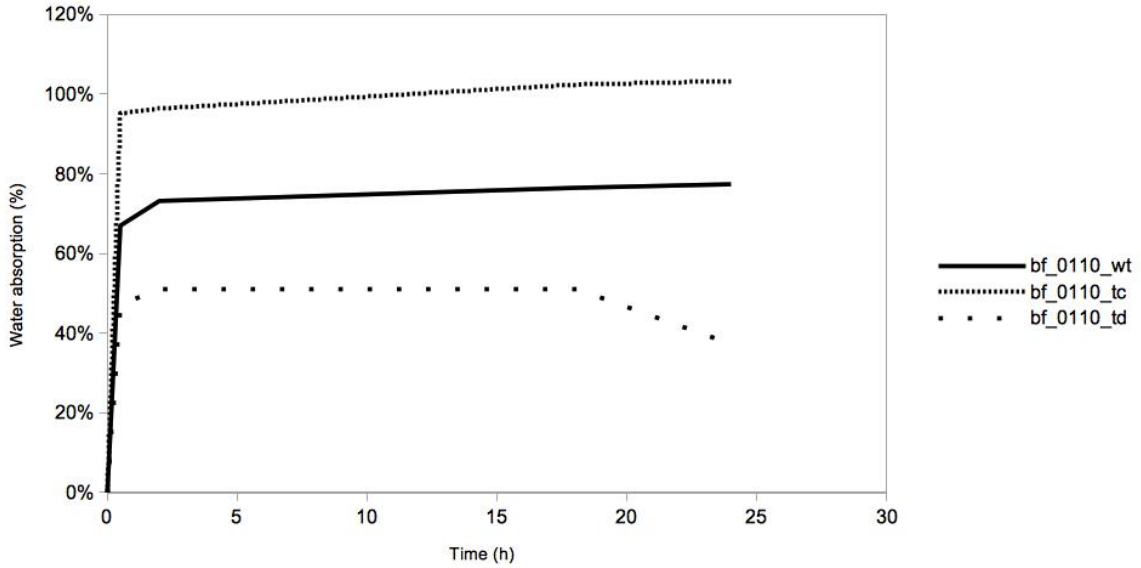

Source: Author.

It is noticed that all evaluated fibers absorbed water. All BF fibers absorbed more or approximatelly 50% within 30 min. With mercerization (Treatment C), the increase of free hydroxyls makes the fiber become more hydrophilic, presenting more than 100% of absorbed water with 18h. However, with acetylation (Treatment D), the BF became less hydrophilic than the previous one.

Another important observation is the rate of the water-absorption index. The natural (BF0110WT) and mercerized fibers (BF0110TC) presented water-absorption throughout all the evaluated time period, always increasing. While the acetylated fibers (BF0110TD), after two hours of immersion, have absorbed practically all the water responsible for their water-absorption.

BF0110TA and BF0110TB were not evaluated because no chemical constituents were fully removed, indicating a water-absorption profile similar to untreated fibers. The thicker fibers were not evaluated either because they presented lower porosity values compared to the thinner ones, indicating lower water-absorption.

4.2 Morphological behavior of bamboo fibers

4.2.1 Microstructure of bamboo fibers

The microstructure of bamboo fibers (morphology with a particular topic on porosity) was observed by SEM, the fibers was prepared following the procedure described in subchapter 3.4.1. Particular attention was paid to the external surface of fibers that were in contact with the PEg matrix. The objective was to characterize the effect of treatments on the fibers.

Figure 4.4 illustrates some SEM micrographics of non-treated BF. They presented a smooth surface layer, which is probably related mainly to the presence of amorphous components of the fiber, such as parenchyma cells (main constituent of the microstructure), extractives, waxes and other fatty residues, due to its vegetable origin associated to the extraction methods. It is also possible to see some grains, maybe associated with starch, which are stored in the bamboo culm after maturation. The structure is basically composed of lignin, which leads to a greater amount of free hydroxyl groups and lower compatibility with the polymer matrix, making the adhesion of the polymer matrix difficult (MELO, 2016).

Figure 4.5 presents the micrographic of BF0110TB, fiber pretreated with boiling water, and shows many rupture of the parenchyma cells, making more apparent the starch grains. The, starch grains, although polar, were only partially solubilized in water, as starch is a mixture of two structurally different polysaccharides.

In contrast, as shown in Figure 4.6, when the fibers are treated with a basic solution, BF0110TC, the starch are completely removed. This treatment also suggests a partial removal of lignin and hemicellulose, influenciating the modification around the surface layer, by favoring the exposure of fibrils (indentations) and globular traits (protrusion). That facilitates the impregnation with a polymeric matrix (RIOS, 2015; MONTEIRO *et al.*, 2011a).

Mercerization followed by acetylation causes superficial changes through the insertion of the acetyl functional group replacing the free hydroxyl groups of the fiber. Figure 4.7 shows that BF0110TD superficially degraded the microfibrils layer at the analyzed surface, where extraction of some fibrils are visible. It can be also observed that the BF is more amorphous, with a spongy aspect, reaffirming the results of porosity and pore size.

Figure 4.4 – SEM images of BF0110WT (a) magnification 100x; and (b) magnification 500x

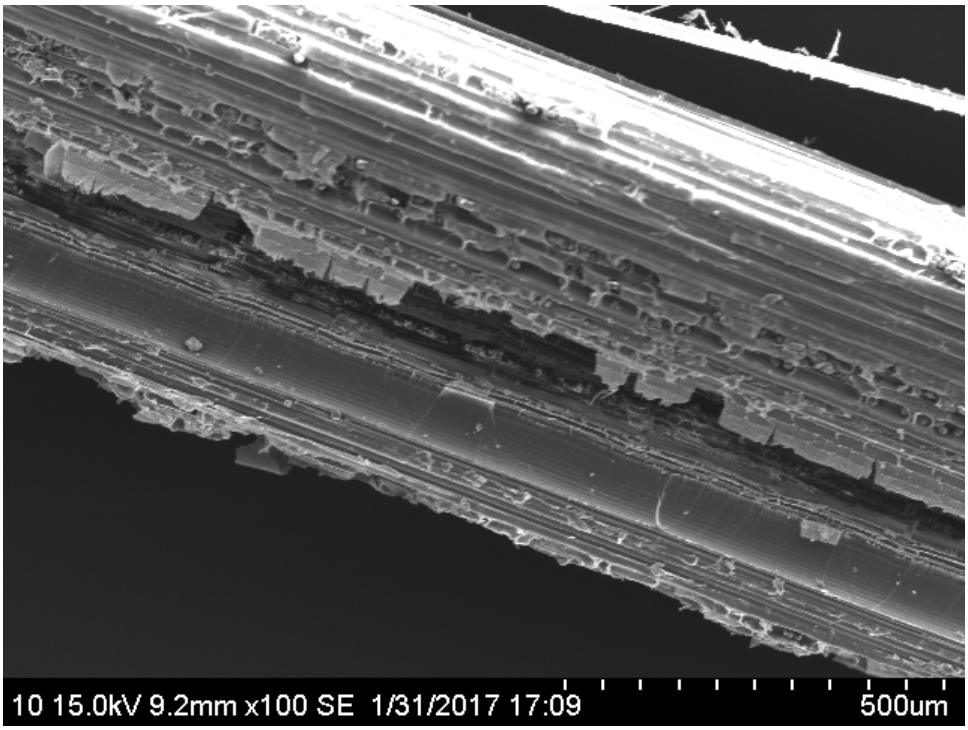

(a)

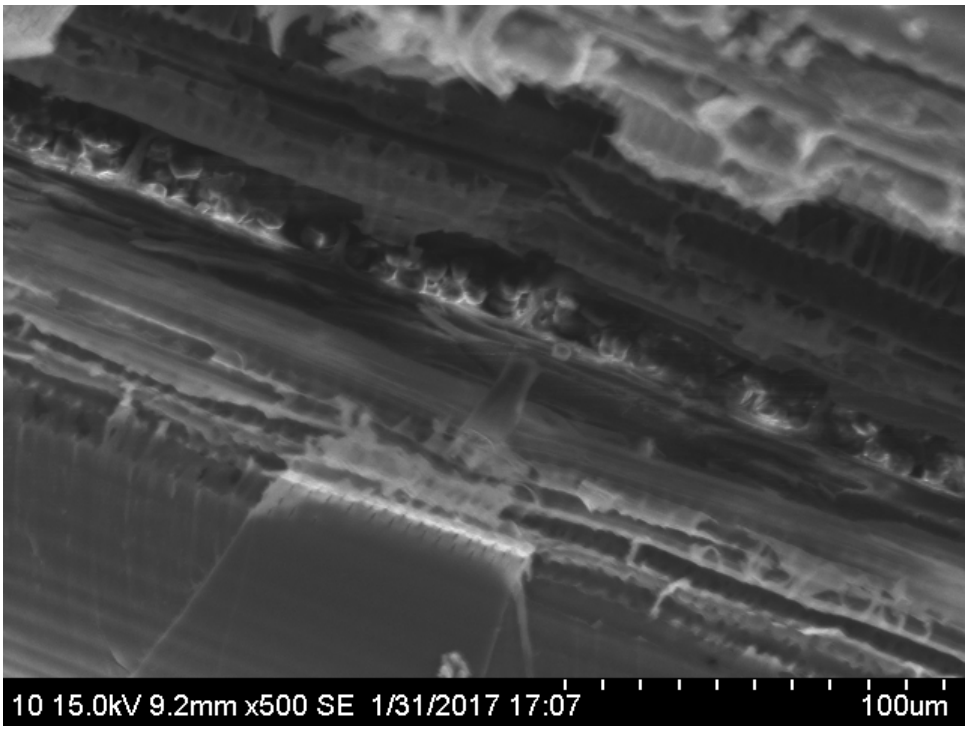

(b)

Source: Author.

Figure 4.5 – SEM images of BF0110TB (a) magnification 100x; and (b) magnification 500x

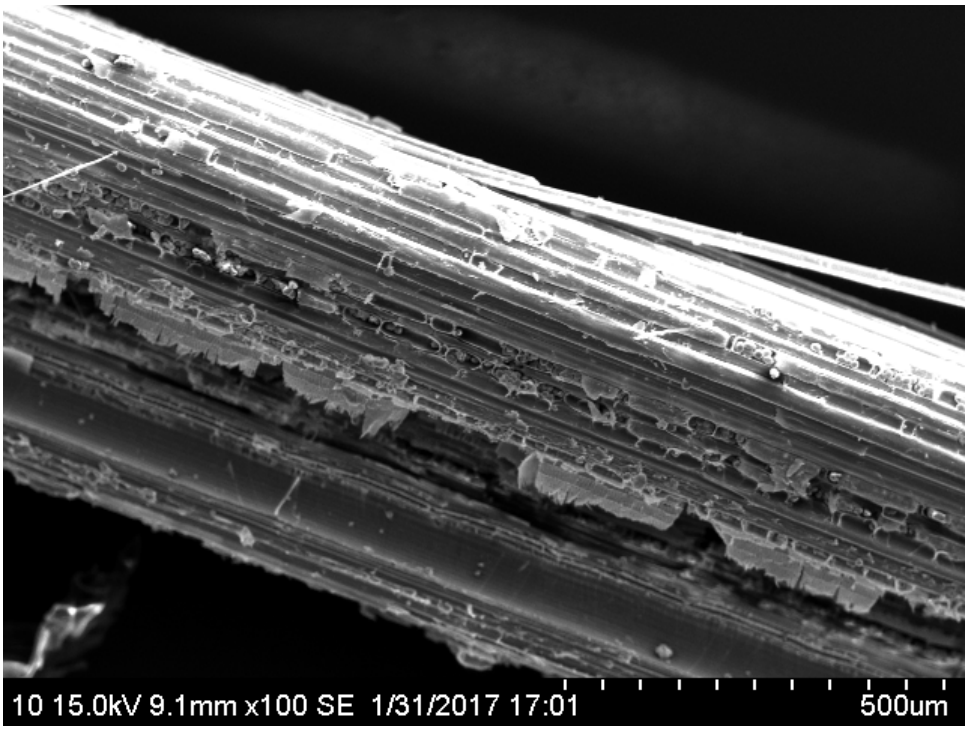

(a)

(b)

Source: Author.

Figure 4.6 – SEM images of BF0110TC (a) magnification 100x; and (b) magnification 500x

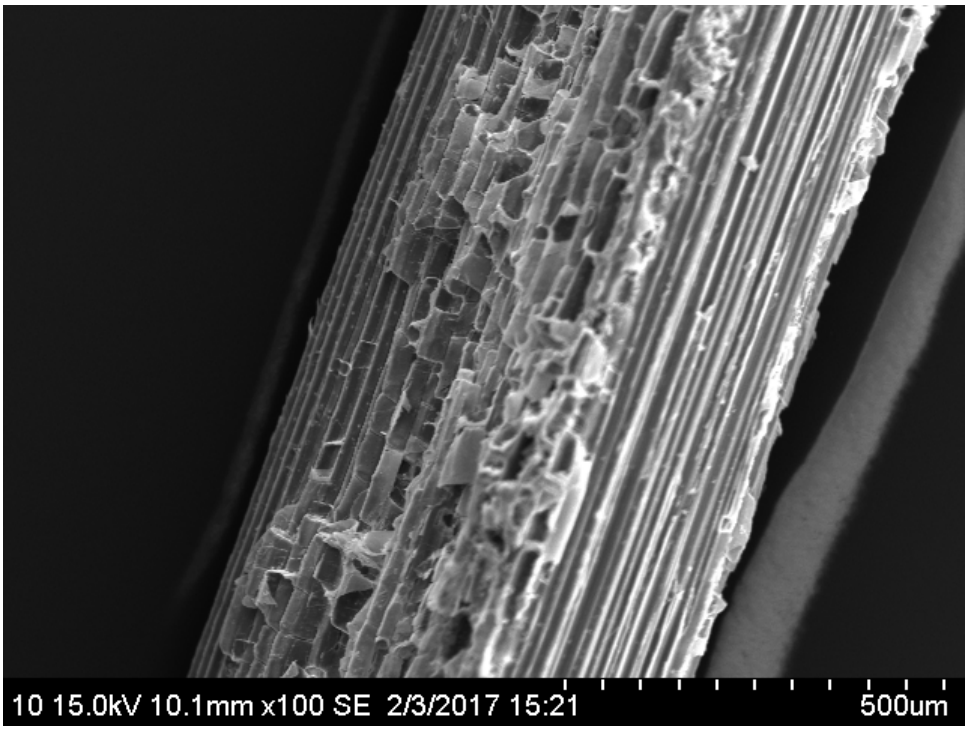

(a)

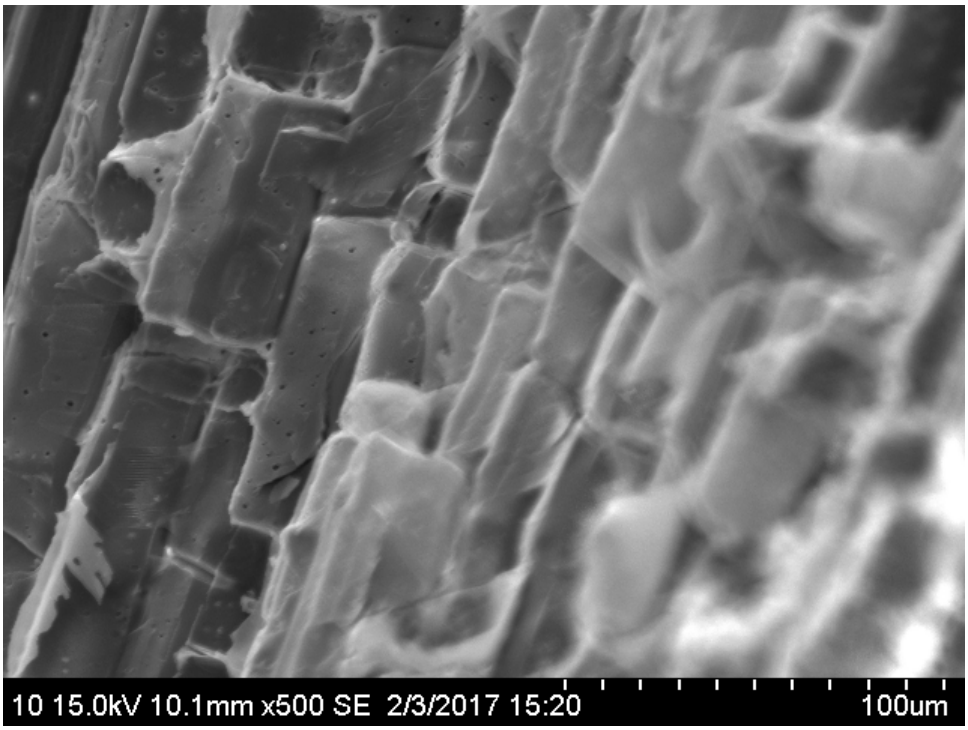

(b)

Source: Author.

Figure 4.7 – SEM images of BF0110TD (a) magnification 100x; and (b) magnification 500x

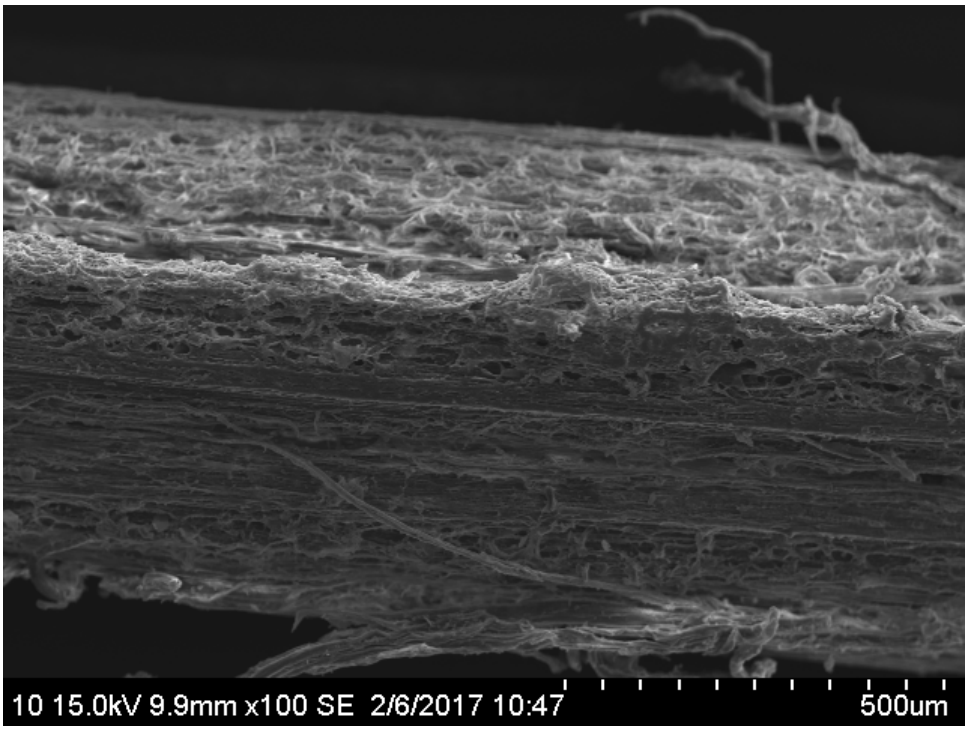

(a)

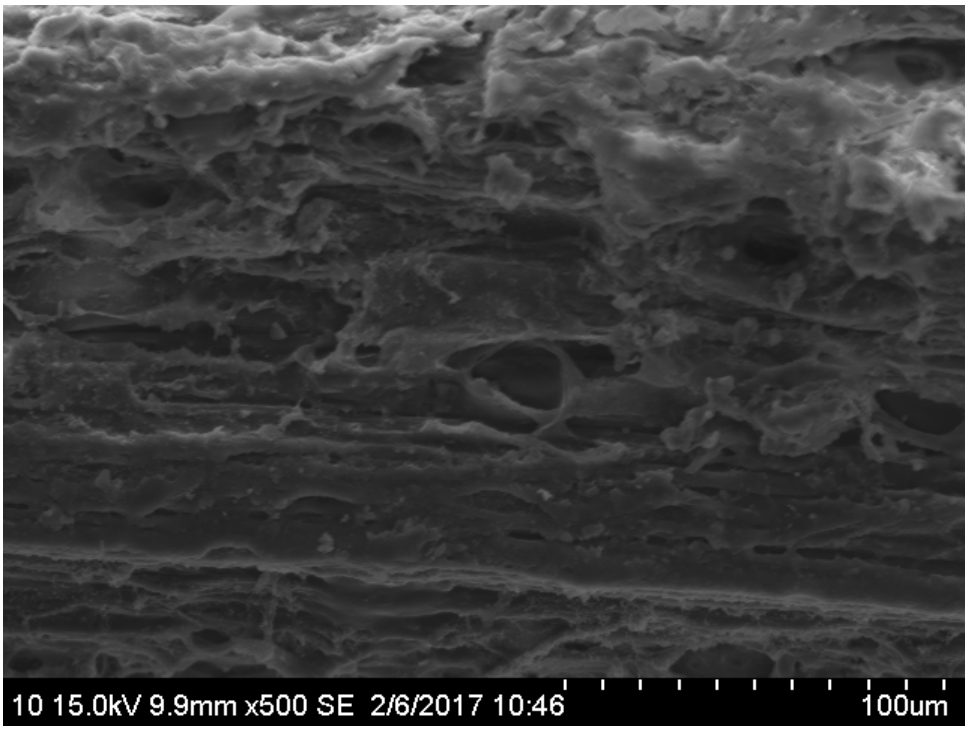

(b)

Source: Author.

4.3 Mechanical behavior of bamboo fibers

4.3.1 Tensile behavior and resistance of bamboo fibers

As mentioned in the literature review, in tension, most fibers tend to fracture in a brittle manner, without any yield or plasticity or some times with small inelastic strain due to progressive damage. Carbon, glass and ceramic fibers are almost completely brittle and fracture without any reduction in cross-sectional area. In contrast, aramid fibers fracture in a ductile manner, although the overall strain to failure stills small. This fracture is very similar to that observed for natural fibers, usually involving fibrillation (HULL & CLYNE, 1996).

Table 4.6 and Figure 4.8 summarize the main results from the BF tensile tests.

Table 4.6 – Average mechanical properties of bamboo fibers in tension

BF	D (mm)	E (GPa)	K/M (GPa^{-1} mm^{-4})	σ (MPa)	m	ε (%)
BF0110WT	0.67 ± 0.12	9.16 ± 3.87	19.92 ± 28.95	193.37 ± 60.38	4.19	2.28 ± 0,75
BF0110TB	0.69 ± 0.14	11.02 ± 3.68	11.01 ± 3.83	215.21 ± 81.44	3.45	1.95 ± 0.41
BF0110TC	0.59 ± 0.13	11.54 ± 5.52	27.00 ± 30.54	253.83 ± 123.75	2.05	2.40 ± 0.67
BF0110TD	0.61 ± 0.12	15.10 ± 9.79	13.77 ± 8.93	281.58 ± 191.23	1.73	1.85 ± 0.44
BF1015WT	1.09 ± 0.15	6.38 ± 2.79	3.19 ± 2.56	126.13 ± 47.36	3.57	2.07 ± 0.75
BF1015TC	1.17 ± 0.07	6.04 ± 1.91	2.10 ± 0.92	117.35 ± 49.55	1.94	1.89 ± 0.36

Source: Author.

Figure 4.8 – Influence of the treatments performed in bamboo fibers on some mechanical properties: (a) tensile strength; (b) Young's modulus; and (c) failure strain

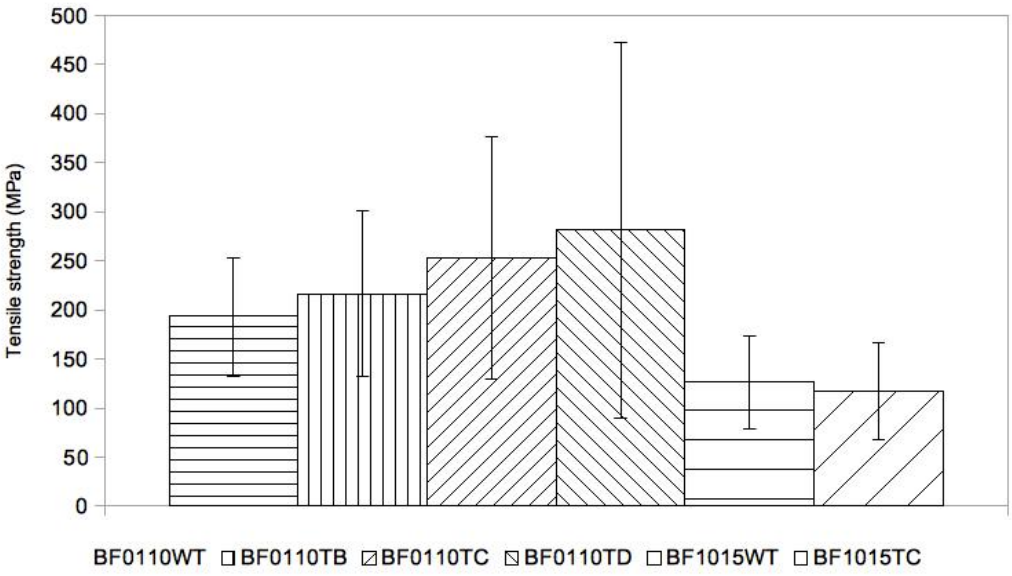

(a)

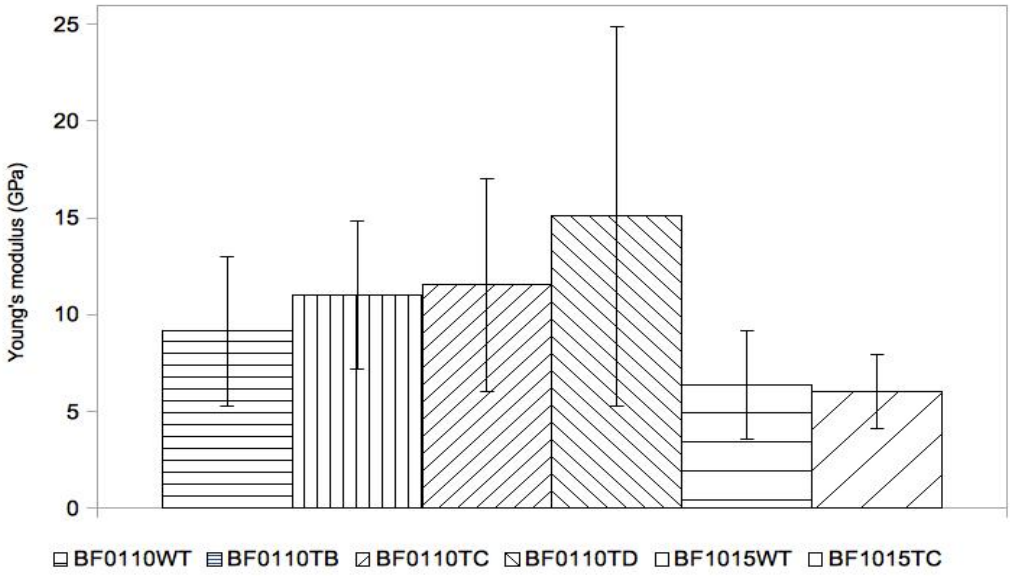

(b)

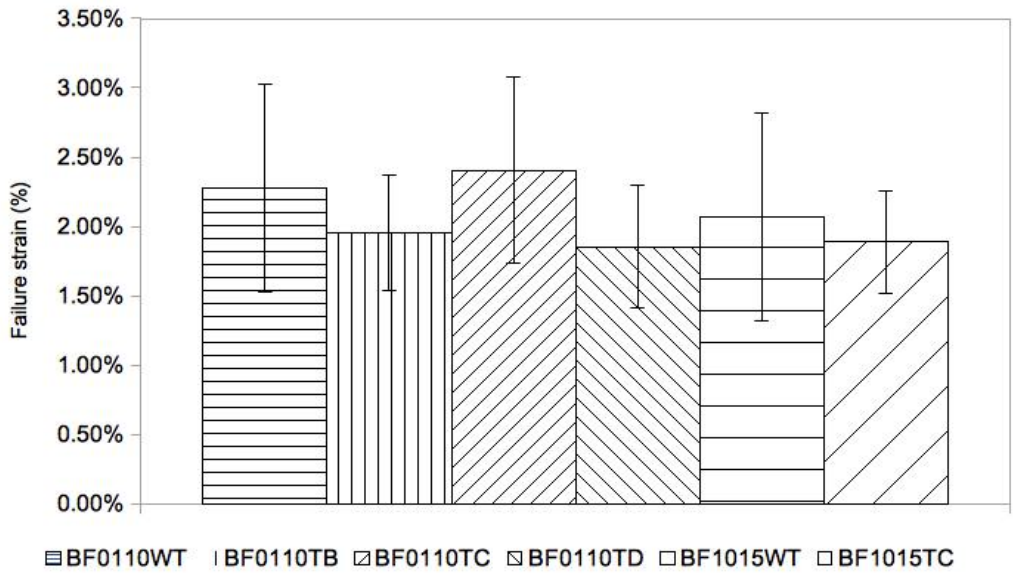

(c)

Source: Author.

Note that both elastic modulus and tensile strength of the treated BF0110 were higher than those non-treated. A small improvement was evident in the elongation at break for BF0110TC, but it decreased for BF0110TB and BF0110TD – BF0110TA had not evaluated, in previous or this section, because it did not presented significant variations in previous physicochemical analyzes. As the heated water (Treatment B) solubilizes part of the natural fiber amorphous superficial component (hemicellulose), the fiber presented slightly more rigid, deforming less than the non-treated fiber, but with enough elasticity to withstand a greater load. However, with the complete removal of hemicellulose and part of lignin (Treatment C) and according to previous discussions, the fiber becomes less dense and less rigid, providing a greater deformation and elasticity. It is also deduced from other studies that, with higher quantity of cellulose (higher percentage of cellulose due to the elimination of hemicellulose and part of lignin), better mechanical properties can be obtained. On the other side, the amount of cellulose content has also a negative effect on other beneficial characteristics of the natural fibers, as that the elongation to break one, which can be observed for BF0110TD, with lignin and a few cellulose content extracted. According to the flexibility, it is dominated by the fiber diameter and the evaluated elastic modulus, presenting a higher result for mercerized BF. Even so, all results presented acceptable values within the group of natural fibers (AL-OQLA *et al.*, 2015; WANG *et al.*, 2011; HULL & CLYNE, 1996).

Figure 4.9(a) shows the variation of Weibull modulus m for BF at different treatments. It can be said that there was an oscillation in the values of m (Table 4.6), not being

possible to perceive the variability in the resistance values. Weibull's modulus is a measure of variability in fiber strength. A high value of m means low variability in resistance. Thus, it can be said that the BF0110TD presented the greater variability in resistance and the BF0110WT the lowest. For comparative effect, it is noteworthy that synthetic fibers have low variability in tensile results. Regarding the size of the cross-sectional dimension, the thicker fibers also showed a decrease in the modulus, indicating the same trend, Figure 4.9(b). Glass and carbon fibers, for example, had a Weibull modulus of 3.3 and 5.7, respectively, in the study by PARDINI & MANHANI (2002).

Characteristics of BF by X-ray Diffraction (XRD) and by Fourier Transform Infrared (FTIR) were carried out in other studies, in order to evaluate the influence of the treatments on the variation of crystallinity index. According to the results presented by MELO (2016), the alkaline base treatment (mercerization) showed a slight increase in the crystallinity content (70.4 ± 0.2%) when compared to that of the untreated fibers (65.7 ± 0.1%). This is mainly due to the extraction of waxes, pectin and lignin from the surface of the fibers, resulting in increase of tensile strength, elastic modulus and failure strain. When the fibers are subjected to the surface acetylation process, the methyl functional groups is introduced into the fiber matrix by replacing the hydroxyls present in their constitution, reducing the interactions by hydrogen bonds present in the fibers, resulting in a crystallinity index of 62.7 ± 0.3%. The results were corroborated with the FTIR analysis.

The diameter of the fibers has a large effect on the way they can be deformed and bent (HULL & CLYNE, 1996). This is the reason that BF1015 presented lower mechanical parameters.

According to some studies, it is common to compare the tensile strength of the materials and their respective bulk density, or specific mass (ASHBY, 1999). Table 4.7 presents this relation for non- and treated BF and other materials for comparison, such as natural fibers (media values from Table 2.3) and some engineering materials, for example steel, iron and PVC (MOTA *et al.*, 2017). A comparison was not made with thicker fibers because they presented lower stress results than the thinner ones.

The BF studied at this work obtained values of the relation between the tensile strength and its specific mass far superior to iron, steel, and PVC, commonly used as engineering materials (MOTA *et al.*, 2017; PERRY, 1999; TITOW, 1984). Comparing to the other vegetable fibers, the values presented by BF appear as average values, motivated by the

high variation of the chemical composition of the fibers, changing their properties, especially the mechanical ones.

Figure 4.9 – Weibull distribution of (a) thinner and (b) thicker non and treated bamboo fibers

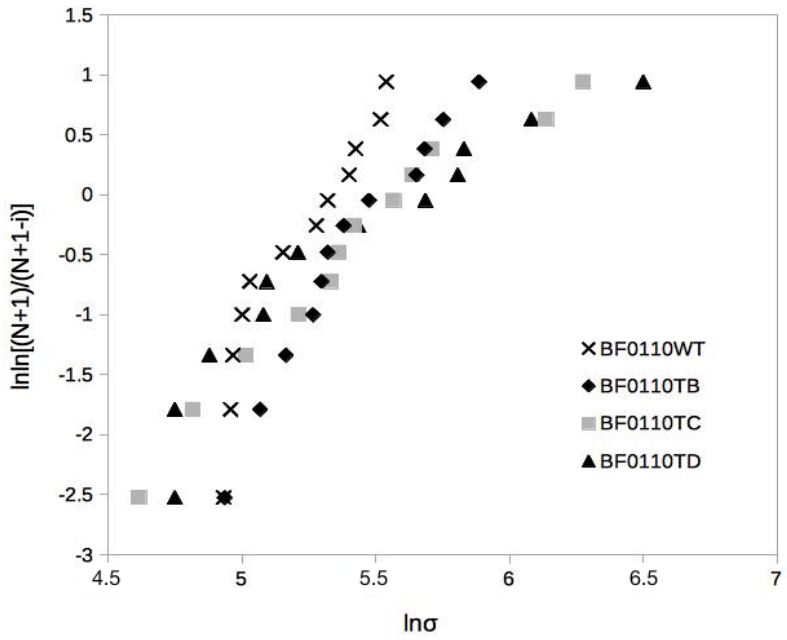

(a)

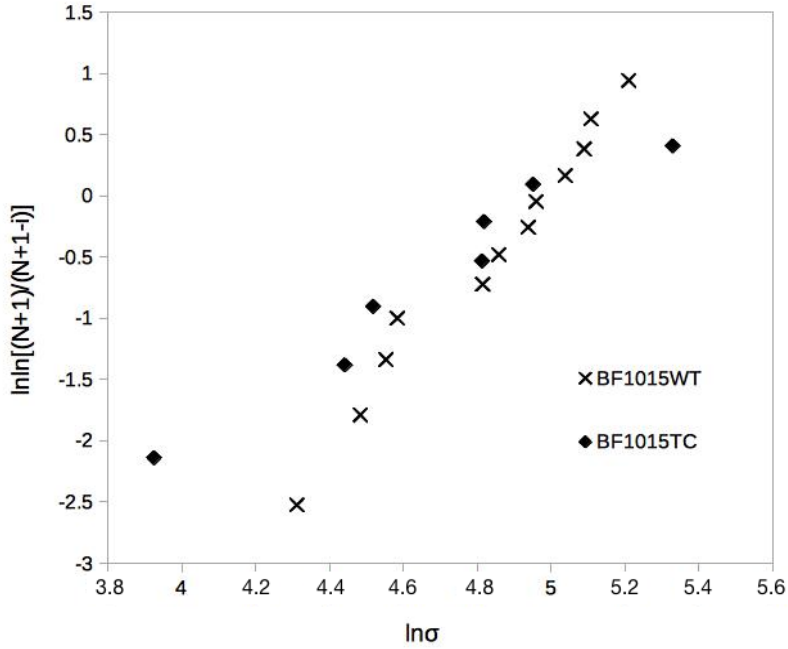

(b)

Source: Author.

Table 4.7 – Comparison of materials efficiencies

Material	σ^* (MPa)	ρ_{bulk} (g/cm^3)	$\sigma^{2/3}/\rho_{bulk}$
BF0110WT	193.37	1.03	32.47
BF0110TB	215.21	1.09	32.95
BF0110TC	253.83	0.98	40.91
BF0110TD	281.58	1.20	35.80
Banana	450.00	1.43	41.07
Coir	157.50	1.39	20.98
Cotton	442.00	1.55	37.44
Curarua	2125.00	0.92	179.66
Flax	922.50	1.48	64.03
Hemp	725.00	1.48	54.53
Jute	600.00	1.46	48.72
Piaçava	127.50	1.46	17.35
Sisal	510.00	1.30	49.10
Steel 303	500.00	7.86	8.01
Cast iron	280.00	7.70	5.56
PVC fibers	70.00	1.45	11.71

*Without the error values.

Source: Author; RIOS (2015); MONTEIRO *et al.* (2011); JOHN & ANANDJIWALA (2008); SATYANARAYANA; GUIMARÃES & WYPYCH (2007); AQUINO (2003); WAMBUA, IVENS & VERPOEST (2003); BLEDZKI & GASSAN (1999); PERRY (1999); TITOW (1984).

5 PHYSICOCHEMICAL AND MECHANICAL BEHAVIOR OF PEg MATRIX

At this chapter, the results of water-absorption index on circular samples of PEg are presented. Then, it also discusses the mechanical behavior of PEg plates through uniaxial mechanical tests.

5.1 Physicochemical behavior of PEg matrix

5.1.1 Water-absorption index of PEg matrix

Table 5.1 and Figure 5.1 present the changes of water-absorption indexes versus time for the PEg matrix. Measurements were made in triplicate.

Table 5.1 – Water-absorption index for PEg matrix

Material	Absorption (%) after							
	0.5 h	**1 h**	**2.5 h**	**4 h**	**5.5 h**	**24 h**	**168 h**	**312 h**
PEg	0.43 ± 0.24	0.22 ± 0.09	0.04 ± 0.00	0.12 ± 0.06	0.12 ± 0.05	0.07 ± 0.02	0.14 ± 0.05	0.25 ± 0.05

Source: Author.

Figure 5.1 – Curves of water-absorption index for PEg matrix

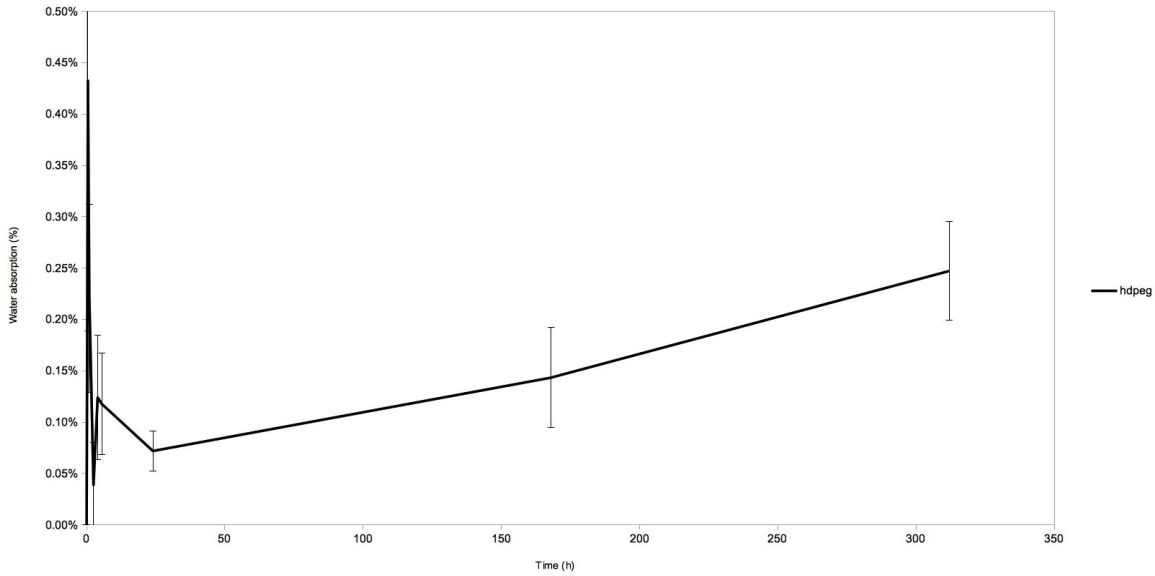

Source: Author.

As observed, the matrix absorbed just a few amount of water and presented a continuous change of the water-absorption index, indicating that the absorption occurs in most part at the beginning. It is possibly due to the organization of the macrostructure after the compression molding. The low water-absorption values by PEg are compatible with data observed for conventional PE (INCOMPLAST, 1977).

5.2 Mechanical behavior of PEg matrix

5.2.1 Uniaxial tensile behavior of pure PEg

The experimental protocols to characterize the tensile behavior of pure compression molded PEg are detailed in subchapter 3.5.2. Results of the tensile drawing for compression molded PEg samples are presented in Figure 5.2.

The experiments were conducted under monotonic loading. Table 5.2 presents the average data for previous mentioned parameters.

Figure 5.2 – Stress-strain curves for compression molded PEg samples deformed until the break at 5 mm/min

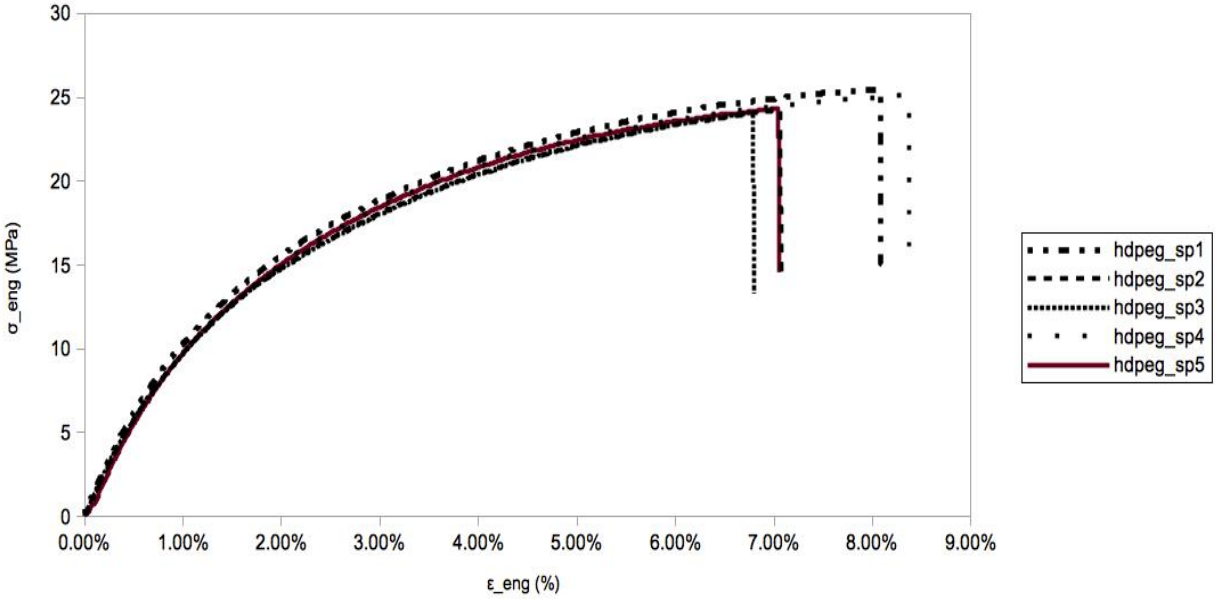

Source: Author.

The pure PEg exhibits a high ductility, comparable to other semicrystalline polymers, such as polypropylene and polyamide (EIRAS & PESSAN, 2009; SCHANG *et al.*,

1996). Their structure consists predominantly of radially oriented lamella in an amorphous matrix. The crystalline lamella can be associated as strong blocks surrounded by an elastic network (the amorphous interlayers) (BURK, 1999).

The deformation proceeds initially with an elastic response for deformation lower than approximately 0.5% and a stress level lower than 5 MPa. The elastic behavior is mainly driven by the amorphous network of the PEg (~ 43%), which has a much lower stiffness than the crystalline part (OLIVEIRA, 2015). As mentioned in the literature, during the initial elastic deformation, crystallographic slip occurs after a reorientation of the crystallites lamellae, which causes the activation of few slip systems lying in favourable orientations. Plastic deformation occurs for higher stresses, but the transition from elastic to elastoplastic behavior is smooth, so that the onset of plastic deformation is difficult to detect without loading-unloading cycles during the test. The irreversible strains occurs in the crystalline part due to slip of lamellae. First, the most favorably oriented lamellae slip, until being stucked by the amorphous phase, then the other oriented lamellae slip. That explains the smooth transition between the two types of behavior (SPIECKERMANN, 2010). Part of the initial hardening observed in the curves is explained by this mechanism.

Until a strain of approximately 6%, the curves are very close showing that, contrary to what was observed for BF, the scattering is very low. The maximum strain (ε_{tmax}) as well as the maximum stress (σ_{max}) are scattered. It is important to observe that the stress is always greater than the tensile strength limit, which is necessary to maintain an increasing and continuous deformation. After that, the failure occurs rapidly. This rapid rupture may be motivated by the type of material processing, as well as the temperature used in this study.

A stress-strain curve for semicrystalline thermoplastics, generally presents an uniform deformation throughout the specimen followed by a maximum in the curve at which necking takes place and propagates until it spans the full gage length of the specimen, a process called drawing (ROYLANCE, 2001). However, as observed in Figure 5.2, after the neck formation, it becomes a little smaller, with local stress increasing with the time, and promotes the specimen rupture. This rapid rupture may have been motivated by the type of material processing, as well as the temperature used. Long-term processing with temperature above the Tg promotes an alteration in the organization of the amorphous fraction, providing an increase in the density and stiffness of the material (constraints on the mobility of the chains) (BACCHI, 2011). Comparing with Table 3.1, regarding the polymer datasheet provided by the manufacturer, the observed results were equivalent.

Table 5.2 – Mechanical properties of PEg plates

Data	PEg - SP1	PEg - SP2	PEg - SP3	PEg - SP4	PEg - SP5
A_i (mm^2)	34.33	37.27	35.33	36.60	32.93
A* (mm^2)	30.79	34.57	32.95	33.54	30.42
w_i (mm)	17.0	19.0	17.5	18.7	18.0
w* (mm)	16.1	18.3	16.9	17.9	17.3
E (GPa)	1.66	1.11	1.11	1.08	1.15
ε_{max} (%)	7.93	6.98	6.78	8.37	7.04
σ_{max} (MPa)	25.40	24.24	24.08	25.13	24.32

Source: Author.

The mechanical parameters of the PEg were within the values provided by Braskem and presented compatible with other studies using the green PE and, also, the conventional one at same conformation temperature (BRASKEM, 2017; HANKEN *et al.*, 2014; PACHECO, 2014).

6 PHYSICOCHEMICAL, MORPHOLOGICAL AND MECHANICAL BEHAVIOR OF PEg COMPOSITES REINFORCED WITH BAMBOO FIBERS

This chapter presents the water-absorption index on circular samples of performed composites. Thus, through the results on tensile testing is possible to evaluate the BF effects as reinforcement in PEg, as well as provides the fields of the failure mechanisms.

6.1 Physicochemical behavior of PEg composites reinforced with bamboo fibers

6.1.1 Water-absorption index of PEg composites reinforced with bamboo fibers

Table 6.1 and Figure 6.1 present the changes of water-absorption indexes versus time for the performed composites. Measurements were made in triplicate.

The composites absorbed water continuously with time and much more than the matrix. For the composites reinforced with the thinner fibers (BF0110), the one that used the non-treated BF presented the worst result: it absorbed almost 4% of water in 24 h and more than 5% in 168 h, stabilizing the water-absorption index. The hydrophilicity is responsible for the higher percentage of water uptake in this composite due to the presence of lignin and hemicellulose component.

The composites reinforced with water treated fibers absorbed between 2 and 4% of water, presenting a constant increase without reaching continuous levels. PEg/BF0110TA presented a lower WAI than PEg/BF0110TB. This may be associated with mass variation after treatments. The water-absorption increase by bamboo fiber reinforcing polymeric composites was already observed in a previous study: the composite with untreated fibers showed absorption of approximately 26% after 2h; while the same composite presented 60% absorption in boiling water after 2h (KUSHWAHA & KUMAR, 2010).

With the mercerization, the increase of free hydroxyls causes the BF to become more hydrophilic, which can be observed for PEg/BF0110TC water-absorption index of 3.53% after 312 h (more than PEg/BF0315TA and a little less than PEg/BF0315TB). This WAI is very similar to that for phenolic composites reinforced with mercerized jute fibers (5% w/v NaOH, 1 h), i.e., more than 3% on the first 24 h. It is also higher than the approximately 2.1% WAI after more than 2 weeks of phenolic composites reinforced with mercerized sisal fibers (4 and 8% w/v NaOH, 1 h) (FROLLINI *et al.*, 2004). On the other hand, the WAI observed for the studied composite is much smaller than that for polyester composite

reinforced with mercerized bamboo (5% w/v NaOH, 30 min) with WAI of approximately 17.5% after 312 h (KUSHWAHA & KUMAR, 2010). This last comparison indicates that the processing form of the composite developed at this study may have guaranteed greater protection of the fibers by the matrix, providing less contact with the medium.

Table 6.1 – Water-absorption index for performed composites of PEg reinforced with BF

Material	Absorption (%) after							
	0.5 h	**1 h**	**2.5 h**	**4 h**	**5.5 h**	**24 h**	**168 h**	**312 h**
PEg/BF0110WT	2.31 ± 0.33	3.07 ± 0.25	2.89 ± 0.25	3.53 ± 0.40	3.16 ± 0.46	3.78 ± 0.58	5.31 ± 0.74	5.53 ± 0.63
PEg/BF0110TA	1.30 ± 0.05	1.53 ± 0.17	1.50 ± 0.18	1.51 ± 0.12	1.85 ± 0.27	2.06 ± 0.32	2.58 ± 0.56	3.17 ± 0.73
PEg/BF0110TB	1.86 ± 0.32	1.64 ± 0.10	1.94 ± 0.08	1.74 ± 0.11	2.02 ± 0.24	2.21 ± 0.31	3.47 ± 0.31	4.06 ± 0.36
PEg/BF0110TC	1.59 ± 0.10	1.46 ± 0.05	1.49 ± 0.16	1.59 ± 0.20	1.74 ± 0.26	2.22 ± 0.37	3.26 ± 0.67	3.53 ± 0.73
PEg/BF0110TD	1.59 ± 0.28	1.34 ± 0.19	1.29 ± 0.34	1.18 ± 0.39	1.27 ± 0.37	1.54 ± 0.52	2.01 ± 0.53	2.10 ± 0.53
PEg/BF1015WT	3.16 ± 2.16	3.97 ± 2.58	4.35 ± 3.07	4.32 ± 2.95	5.14 ± 3.57	5.60 ± 3.82	6.61 ± 3.40	7.57 ± 3.75
PEg/BF1015TC	1.98 ± 0.22	2.53 ± 0.30	2.39 ± 0.22	3.00 ± 0.23	2.68 ± 0.32	3.59 ± 0.48	5.97 ± 1.68	7.09 ± 1.78
PEg/BF0110WT %	2.59 ± 0.07	2.52 ± 0.85	2.27 ± 0.13	2.20 ± 0.41	2.53 ± 0.11	2.91 ± 0.51	3.73 ± 0.86	4.04 ± 0.85
PEg/ BF0110WTX	1.93 ± 0.27	1.31 ± 0.26	1.32 ± 0.11	1.21 ± 0.20	1.64 ± 0.27	1.83 ± 0.34	2.74 ± 1.39	3.85 ± 1.84
PEg/ BF0110WTR	1.28 ± 0.26	1.40 ± 0.17	1.27 ± 0.26	1.12 ± 0.27	1.35 ± 0.35	1.59 ± 0.40	2.86 ± 0.81	3.18 ± 0.82
PEg/ BF0110WT#	6.40 ± 1.04	6.38 ± 1.06	6.13 ± 1.00	6.36 ± 0.98	6.57 ± 1.05	6.74 ± 0.98	7.36 ± 1.13	7.92 ± 1.06

Source: Author.

Figure 6.1 – Curves of water-absorption index for PEg matrix and performed composites of PEg reinforced with BF

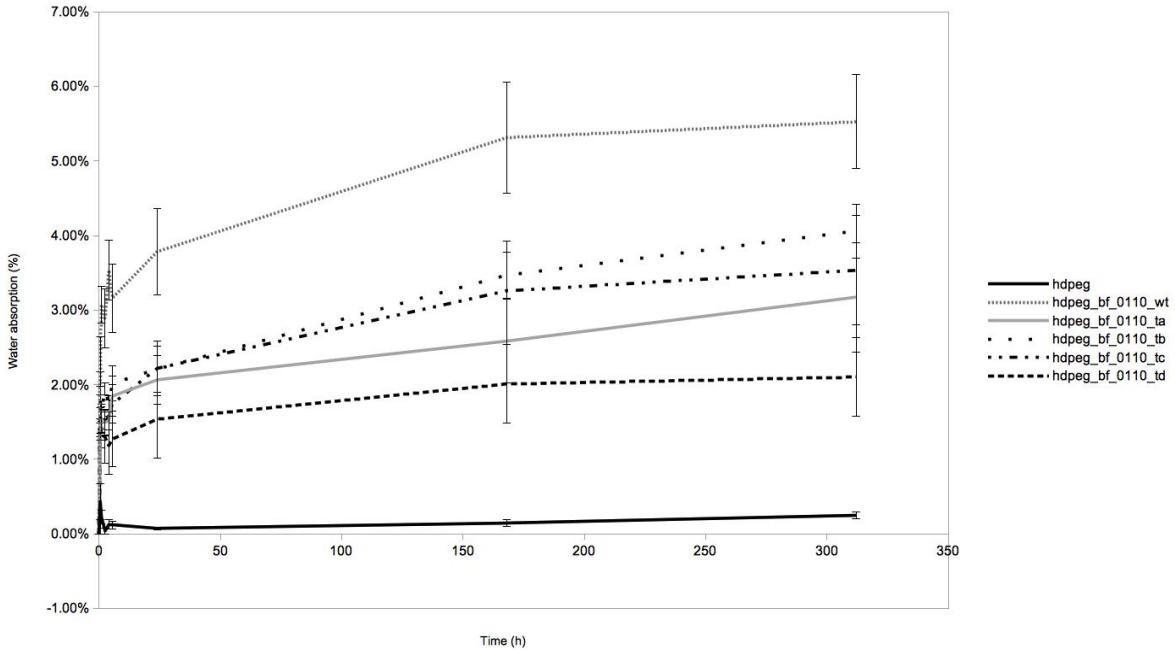

(a)

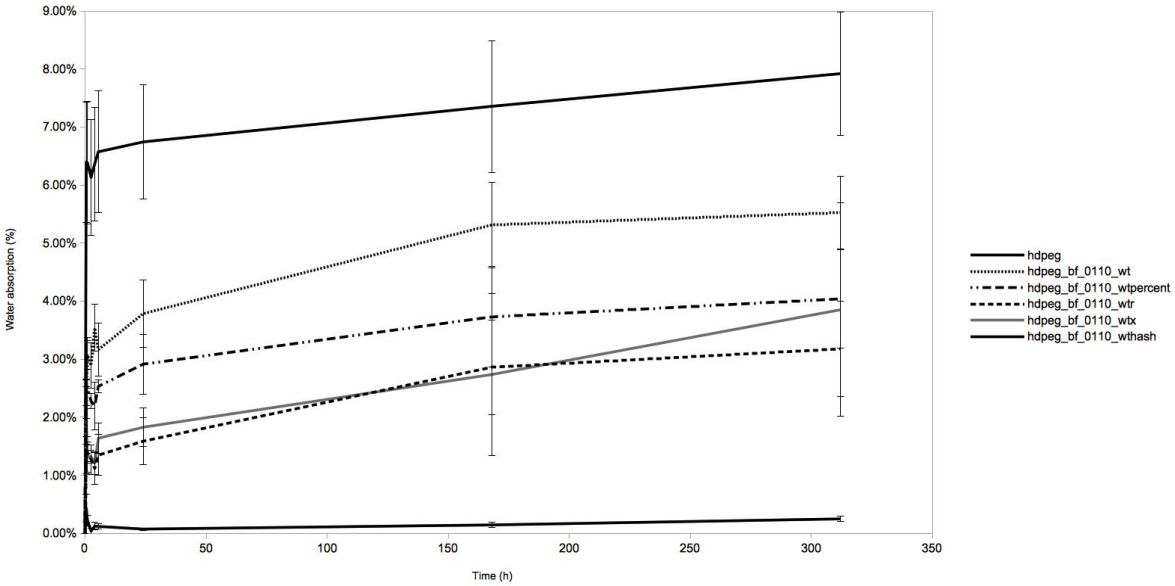

(b)

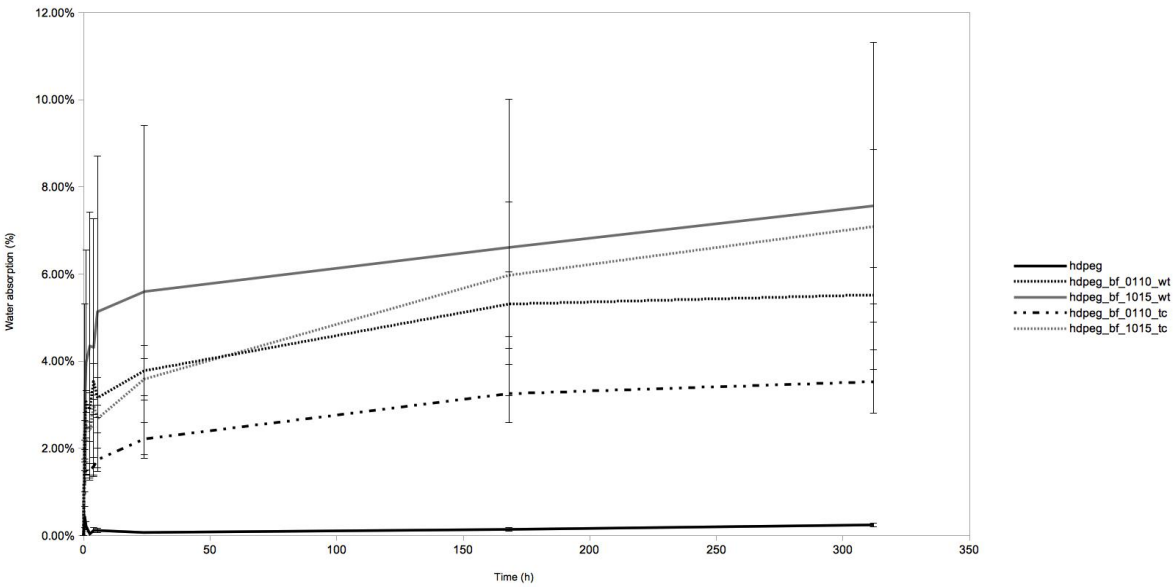

(c)

* peg_bf_0110_wtpercent is referred to PEg/BF0110WT% and peg_bf_0110_wthash is referred to PEg/BF0110WT#.

Source: Author.

The composite reinforced with acetylated fibers (BF0110TD) presented just a 2.10% WAI after 312 h. Compared with the previous results, this composite is perceived to be less hydrophilic than the others. Associated with this, the results for WAI of bamboo fibers were reported to be the smaller one when compared with non-treated and mercerized fibers (MELO, 2016).

Comparing composites reinforced with non-treated BF in different arrangements, the PEg/BF0110WT#, with fibers arranged bidirectionally, presented the highest water-absorption index at all measured periods, even higher than the comparative composite, with long fibers arranged unidirectionally and continuously. As will be presented later (section 6.2), the composite reinforced with fibers in both directions presents numerous faults and bubbles in the macrostructure, which may have resulted in the high entrance of water in contact with the fibers, raising the absorption index.

The other three different composites arrangements presented lower absorption data than PEg/BF0110WT, suggesting materials with a more integrated structure, with better fibers organization and, consequently, less fiber in directly contact with the outer surface of the plate and less voids.

Comparing composites with thinner and thicker fibers non-treated and mercerized, the thicker fibers caused, for both cases, an increase in the absorption index during the

transition period. Thicker fibers presents more volume. This way, for the same quantity of fibers inside the composite, its WAI increases faster due to the increased number of channel and to the increased number of contacts between fibers. Also, thicker fibers are bulkier and may cause more array of fibers at the outer surface of the plate, being in direct contact with the humidity. This way, the water swells through the cell wall of the fibers, where it is absorbed until the saturation of the fiber (more quantity for thicker fibers). The comparative results between the treated reinforces are also consistent with the above discussions.

Although one of the objectives of this study was to investigate the influence of the fiber treatments in adhesion with the polymeric matrix and, consequently, its influence on water-absorption behavior in composites, it was observed from the results that the empty content (voids) of the composite plays an important role. However, there are very few data on this subject in literature. In particular, the influence of voids, as opposed microcracking, is a subject area which has not been widely addressed experimentally (THOMASSON, 1995). This is rather a surprising omission, given the general acceptance of the fact that the presence of voids in composites has an adverse influence on their properties in general. This lack of data may in part be due to the difficulty of producing well-defined composite samples with controlled void content over a large range. Some researches, however, have produced a theoretical analysis which indicates that voids have a diffusivity 15 times greater than that of the composite matrix (WOO & PIGGOTT, 1988). Thus, according to the results presented, it can be assumed that the absorption of water by the polymeric matrix is irrelevant comparing with the absorption by fibers. Therefore, in addition to the differences in absorption motivated by the performed treatments, composites with greater number of failures and voids showed greater absorption of water, providing a linkage between external medium and the fibers inside the composite. Comparing composites with untreated fibers, the absorption results should be similar, however, according to Figure 6.1(c), BF0110WT# showed much higher values, even taking in to account experimental errors. As will be seen in the following section, the composite presented many voids, justifying these results.

As the water-absorption equilibrium had not been reached, the Equations 3.9 and 3.10 must undergo minor changes.

$$\frac{M_{t_{312h}}}{M_s} = k \,.\, t_{312h}{}^{n}$$ **Equation 6.1**

$$\frac{M_t}{M_s} \cdot \frac{M_s}{M_{312h}} = \frac{k \,.\, t^n}{k \,.\, t_{312h}{}^{n}}$$ **Equation 6.2**

$$\frac{M_t}{M_{312h}} = \frac{t^n}{t_{312h}^{\ n}} = t^n . k'^n$$ **Equation 6.3**

Where M_{312h} is the mass gain at time 312 h; and k' = t_{312h}^{-n}.

The values of the parameters n and k' obtained from the fitting curves of water-absorption by the composites are summarized in Table 6.2. Since the most values of the parameter n presented up to 0.5, the composites show a tendency to approach Fickian behavior. When n lies between 0.5 and 1, the diffusion is anomalous. An increase in the k' values is observed for PEg/BF0110WT#, indicating increase in the moisture interaction with the composite material.

The diffusion coefficients (D) calculated are also summarized in Table 6.2.

Figure 6.2 shows the diffusion curve fitting plots for the performed composites. The values of D are also summarized in Table 6.2. Due to the hydrophilic character of natural fibers, the inclusion of water molecules inside the composite material is favored, as demonstrated by the kinetics of the diffusion processes. The values obtained for diffusion coefficients are in agreement with the range of values reported by other authors (KUSHWAHA & KUMAR, 2010; MARCOVICH, REBOREDO & ARANGUREN, 1999; PANTHAPULAKKAL & SAIN, 2007; ROUISON *et al.*, 2005). According to these reports, the values for diffusion coefficient for natural fiber reinforcing composites fall in order of 10^{-12} to 10^{-13} m^2/s.

Figure 6.2 – Diffusion curves fitting plots to determine constants n and k' for the performed composites: (a) PEg/BF0110WT; (b) PEg/BF0110TA; (c) PEg/BF0110TB; (d) PEg/BF0110TC; (e) PEg/BF0110TD; (f) PEg/BF1015WT; (g) PEg/BF1015TC; (h) PEg/BF0110WT%; (i) PEg/BF0110WTX; (j) PEg/BF0110WTR; and (k) PEg/BF0110WT#

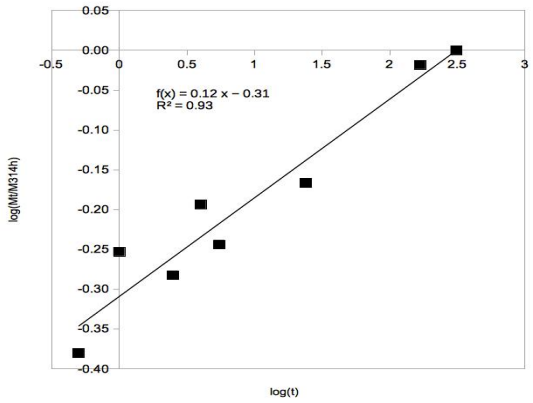

(a)

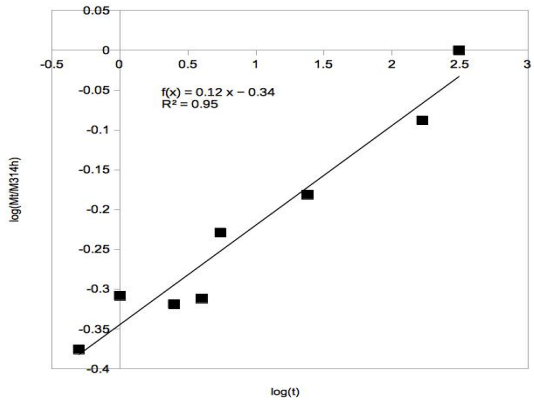

(b)

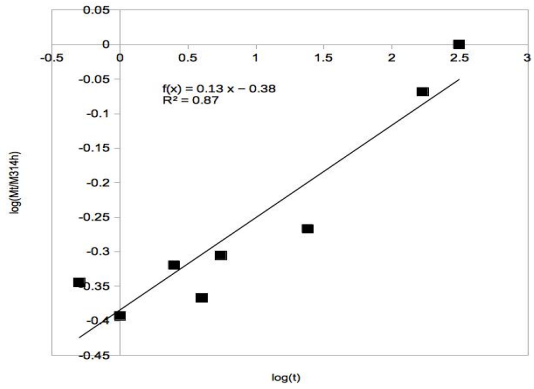

(c)

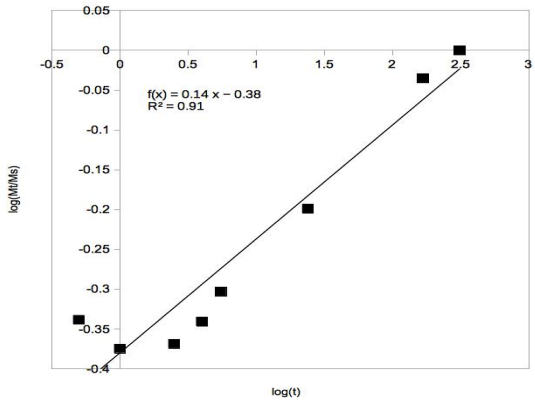

(d)

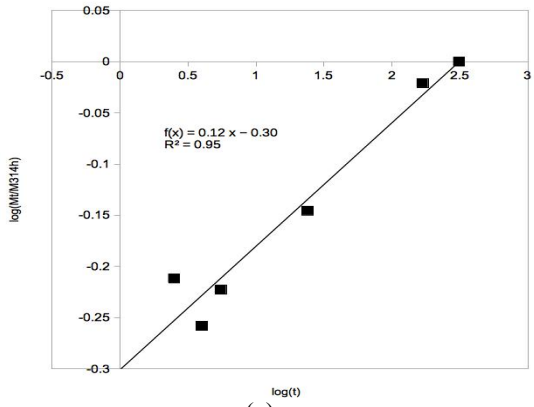

(e)

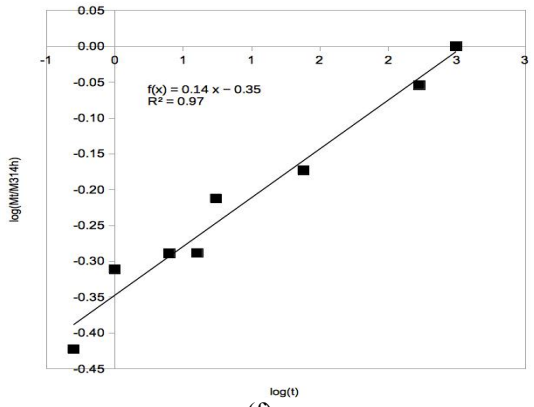

(f)

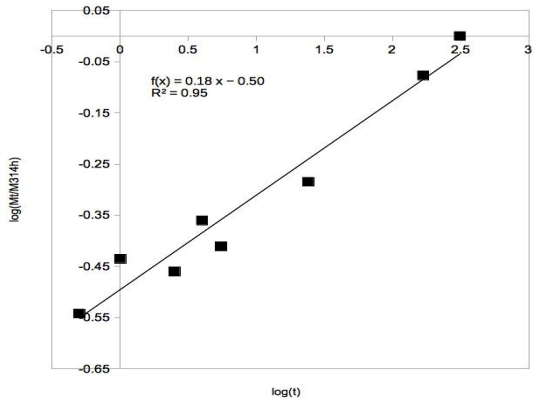

(g)

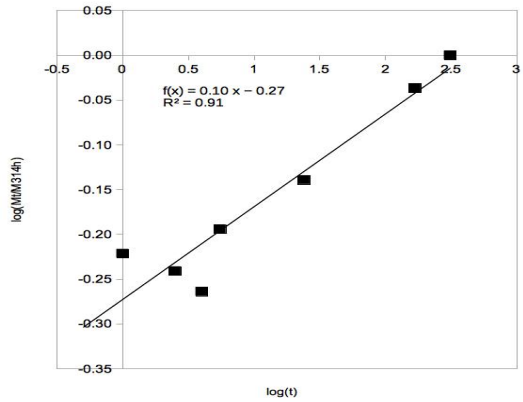

(h)

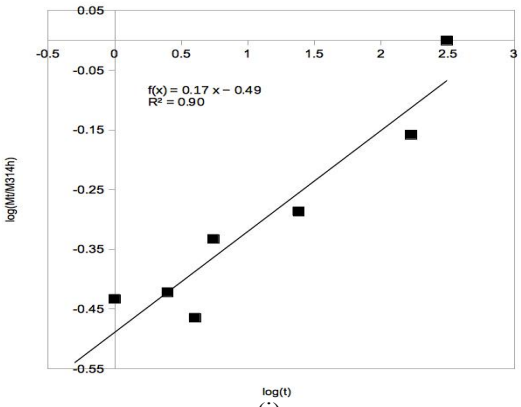

(i)

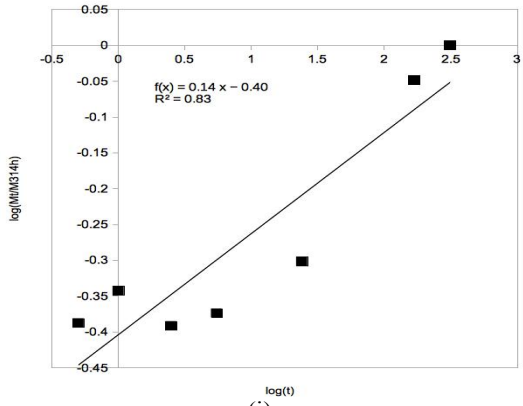

(j)

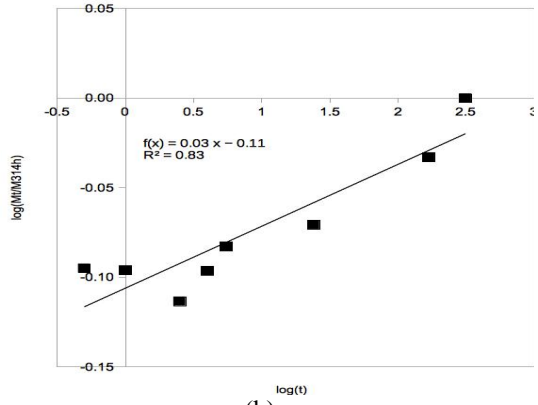

(k)

* PEg_bf_0110_wtpercent is referred to PEg/BF0110WT% and PEg_bf_0110_wthash is referred to PEg/BF0110WT#.

Source: Author.

Table 6.2 – Moisture sorption constants and diffusion coefficient of the performed composites

Composite	n	k'	D x 10^{-12} (m^2/s)
PEg/BF0110WT	0.1240	0.4907	75.05
PEg/BF0110TA	0.1250	0.4525	120.10
PEg/BF0110TB	0.1338	0.4130	140.92
PEg/BF0110TC	0.1430	0.4170	134.90
PEg/BF0110TD	0.1206	0.5001	106.52
PEg/BF1015WT	0.1363	0.4494	76.82
PEg/BF1015TC	0.1847	0.3197	36.43
PEg/BF0110WT%	0.1036	0.5338	91.24
PEg/BF0110WTX	0.1691	0.3243	33.08
PEg/BF0110WR	0.1413	0.3946	50.15
PEg/BF0110W#	0.0346	0.7832	362.25

Source: Author.

6.2 Mechanical behavior of PEg composites reinforced with bamboo fibers

6.2.1 Uniaxial tensile behavior of PEg composites reinforced with bamboo fibers

The average results of the tensile tests for compression molded PEg reinforced with BF are presented in Tables 6.3, 6.5 and 6.6 (complete results are presented in Appendix C, Tables C.1 to C.10). The same analysis conditions were used.

6.2.1.1 PEg reinforced with long bamboo fibers prepared with different treatments

According to the results in Table 6.3, the addition of long BF0110 to PEg matrix in unidirectionally (0° or fibers oriented in direction of the mechanical solicitation) and in a continuously manner promoted a slightly strengthening of its mechanical properties in the loading direction. This can be explained by the transfer capacity of the efforts in the matrix to the reinforcement. The strength increases also with the aggressiveness of treatments. The composites reinforced with treated BF presented increases higher than 30% for maximum stress in all cases (Table 6.4). In general, these results represent that the surface modifiers

provided an effective adhesion between matrix/fiber, resulting in a more resistant and rigid material. Figure 6.3 illustrates a comparative between BF0110 with different treatments, PEg matrix and composites reinforced with these long BF [U (0°),C].

Table 6.3 – Mechanical properties of PEg composites reinforced with non and treated BF0110 [U (0°),C]

Data	PEg/BF0110WT	PEg/BF0110TB	PEg/BF0110TC	PEg/BF0110TD
A_i (mm^2)	48.88 ± 7.38	43.95 ± 2.69	43.66 ± 2.58	41.31 ± 3.74
A* (mm^2)	47.22 ± 8.51	41.45 ± 2.13	41.55 ± 3.68	40.49 ± 3.51
w_i(mm)	18.76 ± 0.75	18.86 ± 0.32	18.48 ± 0.79	18.30 ± 0.23
w* (mm)	18.24 ± 0.84	18.32 ± 0.28	18.02 ± 1.03	17.88 ± 0.34
E (GPa)	1.06 ± 0.13	1.30 ± 0.15	1.24 ± 0.10	1.23 ± 0.12
ε_{max} (%)	1.95 ± 0.38	2.47 ± 0.36	2.58 ± 0.37	3.08 ± 0.06
σ_{max} (MPa)	21.11 ± 6.43	32.78 ± 4.52	33.09 ± 4.17	39.58 ± 3.88
m	2.74	5.82	4.73	7.5

* Maximum values.

Source: Author.

Table 6.4 – Changes in tensile properties of PEg composites reinforced with non and treated BF0110 [U (0°),C] compared to the pure PEg

Material	$\sigma_{composite}/\sigma_{PEg}$* (%)	$E_{composite}/E_{PEg}$ (%)	$\varepsilon_{composite}/\varepsilon_{PEg}$* (%)
PEg/BF0110WT	77.65	86.89	26.96
PEg/BF0110TB	120.76	106.56	34.08
PEg/BF0110TC	121.49	101.64	35.47
PEg/BF0110TD	144.05	100.82	42.46

*The true values were used.

Source: Author.

Figure 6.3 – Comparison of tensile properties of BF0110 with different treatments, PEg matrix and their composites [U (0°),C]

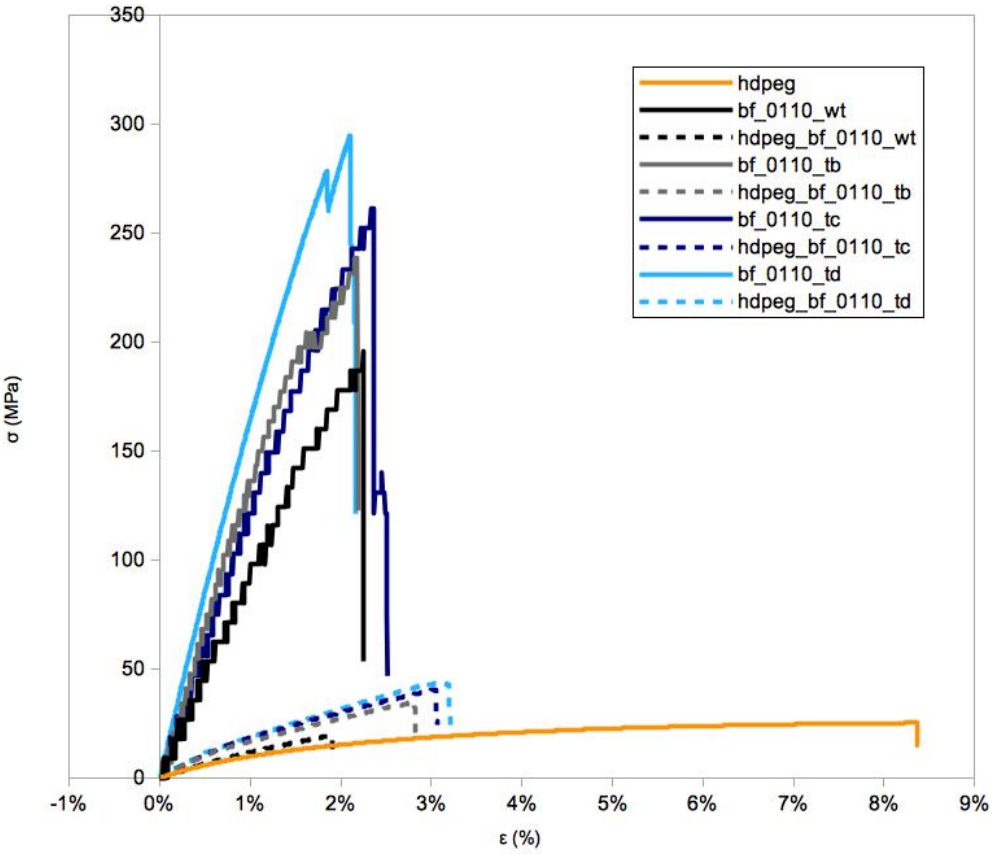

Source: Author.

The maximum strain presented for the reinforced PEg is much smaller than the average value for the matrix and of the same order of magnitude than that of the fibers. However, comparing between the composites, it increases with the performed treatments, reaffirming the improved fiber/matrix interaction according to the intensity of the superficial and bulk modifications.

Figure 6.4 illustrates the variation of Weibull modulus m for PEg/BF0110 with BF at different treatments. It can be said that, in the same way for BF, there was an oscillation in m values (Table 6.3), not being possible to perceive the variability in the resistance values. Since a high m value means low resistance variability, it can be said that PEg/BF0110TD had the highest resistance variability and PEg/BF0110WT the lowest. However, unlike fiber results, PEg/BF0110TC showed less variability than PEg/BF0110TB, indicating resistance results with values closer to each other.

Figure 6.4 – Weibull distribution of PEg/BF0110WT, PEg/BF0110TB, PEg/BF0110TC and PEg/BF0110TD

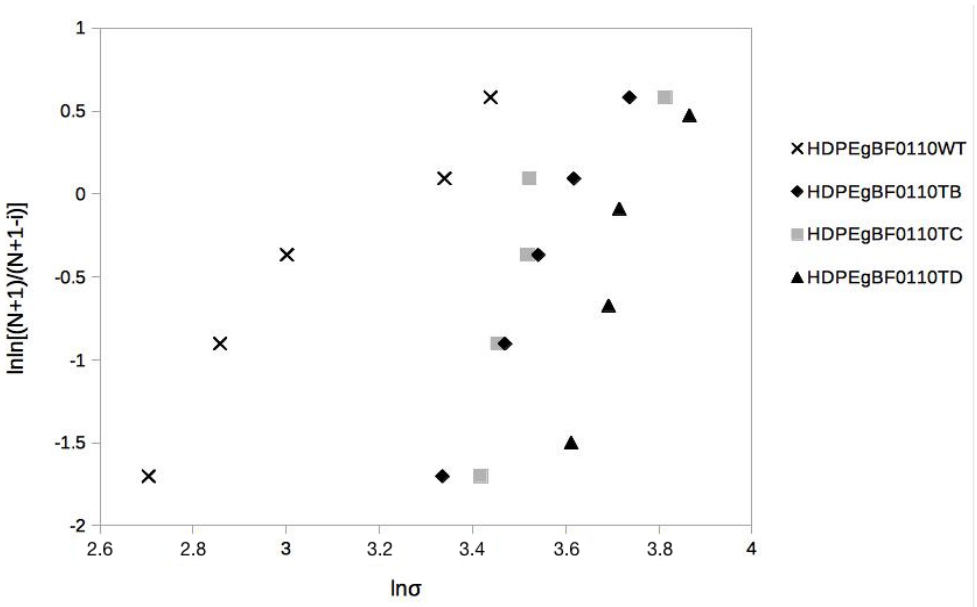

Source: Author.

On the other hand, the elastic modulus values were not directly affected by fiber reinforcement. This was motivated by the end of the test with a rupture of a matrix part of the composite, without necessarily breaking the fibers (in some cases, the matrix slipped through the fibers without breaking them). This fact can be observed in photographs in Figure 6.5, indicating that occurs fiber pull-out, fiber bridging, fiber failure and matrix cracking.

Micromechanical models can help to better understand the influence of fiber in the composite. The Voigt and Reuss mixture models are both simple models and give, for such type of composites, to express lower and higher bounds for elastic properties (DVORAK, 2013). They assume a perfect fiber/matrix interface. The Voigt model is the most appropriate to estimate the elastic properties in the fiber direction. This model has already been applied by Osaka & Onukwuli, 2018 and Freire, Monteiro & Cyrino, 1994.

The composite Young's modulus in fiber direction (E_1) is defined by Equation 6.4, the Voigt model.

$$E_1 = E_f . V_f + E_m . V_m \qquad \textbf{Equation 6.4}$$

Where E and V are the elasticity modulus and the volume fraction, respectively; and f and m are the corresponding indices of composite, fiber and matrix.

Figure 6.5 – Post tensile test samples of some performed composites, illustrating the non-breaking of the reinforcement: (a) PEg/BF0110WT; (b) PEg/BF0110TB; (c) PEg/BF0110TC; and (d) PEg/BF0110TD

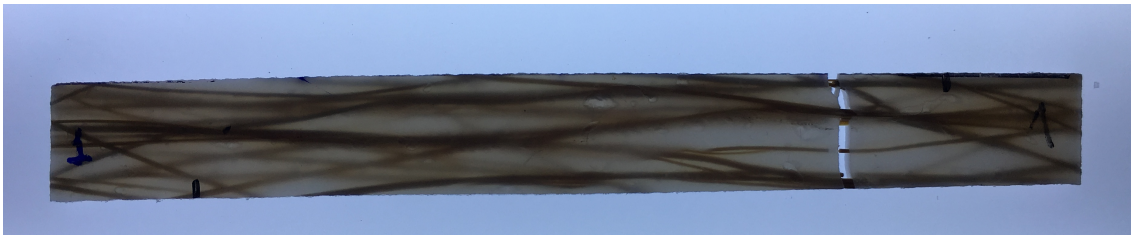

(a)

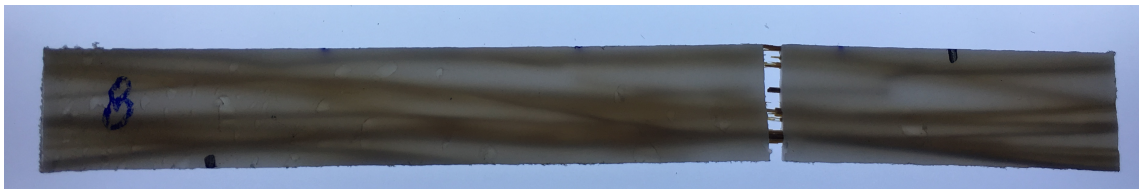

(b)

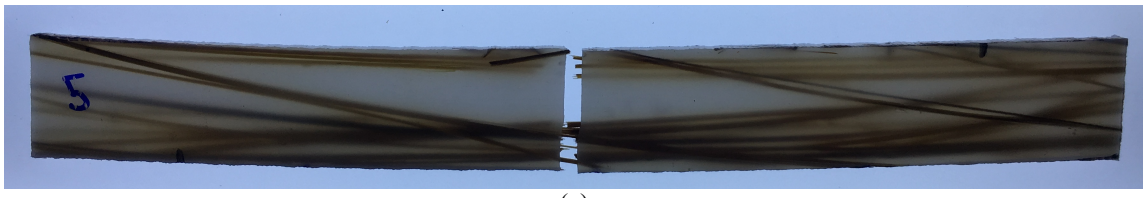

(c)

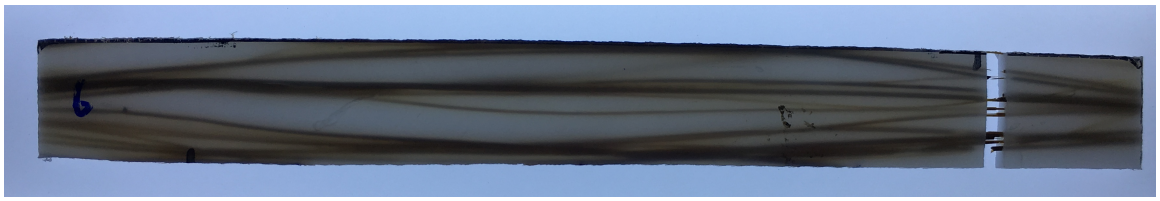

(d)

Source: Author.

It can be observed in Figure 6.6 that the predicted Young's modulus by the Voigt model for the PEg composites reinforced with non and treated long BF0110 aligned in the loading direction are higher than the experimental results. The lower experimental value may be explained in part by misalignement of the fibers as observed in Figure 6.4, nonuniform distribution of fibers in the composite, imperfect fiber/matrix interface reducing the capacity of load transfer to the fibers.

In particular, the interfaces/interphases between the matrix and the fibers play a key role in controlling the overall properties of the composite. Hashin (1990) was one of the pionners proposing a micromechanical model including an imperfect interface to account the influence of weak interface. Many authors have developed different theories to account this effect until today. Amongst them, recently, Gu & He (2016) developed exact connections

between the macroscopic elastic properties of fiber reinforced composite with imperfect interface.

It would be interesting to estimate the properties of the interface via inverse analysis. However, that requires more experimental data than proposed herein which was not the focus of our research.

Figure 6.7 represents other manners of comparing the mechanical properties previously obtained.

Figure 6.6 – Experimental and predicted elastic modulus E_1 of PEg composites reinforced with non and treated BF0110 [U (0°),C]

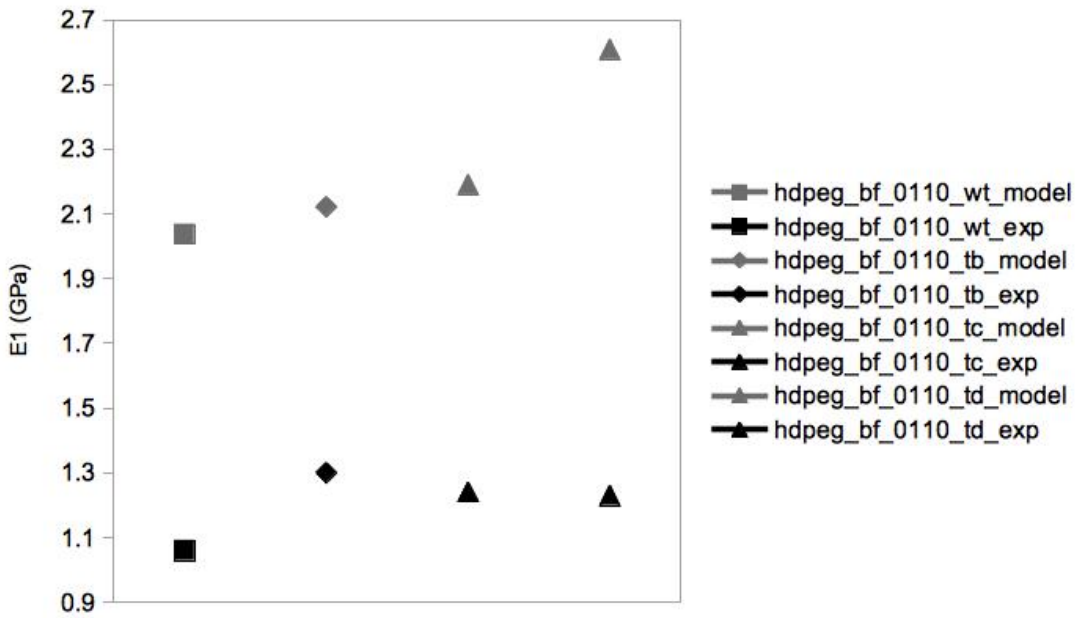

Source: Author.

Figure 6.7 – Mechanical parameter of PEg composites reinforced with non and treated BF0110 [U (0°),C]: (a) tensile strength; (b) elastic modulus; and (c) failure strain

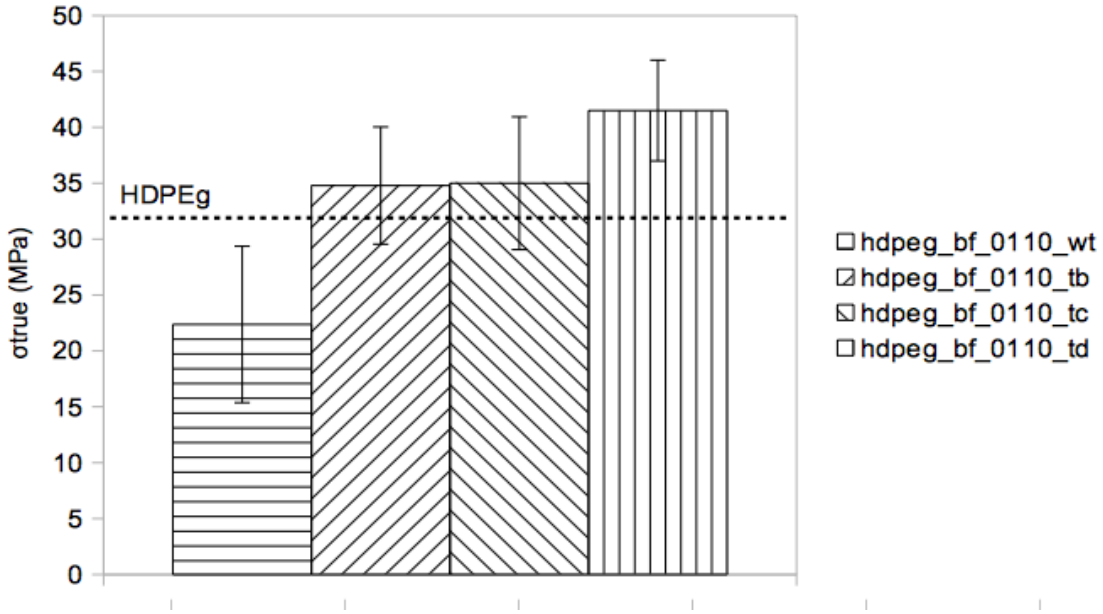

(a)

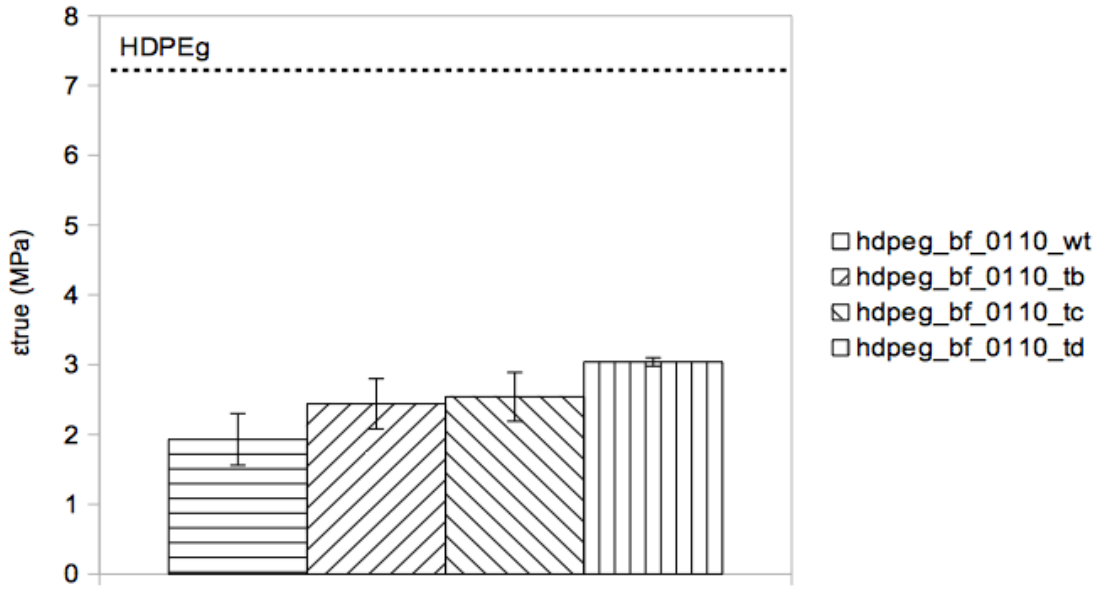

(b)

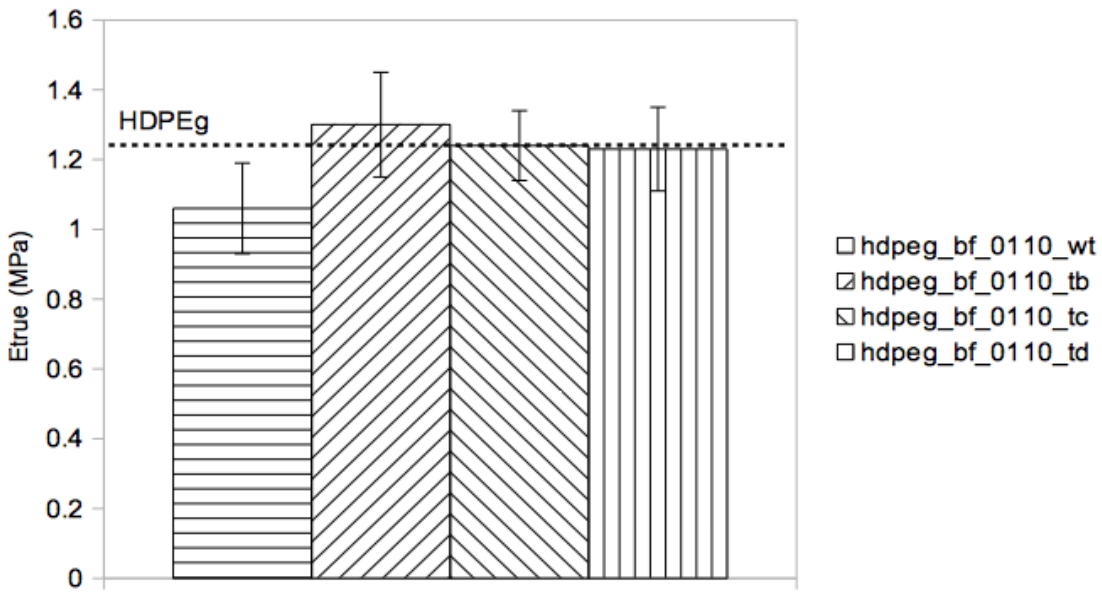

(c)

Source: Author.

6.2.1.2 Influence of some morphological aspects of PEg reinforced with bamboo fibers

Influence of the size of the cross-section area of long bamboo fibers

According to the results in Table 6.5, the addition of long BF1015 to PEg matrix in unidirectionally (0° or fibers oriented in direction of the mechanical solicitation) and in a continuously manner did not improve the mechanical properties of the material – the variability in the strength of the composites did not change either. For the non-treated BF, the maximum stress and the associated strain was lower than the same composite using BF0110. While for the mercerized BF, the composite presented parameter similar to the PEg/BF0110WT. As the composite strength depends on fiber surface area, for the same volume fraction, a composite reinforced with thinner fiber will be stronger than a composite reinforced with thicker fiber (HOSSAIN *et al.*, 2010). Figure 6.8 illustrates the concept of maintaining the same fiber cross-sectional area (A_x) while changing fiber surface area (A_s).

Note that, the volume fraction of the fiber is the same for the BF0110 and BF1015 reinforced composite so that ideally the fiber surface area in the thicker fiber represents half of the fiber surface area in thinner fibers, resulting in less area to be impregnated by the matrix.

Table 6.5 – Mechanical properties of PEg composites reinforced with non-treated and mercerized BF1015 [U (0°),C]

Data	PEg/BF1015WT	PEg/BF1015TC
A_i (mm^2)	43.28 ± 4.39	41.08 ± 3.87
A* (mm^2)	38.18 ± 7.29	37.70 ± 3.65
w_i (mm)	18.67 ± 0.58	18.80 ± 0.84
w* (mm)	17.63 ± 0.67	18.00 ± 0.51
E (GPa)	1.26 ± 0.33	1.35 ± 0.21
ε_{eng_lenght}* (%)	1.27 ± 0.01	1.84 ± 0.21
$\varepsilon_{true_length}$ (%)	1.26 ± 0.01	1.83 ± 0.20
ε_{true_width} (%)	-5.71 ± 3.24	-4.30 ± 2.01
σ_{eng}* (MPa)	16.49 ± 4.17	23.96 ± 3.90
σ_{true} (MPa)	18.65 ± 5.65	26.10 ± 4.23
m	2.54	4.96

* Maximum values.

Source: Author.

Figure 6.8 – Illustration of a simplified concept of composite materials with same volume fraction, where $D_L = 2D_T$

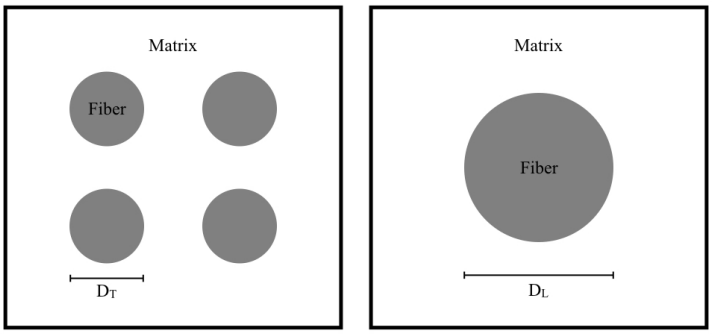

Source: Author.

Figure 6.9 illustrates a comparative of the experimental and calculated elastic modulus E_1 for the PEg composites reinforced with non-treated and mercerized BF1015 continuously aligned in load direction. The values for the composites did not change significantly with the aggressiveness of the BF treatment. Actually, it was expected, since their own elastic modulus did not vary and was smaller than the values of thinner fibers.

According to the results in Table 6.6, the addition of long and non-treated BF0110 to PEg matrix in different directions caused a decrease on its mechanical properties compared to the longitudinal direction, except the BF in braids longitudinally oriented.

Figure 6.9 – Experimental and predicted elastic modulus E_1 of PEg composites reinforced with non-treated and mercerized BF1015 [U (0°),C]

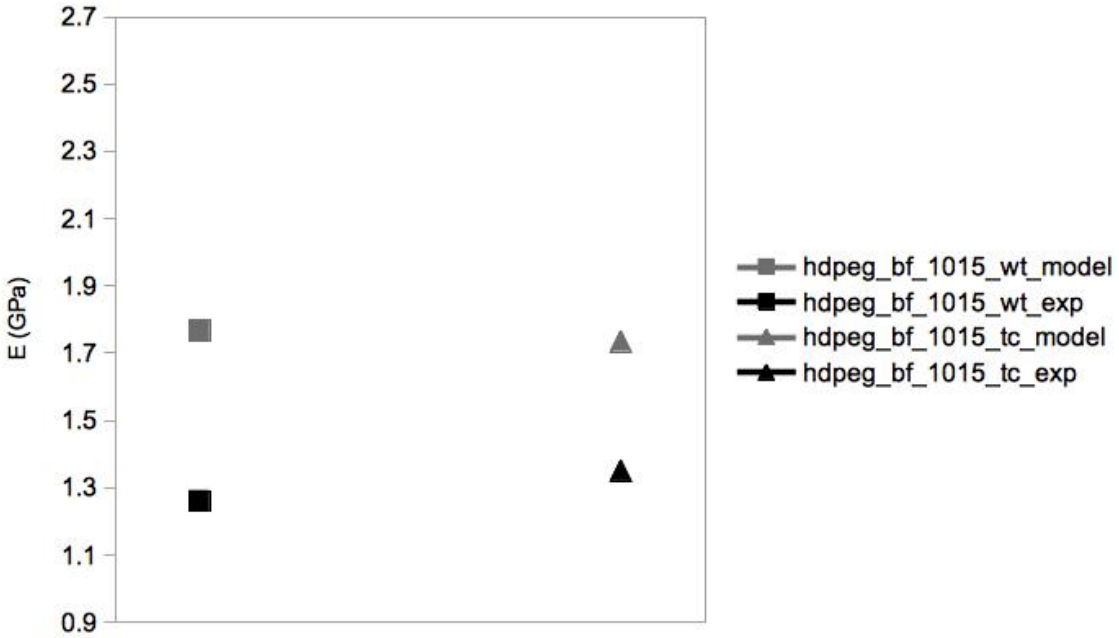

Source: Author.

Influence of long bamboo fibers orientation

Considering the fiber without treatment and oriented in 45°, the composite presented results similar to the one oriented longitudinally (Table 6.6 and Figure 6.10). Despite the greater variability in strength compared to fiber composite at 0° (Figure 6.11), this results suggests that until this degrees of orientation, the mechanical properties of the composite will not differ from the totally straight fibers and the composites can be performed without a rigorous orientation, since they present a natural curvature.

When comparing samples loaded in the direction oriented at 45° from the fibers alignment, it is observed that the two main properties, namely the elastic modulus and the tensile strength are significantly changed in comparison to the previous values for samples loaded in the same direction than that of the fibers. According to other studies, these effects on mechanical properties also can be observed at different fracture modes, like brittle fracture of the matrix and breaking of the fibers gradually depending on the fiber orientation angle. For 0°, the failure presented irregular and the crack propagates in different directions because of the high strength of the fiber in the longitudinal direction. While for 45°, the failure starts by shear and splitting of the matrix parallel to the direction of reinforcement. Not present at this work, but also important for comparison, for 90°, the failure occurs by breaking of the

matrix and the crack propagates in direction perpendicular to the load direction (ABD-ALI & MADEH, 2016; SOUSA, UJIKE & KADOTA, 2016).

Table 6.6 – Mechanical properties of PEg composites reinforced with non-treated BF0110 in different fiber direction

Data	PEg/BF0110WT%	PEg/BF0110WTX	PEg/BF0110WTR	PEg/BF0110WT#
A_i (mm^2)	35.78 ± 0.44	37.39 ± 1.48	38.91 ± 3.21	41.48 ± 1.36
A* (mm^2)	33.50 ± 1.02	35.91 ± 1.72	36.54 ± 3.35	39.61 ± 1.70
w_i (mm)	18.40 ± 0.61	18.92 ± 0.79	18.66 ± 1.27	18.75 ± 0.29
w* (mm)	17.80 ± 0.50	18.54 ± 0.83	18.08 ± 1.26	18.33 ± 0.55
E (GPa)	0.72 ± 0.09	1.46 ± 0.20	0.70 ± 0.04	1.00 ± 0.11
ε_{eng_lenght}* (%)	2.06 ± 0.71	1.82 ± 0.55	1.80 ± 0.22	0.95 ± 0.30
$\varepsilon_{true_length}$ (%)	2.03 ± 0.70	1.80 ± 0.54	1.79 ± 0.22	0.94 ± 0.30
ε_{true_width} (%)	-3.31 ± 1.43	-2.04 ± 0.73	-3.17 ± 1.65	-2.32 ± 1.80
σ_{eng}* (MPa)	14.60 ± 2.99	25.60 ± 8.50	13.20 ± 1.24	8.98 ± 2.63
σ_{true} (MPa)	15.54 ± 2.72	26.73 ± 9.11	14.09 ± 1.58	9.37 ± 2.59
m	4.42	2.66	6.68	2.90

* Maximum values.

Source: Author.

Influence of the long bundles of braided bamboo fibers

If the mechanical properties are at least comparable to braided fabrics, it would be also very interesting for composite reinforcements due to their characteristics, such as multiaxial orientation, conformability, excellent damage tolerance and low cost (FANGUEIRO *et al.*, 2006). For that reason, such type of composite were also characterized and must be considered as a preliminary investigation. Only the fiber without treatment has been investigated. The total yarns were not counted, but some braids with three rovings were prepared. A typical distribution of the fibers in the composite is shown in Figure 6.12.

A typical true strain versus stress curve obtained via tensile test with a load applied in fiber direction is show in Table 6.6 and in Figure 6.13.

Figure 6.10 – Comparison of tensile properties of BF0110 without treatment, PEg matrix, PEg/BF0110WT and PEg/BF0110WT%

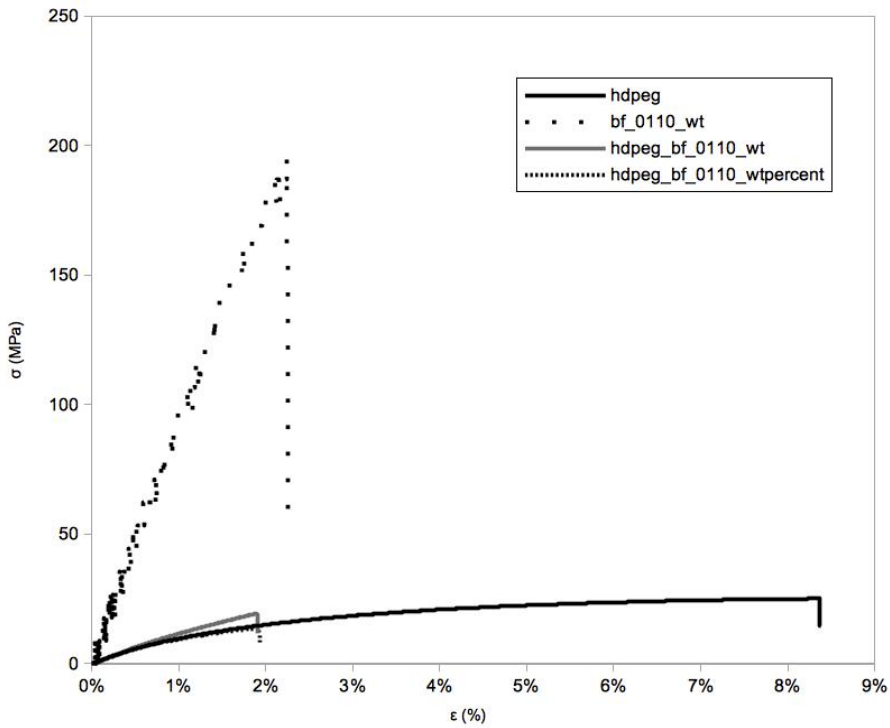

Source: Author.

Figure 6.11 – Weibull distribution of PEg/BF0110WT%, PEg/BF0110WTX, PEg/BF0110WTR and PEg/BF0110WT#

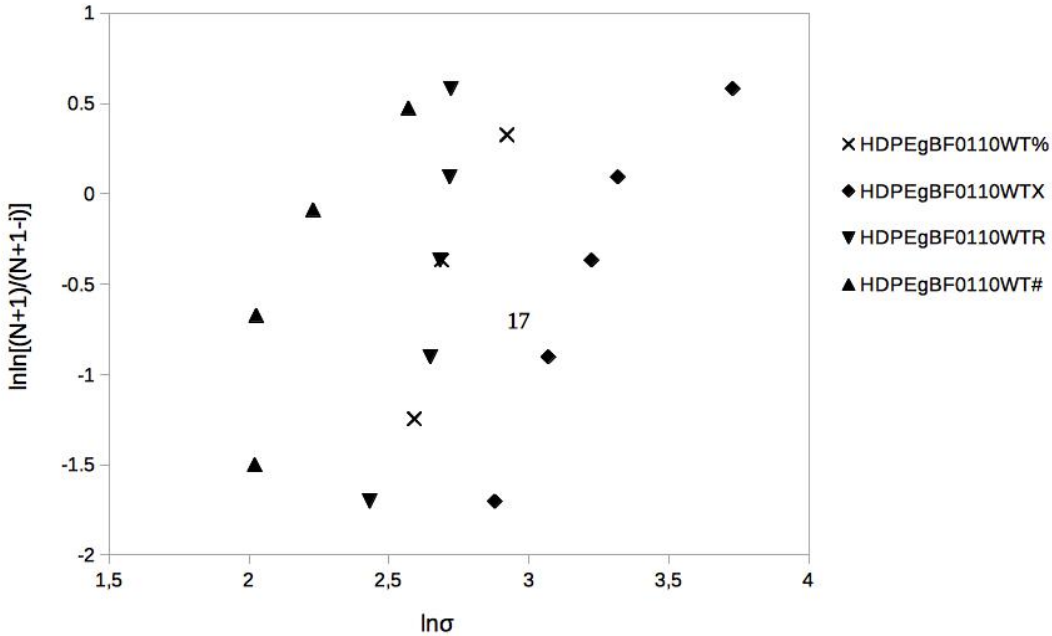

Source: Author.

Figure 6.12 – Sample of Peg/BF0110WTX

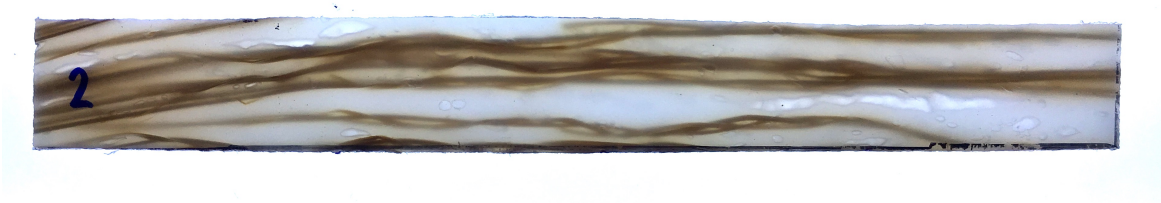

Source: Author.

Figure 6.13 – Comparison of tensile properties of BF0110 without treatment, PEg matrix, PEg/BF0110WT and PEg/BF0110WTX

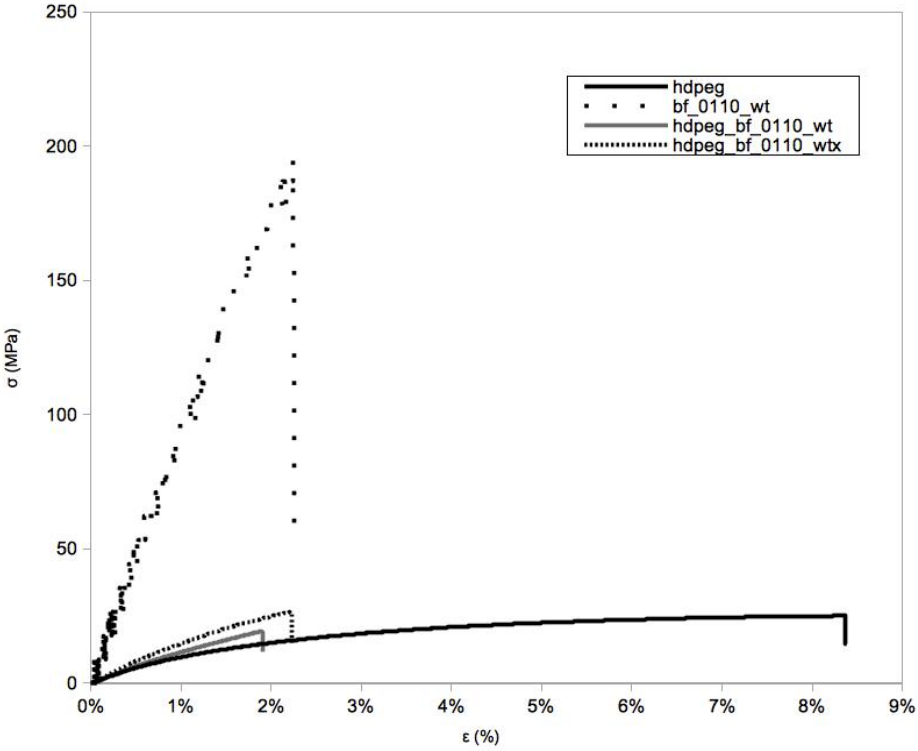

Source: Author.

The increase of the maximum stress is due to higher modulus of braided yarn that carries more loads. This enhancement of the tensile properties of the composites has been observed by RAJESH & PITCHAIMANI (2017). In our study, although the similarity of the variability in strength compared to the 0° fiber composite indicates reproducibility of the values, the results are not better than the PEg/BF0110WT. The low elastic stiffness measured suggests that there are weak interactions between the fibers and matrix, due to the manufacturing process of the plate. Probably, mercerized and acetylated fibers would have

greater interaction with the polymer. Despite this, due to the lack of mobility of the braid, as a set of fibers, the deformation of the composite is very low, because the braid can not deform as a fiber unit. However, when the braids are stretched, the induced waviness of the braided fibers provides a kind of elasticity until the fibers get closer (braid tighter).

Influence of the bamboo fibers length and randomly orientation

For the composites reinforced with short and randomly oriented fibers (PEg/BF0110WTR), it can be seen in Table 6.6 and Figure 6.14 that the tensile strength and the elastic modulus has decreased. As already commented at the literature review, if short fibers are arranged discontinuously and randomly in a composite, the final product can presents an isotropic physical and mechanical properties in the plane of the composite and for the same volume fraction content of fibers. These values parameters are normally lower than the composite with long fibers (MELO, 2016; MALLICK, 2007). The comparison between the values, calculated and obtained experimentally, follow the same difference presented by the previously demonstrated composites. In addition, the Weibull modulus indicated high variability of tensile strength values.

Influence of bamboo fibers oriented in 0 and 90°

For the composite systems consisting of two phases, with continuous reinforcements, part of fibers oriented in the loading direction and part of fiber oriented in the perpendicular direction (PEg/BF0110WT#), the mechanical properties was the worst. As can be observed in Figure 6.15, the composite presented many defects due to the fibers organization, presenting as a tension accumulation and easily breaking. For the elastic modulus evaluation, this composite can be represented by Equation 6.4, with k_{reinf} = ½, remaining between the two extreme mixture models, the Voigt model, with k_{reinf} = 1 (upper limit), and the Reuss model (lower limit) (FREIRE, MONTEIRO & CYRINO, 1994). This last corresponds to the case where the composite is request in transverse direction (E_2), represented by Equation 6.5. This model assumes that the fibers and matrix experience the same stress when the composite is loaded in the direction transverse to the fibers (OSAKA & ONUKWULI, 2018).

$$E_2 = \frac{E_f . E_m}{E_f . V_m + E_m . V_f}$$ **Equation 6.5**

Figure 6.14 – Comparison of tensile properties of BF0110 without treatment, PEg matrix and PEg/BF0110WTR

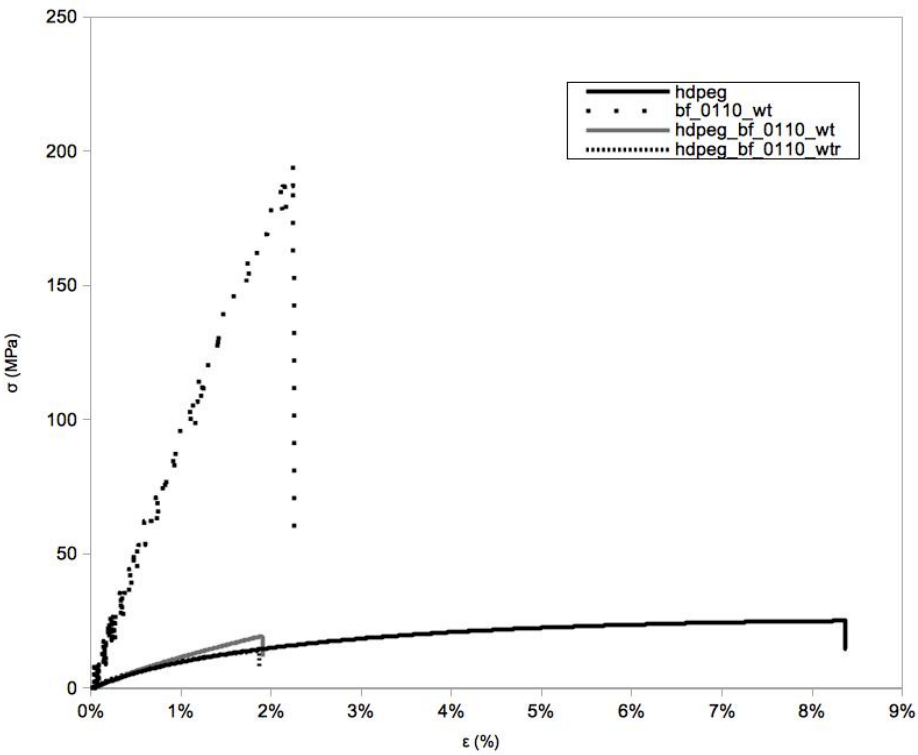

Source: Author.

Figure 6.15 – Post tensile test samples of PEg/BF0110WT#

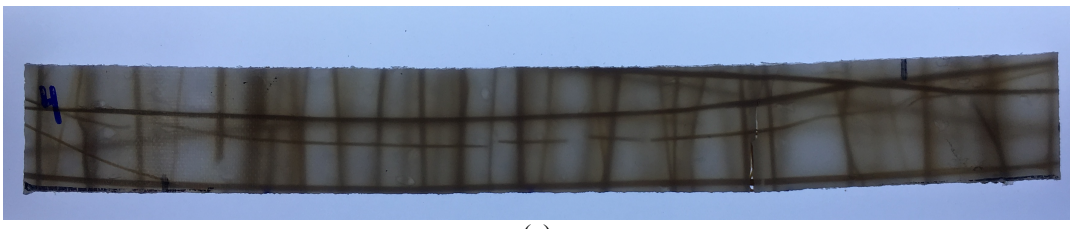

(a)

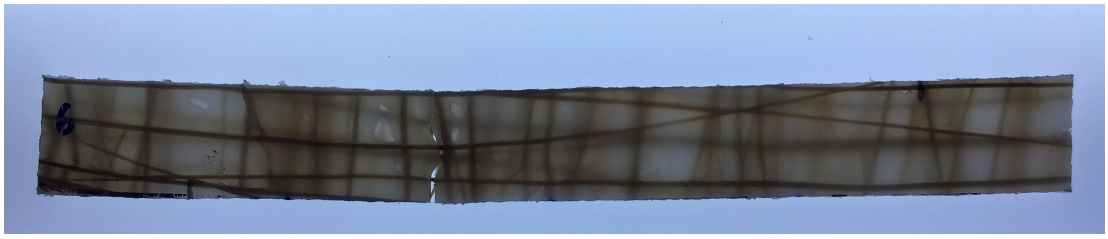

(b)

Source: Author.

Table 6.7 presents a comparison between the elastic modulus calculated and experimentally obtained for PEg/BF0110WT# and the extreme values calculated for the same volumetric fiber fraction reinforcing a composite. According to the difference between the experimental and calculated elasticity moduli previously observed, it can be observed that the modeled elastic modulus of PEg/BF0110WT# is between the modeled value of PEg/BF0110WT and the theoretical PEg/BF0110WT_, inducing that the its experimental elastic modulus is also between the maximum and minimum experimental values.

Table 6.7 – Comparative between Young's modulus of PEg/BF0110WT# and calculated Young's modulus using Voigt model (PEg/BF0110WT) and Reuss model (theoretical Peg/BF0110WT_)

Material	**E (experimental) (GPa)**	**E (Equation 4.20) (GPa)**	**E (Equation 4.25) (GPa)**
PEg/BF0110WT	1.06 ± 0.13	2.04 (k_{reinf} = 1)	-
PEg/BF0110WT#	1.00 ± 0.11	1.57 (k_{reinf} = ½)	-
PEg/BF0110WT_	-	-	1.34

Source: Author.

Figure 6.16 presents comparisons between the BF, the matrix and the performed composite PEg/BF0110WT#. In all cases, the matrix has the higher failure strain, but also it fail first. During the tensile test of composites, above the maximum stress presented by the matrix, it starts to undergo microcracking. The composite subsequently extends with little further increase in the applied stress. As matrix cracking continues, the load is transferred progressively to the fibers until it will be carried entirely by them (HULL & CLYNE, 1996).

Figure 6.16 – Comparison of tensile properties of BF0110 without treatment, PEg matrix and PEg/BF0110WT#

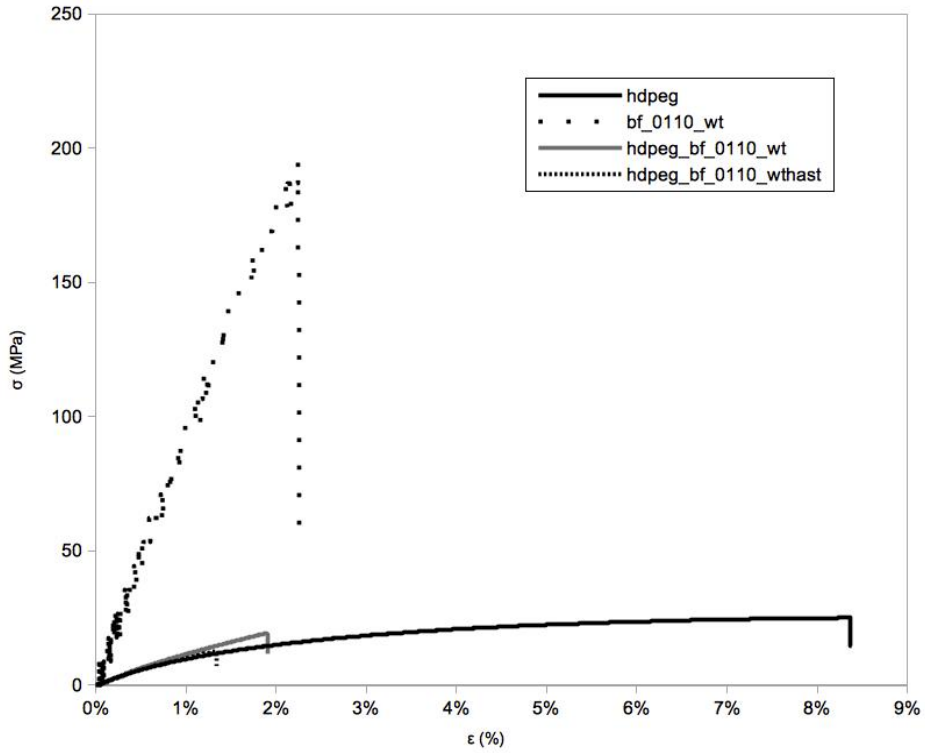

Source: Author.

7 CONCLUSIONS AND PERSPECTIVES

This study was motivated by the development of environment friendly composites based on PEg reinforced by bamboo fibers. For such composites, the fibers played two roles: i) replacing a part of the PEg by a natural vegetable product that is easy to product, to reprocess or eliminate after use, reducing the quantity of polymeric material without reducing its mechanical properties; and/or ii) improving the physical and mechanical properties of the composite material. Bearing these considerations in mind, this study presented encouraging results for the application of treated BF as reinforcement in green polymeric composites.

The treatments improve the mechanical performance of the fibers and facilitate the impregnation by the polymeric resin. Consequently, slightly improved mechanical properties of the composite are obtained comparing to those without treated bamboo fibers.

Various morphological and physical parameters of the basic compounds (PEg and fibers) and the composites was determined, such as mass variation of BF after the treatments, average diameter of BF, apparent and bulk densities of BF, porosity and pore size of BF, and swelling index of the PEg plate and composites reinforced with BF. In general, the fibers presented very sensitive to the treatments. In particular a significantly mass variation was observed according to the aggressiveness of the processing. The size of the BF were characterized, in particular to correlate the cross-section shape with others properties measured in this part or in the composite. It was found that non-circular shape can be considered as a second-order effect on some properties in comparison to the influence of other parameters, such as the proper dimension. The densities and the porosity of thinner fibers were increased with aggressiveness of the treatments, justified by the fact that they were naturally more compact. In general, the mercerization caused size pore growing, increasing the percentage of macropores. Moreover, the acetylation induced the appearance of new mesopores, changing the percentage of macropores and, this way, resulting in a decrease of average diameter of the presented pores in BF. Due to the hydrophilic character of natural fibers, the penetration of water molecules inside the composite material was favored, as demonstrated by the kinetics of the diffusion processes. The results also suggested that the interaction between matrix and treated fibers were improved, reducing any empty spaces between them that might allow some contact with moisture.

Other aspects were observed qualitatively, such as irregularities at the fiber surface, presence of impurities and their cleaning after the BF treatments. Also the presence of

defects, such as some voids, at the composites were observed.

Concerning the mechanical behavior of the materials, some parameters such as elastic modulus, maximum tensile strength and maximum tensile strain were determined. The dimension and the surface treatments of BF directly influenced the mechanical properties. Larger cross-sectional area BF presented lower mechanical parameters, but, for them, the treatments had not a significative influence. Thinner fibers presented as less dense and less rigid, resulting in a greater deformation and elasticity. Even presenting improvement, the mechanical properties could be better when using other processes of acquiring fibers, such as chemical isolation, or even using other types of bamboo units, such as vascular bundles, fibers bundles and bamboo strips (WANG & CHEN, 2017).

According to the mechanical behavior of the performed composites, the addition of long fibers in matrix, unidirectionally and in a continuously manner, promoted a strengthening on its properties, transferring capacity of the efforts in the matrix to the reinforcement. This behavior was also increased with the aggressiveness of the BF treatments. Even though, the composite maximum strain was smaller than the average value for the matrix, it also increased with the performed treatments, indicating an improved fiber/matrix interaction. On the other hand, the elastic modulus values of the composites were not directly affected. The trend can be roughly explained using a simple micro-mechanical models based on mixture rule law. For long and larger BF reinforcing PEg, also unidirectionally and in a continuously manner, the mechanical properties of the material were not improved. This occurred because the composite strength depends on fiber surface area; that is, for the same volume fraction, a composite reinforced with thinner BF will be stronger than the one reinforced with larger fibers.

Evaluating the fiber orientation, it was possible to confirm that aligned continuous fibers presented a higher tensile strength when a load was applied along the direction of the fibers. Also important is the fiber length: the tensile strength increased with the fiber length (MALLICK, 2007; MELO, 2016). For the composites reinforced with short fiber discontinuously and randomly arranged, the final material presented an isotropic mechanical and physical parameters in the composite plane. Also, lower values of mechanical properties were observed when compared with the long fiber in any arrangement direction. Analyzing the composites bidirectionally reinforced, the results were the lowest, however they were within expected ranges.

According to the obtained results, it was found that the produced composites were

light and presented good mechanical properties, while steels, commonly used in the automotive industry, despite having high yield strength, are very heavy. This indicates that the use of natural fiber reinforced polymer composites in the automotive industry can reduce overall weight and fuel consumption. Thus, for the initial application in the faring and internal car finishes, the PEg composites reinforced with mercerized and acetylated long bamboo fibers presented themselves as possible and seemingly viable innovation.

7.1 Suggestions for future works

The results obtained during this work suggests future researches. In particular in:

- To utilize fibers with different volume fractions in the polymeric matrix, in order to evaluate mechanical parameters changes;
- To make or manufacture composites with bamboo fibers obtained by different processes, such as by chemical isolation;
- To refine the plate production method by compression molding in order to decrease the amount of voids inside the material, in order to obtain properties with low standard deviation values;
- To study parameters that were not evaluated at this study, such as: multiaxial behavior flexural modulus, biodegradability and thermal stability;
- To evaluate theoretical model to predict the mechanical properties of the studied composites;
- To evaluate the use of different phase compatibilizers, modifying not only the dispersed phase, but also the continuous one. It is also indicated that a third compatibilizing phase is inserted between fiber and matrix, creating a compatibilizing surface.

REFERENCE

ABD-ALI, Nabel Kadum; MADEH, Ahmed Raee. Effect of fiber orientation angles on mechanical behavior of car bumper composite. **Kufa Journal of Engineering**, v. 7, n. 3, p. 27-37, 2016.

ASSOCIAÇÃO BRASILEIRA DA INDÚSTRIA DE PLÁSTICO. **Perfil 2014**. Indústria Brasileira de Transformação de Material Plástico, 2015. Available at: <http://file.abiplast.org.br/download/links/2015/perfil_abiplast_2014_web.pdf>. Access on: October 6th 2017.

ADEKUNLE, Kayode Feyisetan. Surface treatments of natural fibers – A review: Part 1. **Open Journal of Polymer Chemistry**, v. 5, p. 41-46, 2015.

ADEKUNLE, Kayode; AKESSON, Dan; SKRIFVARS, Mikael. Biobased composites prepared by compression molding with a novel thermoset resin from soybean oil and a natural-fiber reinforcement. **Journal of Applied Science**, v. 116, n. 3, p. 1759-1765, 2010.

AGARWAL, Bhagwan D.; BROUTMAN, Lawrence J.; CHANDRASHEKHARA, K. **Analysis and performance of fiber composites**, 4th ed., New Jersey: John Wiley & Sons, 2006. 576 p.

AL-OQLA, Farias M.; SALIT, Mohd Sapuan; ISHAK, Mohamed Ridzwan; AZIZ, Nuraini Abdul. Selecting natural fibers for bio-based materials with conflicting criteria. **American Journal of Applied Sciences**, v. 12, n. 1, p. 64-71, 2015.

ALVES, Cristiano; SILVA, Arlindo; REIS, Luis; FERRAO, Paulo; FREITAS, Manuel José. Chapter 14 – Sustainable Design of Automotive Components Through Jute Fiber Composites: An integrated approach. *In:* CHIABERGE, Marcello. **New Trends and Developments in Automotive Industry.** InTech, 2011.

ALVIN, Kenneth L.; MURPHY, Richard James. Variation in fibre and parenchyma wall thickness in culms of the bamboo Sinobambusa tootsik. **International Association of Wood Anatomists Bulletin**, v. 9, n. 4, p. 353-361, 1988.

AMIDON, Thomas Edward; WOOD, Christopher D.; SHUPE, Aalan M.; WANG, Yang; GRAVES, Mitchell; LIU, Shijie. Biorefinery: Conversion of woody biomass to chemicals, energy and materials. **Journal of Biobased Materials and Bioenergy**, v. 2, n. 2, p. 100-120, 2008.

ANDERSON, T. L. **Fracture mechanics – Fundamentals and applications**, 3rd ed., Boca Raton: Taylor & Francis, 2005. 640 p.

ANDRADES, R. C; PEREIRA, N. C. Influência da mercerização nas propriedades dinâmico mecânicas de compósitos de polietileno de alta densidade reforçado com fibras de juta. *In:* 13° CONGRESSO BRASILEIRO DE POLIMEROS, 2015, Natal. **Anais…** Natal: 13° CBPOL, 2015.

AQUINO, Regina Coeli Martins Paes. **Desenvolvimento de compósitos de fibras de**

piaçava da espécie *Attalea funifera mart* e matriz de resina poliéster. 2003. 139 f. Tese (Doutorado em Engenharia e Ciências de Materiais) – Centro de Ciências e Tecnologia, Universidade Estadual do Norte Fluminense, Campos dos Goytacazes, 2003.

ARAUJO, A. V. C.; SCIENZA, L. C.; SOARES, A. L. A.; MARTINS, V. Avaliação do efeito do reprocessamento nas propriedades térmicas do polietileno de alta densidade (PEAD) verde por calorimetria exploratória diferencial (DSC). *In:* 5° CONGRESSO INTERNACIONAL DE TECNOLOGIA PARA O MEIO AMBIENTE, 2016, Bento Gonçalves. **Anais…** Bento Gonçalves: 5° CITMA, 2016.

ARAUJO, Joyce Rodrigues de. **Compósitos de polietileno de alta densidade reforçados com fibra de curaua obtidos por extrusão e injeção.** 2009. 141 f. Dissertaçao (Mestrado em Quimica) – Instituto de Quimica, Universidade Estadual de Campinas, Campinas, 2009.

ASHBY, Michael F. **Materials Selection in Mechanical Design**, 2nd ed., Burlington: Butterworth-Heinemann, 1999. 624 p. chapter 3.

ASHBY, Michael F.; JONES, David R. H. **Engineering Material 2: An Introduction to Microstructures**, 3rd ed., Oxford: Butterworth-Heinemann, 2006. 576 p. chapter 25.

ASTM D3039. **Standard Test Method for Tensile Properties of Polymer Matrix Composite Materials**, ASTM International, West Conshohocken, PA.

ASTM D638. **Standard Test Method for Tensile Properties of Plastics**, ASTM International, West Conshohocken, PA.

ASTM D6400-04. **Standard Specification for Compostable Plastics**, ASTM International, West Conshohocken, PA, 2004.

ASTM D6866-18. **Standard Test Method for Determining the Biobased Content of Solid, Liquid, and Gaseous Samples Using Radiocarbon Analysis**, ASTM International, West Conshohocken, PA, 2018.

BACCHI, Renato Vieira. **Análise das imagens de ruptura de corpos de prova de polipropileno em ensaios de tração obtidas através de câmera de alta viscosidade.** 2011. 74 f. Dissertaçao (Mestrado em Quimica) – Instituto de Quimica, Universidade Estadual de Campinas, 2011.

BARBOSA, Anderson de Paula. **Características estruturais e propriedades de compositos poliméricos reforçados com fibras de buriti.** 2011. 141 f. Tese (Doutorado em Engenharia e Ciências de Materiais) – Centro de Ciência e Tecnologia, Universidade Estadual do Norte Fluminense Darcy Ribeiro, Campos dos Goytacazes, 2011.

BARROS, Alysson Régis de Freitas. **Compósitos híbridos: Desenvolvimento de configuração e efeitos de umidificação.** 2006. 110 p. Dissertaçao (Mestrado em Engenharia Mecânica) – Programa de Pos-graduaçao em Engenharia Mecânica, Centro de Tecnologia, Universidade Federal do Rio Grande do Norte, Natal, 2006.

BAUMGART, F. Stiffness – an unknown world of mechanical science? **Injury**, v. 31, p. SB14-SB23, 2000.

BECKERMANN, G. W.; PICKERING, K. L. Engineering and evaluation of hemp fibre reinforced polypropylene composites: Fibre treatment and matrix modification. **Composites: Part A**, v. 39, n. 6, p. 979-988, 2008.

BELLOLI, Rodrigo. **Polietileno verde do etanol da cana-de-açucar brasileira. Biopolímero de classe mundial.** 2010. 34 f. Monografia (Graduaçao em Engenharia Quimica) – Departamento de Engenharia Quimica, Faculdade de Engenharia, Universidade Federal do Rio Grande do Sul, Porto Alegre, 2010.

BHATTACHARYA, Sati N.; KAMAL, Musa R.; GUPTA, Rahul K. **Polymeric Nanocomposites: Theory and Practice**, Cincinnati: Hanser, 2007. 396 p. chapter 1.

BISANDA, Elias T. N.; ANSELL, Martin P. The effect of silane treatment on the mechanical and physical properties of sisal-epoxy composites. **Composites Science and Technology**, v. 41, n. 2, p. 165-178, 1991.

BLEDZKI, Andrzej K.; GASSAN, J. J. Composites reinforced with cellulose based fibers. **Journal of Progress in Polymer Science**, v. 24, n. 2, p. 221-274, 1999.

BLEDZKI, Andrzej. K.; AL-MAMUN, Abdullah; LUCKA-GABOR, M. M.; GUTOWSKI, Voytek. S. The effects of acetylation on properties of flax fibre and its polypropylene composites. **eXPRESS Polymer Letters**, v. 2, n. 6, p. 413-422, 2008.

BLEDZKI, Andrzej K.; REIHMANE, Skaidrite; GASSAN, J. J. Properties and modification methods for vegetable fibers for natural fibers composites. **Journal of Applied Polymer Science**, v. 59, p. 1329-1336, 1996.

BRASKEM. **I'm greenTM**, 201-?a. Available at: <http://www.plasticoverde.braskem.com/site.aspx/Im-greenTM-Polyethylene>. Access on: 6 October 2017.

BRASKEM. **Green polyethylene biopolymer, innovation transforming plastic into sustainability**, 201-?b. Available at: <http://www.braskem.com.br/Portal/Principal/Arquivos/Download/Upload/Catalogo-PE-Verde.pdf>. Access on: 4 December 2017.

BRASKEM. **I'm greenTM Polyethylene. Certifications**, 201-?c. Available at: <http://www.braskem.com/site.aspx/Certifications-pe>. Access on: 22 November 2017.

BRITISH PLASTICS FEDERATION. **Polyethylene (High Density) HDPE**, 201-?. Available at: <http:// www.bpf.co.uk/plastipedia/polymers/HDPE.aspx>. Access on: 4 October 2017.

BRITO, Gustavo F.; AGRAWAL, Pankaj; ARAUJO, Edcleide M.; MELO, Tomas Jeferson A. Biopolímeros, polímeros biodegradáveis e polímeros verdes. **Revista Eletrônica de Materiais e Processos**, v. 6, p. 127-139, 2011.

BURK, Patrick Earl H. **The tensile deformation process of polypropylene at high pressure.** 1999. Thesis (PhD in Applied Science) – Graduate Department of Metallurgy and Material Science, University of Toronto, Toronto, 1999.

CAETANO, L. F.; GRAIFF, A. G.; GARCEZ, E. O.; BERNARDI, S. T.; SILVA FILHO, L. C. P. Compósito de matriz cimêntica reforçada com fibras. *In:* II SEMINARIO DE PATOLOGIA DAS EDIFICAÇOES "Novos Materiais e Tecnologias Emergentes", 2004, Porto Alegre. **Anais…** Porto Alegre, 2004.

CAMPBELL, F. C. **Structural composite materials.** 1st ed. Ohio: ASM International, 2010. 612 p.

ASHBY, Michael F. **Materials Selection in Mechanical Design**, 2nd ed., Burlington: Butterworth-Heinemann, 1999. 624 p. chapter 3.

CANEVALORO JR, Sebastiao V. **Técnicas de caracterização de polímeros.** 1st ed. Sao Paulo: Artliberr, 2004.

CANTWELL, Wesley J.; MORTON, John. The impact resistance of composite materials – A review. **Composites,** v. 22, n. 5, p. 347-362, 1991.

CHANG, Fuxiang; KWON, Jin Heon; KIM, Namhun H.; ENDO, Takashi; LEE, Seung Hwan. Effect of hot-compressed water treatment of bamboo fiber on the properties of polypropylene/bamboo fiber composite. **BioResources**, v. 10, n. 1, p. 1366-1377, 2015.

CHAWLA, Nikhilesh; KERR, M.; CHAWLA, K. K. Monotomic and cyclic fatigue behavior of high- performance ceramic fibers. **Journal of the American Ceramic Society**, v. 88, n. 1, p. 101-108, 2005.

CHEUNG, Hoi-Yan.; HO, Mei-po; LAU, Kin-tak; CARDONA, Francisco; HUI, David. Natural fibre-reinforced composites for bioengineering and environmental engineering applications. **Composites: Part B**, v. 40, n. 7, p. 655-663, 2009.

CHODAK, Ivan. High modulus polyethylene fibres preparation properties and modification by crosslinking. **Progress in Polymer Science**, v. 23, n. 8, p. 1409-1442, 1998.

CLARKE, John L. **Structural Design of Polymer Composites.** EuroComp Design Code and Handbook. 1st ed. London: E & FN SPON, 1996. 762 p.

CORREIA, M. A. P. **Utilização de bambu na construção.** 2014. 91 p. Dissertaçao (Mestrado Integrado em Engenharia Civil) - Faculdade de Engenharia da Universidade de Porto, 2014.

COSTA, Milene Muniz Eloy. **Estudo da compatibilidade de poli-hidroxibutirato (PHB) para recobrimento de grânulos de uréia**. 2012. 140 f. Dissertaçao (Mestrado em Engenharia Industrial) – Programa de Pos-graduaçao em Engenharia Industrial, Escola Politécnica, Universidade Federal da Bahia, Salvador, 2012.

COSTA, Milene Muniz Eloy; MELO, Santino Loruan S.; SANTOS, Joao Victor M.; ARAUJO, Eduardo A.; CUNHA, Gustavo P.; DEUS, Enio Pontes; SCHMITT, Nicolas. Influence of physical and chemical treatments on the mechanical properties of bamboo fibers. **Procedia Engineering**, v. 200, p. 457-464, 2017.

COUTINHO, Fernanda M. B.; MELLO, Ivana L. DE SANTA MARIA, Luiz C. Polietileno:

Principais tipos, propriedades e aplicações. **Polímeros: Ciência e Tecnologia,** v. 13, n. 1, p. 1-13, 2003.

THE CORPORATE SOCIAL RESPONSIBILITY NEWSWIRE. **Dow and Crystalsev announce plans to make polyethylene from sugar cane in Brazil**, 2007. Available at: <http://www.csrwire.com/press_releases/25930-Dow-and-from-Sugar-Cane-in-Brazil>. Access in: 23 October 2017.

DAI, D.; FAN, M. Chapter 1 – Wood fibres as reinforcements in natural fibre composites: structure, properties, processing and applications**.** *In:* HODZIC, Alma; SHANKS, Robert. **Natural fibre composites:** Materials, Processes and Applications, Woodhead Publishing, 2014.

DAVISON, Brian H.; PARKS, Jerry; DAVIS, Mark F; DOROHOE, Bryon S. Chapter 3 - Plant cell walls: Basics of structure, chemistry, accessibility and the influence on conversion. *In:* WYMAN, Charles E. (Org.). **Aqueous pretreatment of plant biomass for biological and chemical conversion to fuels and chemicals**, 1st ed., West Sussex: Jonh Wiley & Sons, 2013. 566 p.

DEFOIRDT, Nele; BISWAS, Subhankar; VRIESE, Linde De; TRAN, Le Quan Ngoc; ACKER, Joris Van; AHSAN, Qumrul; GORBATIKH, Larissa; VUURE, A. W. Van; VERPOEST, I. Assessment of the tensile properties of coir, bamboo and jute fibre. **Composites: Part A**, v. 41, n. 5, p. 588-595, 2010.

DIHARJO, Kuncoro; PERMANA, Andy; ARSADA, Robbi; ASMORO, Gundhi; BUDIONO, Herru Santosa; FIRDAUS, Yohanes. Effect of acetylation treatment and soaking time to bending strength of sugar palm fiber composite. **AIP Conference Proceedings – International Conference on Enginnering, Science and Nanotechnology.** Indonesia: American Institute of Physics, 2017.

DONNET, Jean-Baptist; BANSAL, Roop Chand. **Carbon Fibers.** 3rd ed., New York: Marcell-Dekker, 1998. 470 p.

DOW CHEMICAL. **Santa Vitoria Açúcar e Álcool inicia as operaçoes da planta de etanol**, 2016. Available at: <http://www.dow.com/brasil/noticias/release.aspx?id=253>. Access on: 23 October 2017.

DRZAL, Lawrence T.; RICH, Michael J.; LLOYD, Pamela F. Adhesion of graphite fiber to epoxy matrices: I. The role of fiber surface treatment. **The Journal of Adhesion**, v. 16, n. 1, p. 1-30, 1983.

DVORAK, George J. **Micromechanics of composite materials**, New York: Springer, 2013. 442 p.

EIRAS, Daniel; PESSAN, Luiz Antonio. Mechanical properties of polypropylene/calcium carbonate nanocomposites. **Materials Research**, v. 12, n. 5, p. 517-522, 2009.

FANGUEIRO, Raul; PEREIRA, C. Gonilho; JALALI, Said; ARAUJO, Mario Duarte de. Mechanical properties of braided reinforced composites. *In:* 6a FEIRA INTERNACIONAL DE APLICACIONES TÉCNICAS DE LOS MATERIALES TEXTILES, 2006, Valência.

Anais… Valência: ApliMatec06, 2006.

FARUK, Omar; BLEDZKI, Andrzej K.; FINK, Hans-Peter; SAIN, Mohini. Progress report on natural fiber reinforced composites. **Macromolecular Materials and Engineering**, v. 299, n. 1, p. 9-26, 2012.

FENTAHUN, Mekonnen Asmare; SAVAS, Mahmut Ahsen. Materials used in automotive manufacture and material selection using ashby charts. **International Journal of Materials Engineering**, v. 8, n. 3, p. 40-54, 2018.

FIDELIS, Maria Ernestina Alves. **Desenvolvimento e caracterização mecânica de compósitos científicos têxteis reforçados com fibras de juta.** 2014. 266 f. Tese (Doutorado em Engenharia Civil) – Programa de Pos-graduaçao em Engenharia Civil, Instituto Alberto Luiz Coimbra de Pos-graduaçao e Pesquisa de Engenharia, Universidade Federal do Rio de Janeiro, Rio de Janeiro, 2014.

FRANK, Robert R. **Bast and other plant fibres,** Cambridge: Woodhead Publishing Limited, 2005. 397 p.

FREIRE, Estevao; MONTEIRO, Elisabeth E. C.; CYRINO, Julio C. R. Propriedades mecânicas de compositos de polipropileno com fibra de vidro. **Polímeros**, v. 4, n. 3, p. 25-32, 1994.

FRIEDRICH, Klaus; BREUER, Ulf. Chapter 4 – Natural fibers: Theur composites and flammability characterization. *In:* **Multifunctionality of Polymer Composites,** 1st ed., William Andrew, 2015. 996 p.

FROLLINI, Elisabete; PAIVA, Jane M. F.; TRINDADE, Wanderson G.; RAZERA, Ilce A. Tanaka; TITA, Sandra P. Chapter 12 – Plastics and composites from lignophenols**.** *In:* WALLENBERGER, Frederick T.; WESTON, Norman. **Natural Fibers, Plastics and Composites**, Massachusetts: Kluwer Academic Publishers, 2004. 370 p.

FU, Shao-Yun; HU, Xiao; YUE, Chee-Yoon. Effects of fiber length and orientation distributions on the mechanical properties of short-fiber reinforced polymers: A review. **Materials Science Research International**, v. 5, n. 2, p. 74-83, 1999.

FU, Shao-Yun; LAUKE, Bernd; MAI, Yiu-Wing. Chapter 2 – Extrusion compounding and injection moulding**.** *In:* **Science and Engineering of Short Fibre Reinforced Polymer Composites**, 1st ed., Woodhead Publishing Limited, 2009. 364 p.

GABRIEL, L. H. **Chapter 1 – History and Physical Chemistry of HDPE**, 2010. Available at: <http://www.plasticpipe.org/pdf/chapter-&_history_physical_chemistry_hdpe.pdf>. Access on: 4 December 2017.

GAMSTEDT, E. Kristofer; SKRIFVARS, Mikael; JACOBSEN, Torben K.; PYRZ, Ryszard. Synthesis of unsaturated polyesters for improved interfacial strength in carbon fibre composites. **Composites: Part A**, v. 33, n. 9, p. 1239-1252, 2002.

GASSAN, Jochen; BLEDZKI, Andrzej K. Alkali treatment of jute fibers: Relationship between structure and mechanical properties. **Journal of Applied Polymer Science**, v. 71, n.

4, p. 623-629, 1999.

GECKELER, Kurt E.; RUPP, Frank; GEIS-GERSTORFER, Jürger. Interfaces and interphases of (bio)materials: Definitions, structures and dynamics. **Advanced Materials**, v. 9, n. 6, p. 513- 518, 1997.

GENEROSO, Andressa Leal; SANTOS, Jardel Oliveira; CARVALHO, Virginia Silva; SACOMAN, Nayara Niele; RODRIGUES, Rosana. Proposal for qualitative and quantitative descriptors to characterize bamboo germplasm. **Revista Ciência Agronômica**, v. 47, n. 1, p. 47-55, 2016.

GOMES, Maycon de Almeida. **Propriedades mecânicas de compositos poliméricos reforçados com fibras de folhas de abacaxizeiro (PALF).** 2015. 138 f. Tese (Doutorado em Engenharia e Ciência de Materiais) – Centro de Ciências e Tecnologia, Universidade Estadual do Norte Fluminense, Campos dos Goytacazes, 2015.

GOTRO, Jeff. Polymer composites. Part 3: Common reinforcements used in composites. *In:* **Polymer Innovation Blog**, 2016. Available at: <http://www.polymerinnovationblog.com/polymer-composites-part-3-common-reinforcements-used-composites/>. Access on: 4 December 2017.

GU, J. J.; HE, Qichang C. Exact connections between the effective elastic modulli of fibre-reinforced composites with general imperfect interfaces. **International Journal of Solids and Structures**, v. 104-105, p. 65-72, 2017.

GUIMARÃES Jr., Mario; BOTARO, Vagner Roberto; NOVACK, Katia Monteiro; FLAUZINO NETO, Wilson Pires; MENDES, Lourival M.; TONOLI, G. H. D. Preparation of cellulose nanofibrils from bamboo pulp by mechanical defibrillation for their applications in biodegradable composites. **Journal of Nanoscience and Nanotechnology**, v. 15, n. 9, p. 1-18, 2015.

GUIMARÃES Jr., Mario; NOVACK, Katia Monteiro; BOTARO, Vagner Roberto. Caracterização anatômica da fibra de bambu (*Bambusa vulgaris*) visando sua utilização em compositos poliméricos. **Revista Iberoamericana de Polímeros**, v. 11, n. 7, p. 442-456, 2010.

HALLAL, Ali; ELMARAKBI, Ahmed; SHAITO, Ali; EL-HAGE, Hicham. Chapter 1 – Overview of composite materials and their automotive applications**.** *In:* ELMARAKBI, Ahmed. **Advanced Composite Materials for Automotive Applications:** Structural integrity and crashworthiness, West Sussex: John Wiley & Sons, 2013. 472 p.

HANKEN, R. B. L.; AGRAWAL, P.; OLIVEIRA, A. D. B; MELO, T. J. A. Propriedades mecânicas e reológicas de bionanocompósitos de BIOPE/vermiculita organofílica. *In:* 21° CONGRESSO BRASILEIRO DE ENGENHARIA E CIÊNCIAS DOS MATERIAIS, 2014, Cuiaba. **Anais…** Cuiaba: 21° CBECIMAT, 2014.

HASHIN, Zvi. Thermoelastic properties of fiber composites with imperfect interface. **Mechanics of Materials**, v. 8, n. 4, p. 333-348, 1990.

HILL, Callum A. S.; ABDUL KHALIL, H. P. S.; HALE, Mike David. A study of the potential

of acetylation to improve the properties of plant fibres. **Industrial Crops and Products**, v. 8, n.1, p. 53-63, 1998.

HOLLAWAY, L. **Polymer Composites for Civil and Structural Engineering.** 1st ed., New Delhi: Springer Science+Business Media Dordrecht, 1993. 259 p.

HOSSAIN, N. M.; MILLIREN, E. C.; WOO, Kyeongsik; JENKINS, C. H. The effect of fiber diameter on the strength of lightweight composites. *In:* 51st STRUCTURES, STRUCTURAL DYNAMICS AND MATERIALS CONFERENCE, 2010, Orlando. **Annals…** Orlando: 51st AIAA/ASME/AHS/ASC, 2010.

HUDA, Masud S.; DRZAL, Lawrence T.; MOHANTY, Amar K.; MISRA, Manjusri. Effect of fiber surface- treatments on the properties of laminated biocomposites from poly(lactic acid) (PLA) and kenaf fibers. **Composites Science and Technology**, v. 68, n. 2, p. 424-432, 2008.

HULL, Derek; CLYNE, T. W. **An introduction to composite materials**. 2nd ed., New York: Cambridge University Press, 1996. 326 p.

HULT, J. Chapter 1 – Introduction**.** *In:* HULT, J.; RAMMERSTORFER, F. G. **Engineering Mechanics of Fibre Reinforced Polymers and Composite Structures**, New York: Springer-Verlag Wien, 1994. 314 p.

IMRE, Balazs; PUKANSZKY, Bela. Compatibilization in bio-based and biodegradable polymer blends. **European Polymer Journal**, v. 49, n. 6, p. 1215-1233, 2013.

INCOMPLAST. **Polietileno (PEAD)**, 1977 Available at: <http://www.incomplast.com.br/polietileno-pead>. Access on: 4 December 2017.

JAHAN, Arfin; RAHMAN, M. Mahbubur; KABIR, Humayun; KABIR, Alamgir; AHMED, Farid; HOSSAIN, Abul; GAFUR, A. Comparative study of physical and elastic properties of jute and glass fiber reinforced LDPE composites. **International Journal of Scientific & Technology Research**, v. 1, n. 10, p. 68-72, 2012.

JESSON, David A.; WATTS, John F. The interface and interphase in polymer matrix composites: Effect on mechanical properties and methods for identification. **Polymer Reviews**, v. 52, n. 3, p. 321-354, 2012.

JOHN. Maya Jacob; ANANDJIWALA, Rajesh D. Recent developments in chemical modification and characterization of natural fiber-reinforced composites. **Polymer Composites**, v. 29, n. 2, p. 187-207, 2008.

KAKROODI, A. R.; KAZEMI, Y.; CLOUTIER, A.; RODRIGUE, D. Chapter 9 – Mechanical performance of polyethylene (PE)-based biocomposites. *In:* MISRA, Manjusri; PANDEY, Jitendra Kumar; MOHANTY, Amar. **Biocomposites: Design and Mechanical Performance**, Elsevier, 2015. 524 p.

KALIA, Susheel; KAITH, Balbir Singh; KAUR, Inderjeet. Pretreatments of natural fibers and their application as reinforcing material in polymer composites: A review. **Polymer Engineering and Science**, v. 49, n. 7, p. 131-135, 2009.

KARMAKAR, S. R. Chapter 9. Mercerization. *In:* **Textile Science and Technology:** Chemical Technology in the Pre-treatment Processes of Textiles, Elsevier, 1999. DOI: 10.1016/s0920-4083(99)80010-3.

KUSHWAHA, Pradeep K.; KUMAR, Rakesh. Studies on water absorption of bamboo-polyester composites: Effect of silane treatment of mercerized bamboo. **Polymer-Plastics Technology and Engineering**, v. 49, n. 1, p. 45-52, 2010.

JAIN, Ravi; LEE, Luke. Chapter 1. Introduction. *In:* **Fiber Reinforced Polymer (FRP) Composites for Infrastructure Applications:** Focusing on Innovation Technology Implementation and Sustainability, Dordrecht: Springer Science, 2012. 280 p.

LEVY NETO, Flaminio; PARDINI, Luiz Claudio. **Compósitos estruturais.** Ciências e Tecnologia. Sao Paulo: Edgar Bücher, 2006. 313 p.

LI, Xue; TABIL, Lope G.; PANIGRAHI, Satyanarayan. Chemical treatments of natural fiber for use in natural fiber-reinforced composites: A review. **Journal of Polymers and the Environment**, v. 15, n. 1, p. 25-33, 2007.

LUO, S.; NETRAVALI, Anil N. Interfacial and mechanical properties of environment-friendly "green" composites made from pineapple fibers and poly(hydroxybutyrate-co-valerate) resin. **Journal of Materials Science**, v. 34, p. 3709-3719, 1999.

MADHUKAR, Madhu S.; DRZAL, Lawrence T. Fiber-matrix adhesion and its effect on composite mechanical properties: I. Inplane and interlaminar shear behavior of graphite/epoxy composites. **Journal of Composite Materials**, v. 25, p. 932-957, 1991.

MALLICK, P. K. **Fiber-reinfoced composites:** Materials, Manufacturing, and Design. 3rd ed., Michigan: Taylor & Francis Group, 2007. 619 p.

MANO, Eloisa Biasotto. **Polímeros como Materiais de Engenharia.** 1a ed., Sao Paulo: Edgar Blücher, 2000. 218 p.

MAR-BAL INCORPORATED. **History of Composite Materials,** 201-?. Available at: <http://www.mar-bal.com/language/en/applications/history-of-composites/>. Access on: 26 September 2017.

MARCOVICH, N. E.; REBOREDO, M. M., ARANGUREN, M. I. Moisture diffusion in polyester-woodflour composites. **Polymer**, v. 40, p. 7313-7320, 1999.

MARINHO, Luis Fernando; ANTUNES, Adelaide Maria de Souza. Chapter 3 – Petroquímica básica. *In:* ANTUNES, Adelaide Maria de Souza. **Setores da Industria Quimica Orgânica,** Rio de Janeiro: E-paper Serviços Editorias Ltda, 2007. 242 p.

MARINHO, Nelson Potenciano; NISGOSKI, Silvana; KLOCK, Umberto; ANDRADE, Alan Sulato de; MUNIZ, Graciela Inês Bolzon de. Analise quimica do bambu-gigante (Dendrocalamus gigantes Wall. ex Munro) em diferentes idades. **Ciência Florestal**, v. 22, n. 2, p. 417-422, 2012.

MARINHO, Nelson Potenciano; NISGOSKI, Silvana; MUNIZ, Graciela Inés Bolzon de.

Avaliação das dimensões das fibras de colmo de bambu, *Dendrocalamus gigantes (Wall) Munro*, em diferentes idades. **Ciência Florestal**, v. 24, n. 1, p. 251-256, 2014.

MASUELLI, Martin Alberto. Chapter 1. Introduction of fibre-reinforced polymers – Polymers and composites: concepts, properties and processes. *In:* MASUELLI, Martin Alberto. **Fiber Reinforced Polymers:** The Technology Applied for Concrete Repair. IntechOpen, 2013. DOI: 10.5772/3162.

MCCUSKER, Lynne B. IUPAC nomenclature of ordered microporous and mesoporous materials ans its application to non-zeolite microporous mineral phase. **Review in Minerology & Geochemistry**, v. 57, n. 1, p. 1-16, 2005.

MELO, Santino Loruan Silvestre de. **Investigação das propriedades mecânicas e adesão interfacial dos compósitos de polipropileno virgem e reciclado reforçados com fibras e microfibras de bambu.** 2016. 81 f. Dissertaçao (Mestrado em Engenharia e Ciência de Materiais) – Programa de Pos-graduaçao em Engenharia e Ciência de Materiais, Departamento de Engenharia Metalurgica e de Materiais, Universidade Federal do Ceara, Fortaleza, 2016.

MIRANDA, Cleidiene S.; FIUZA, Raigenis P.; CARVALHO, Ricardo F.; JOSÉ, Nadia M. Efeito dos tratamentos superficiais nas propriedades do bagaço da fibra de piaçava *Attalia funifera martius*. **Quimica Nova**, v. 38, n. 2, p. 161-165, 2015.

MISHRA, S.; MISRA, Manjusri; TRIPATHY, S. S.; NAYAK, Sanjeev K.; MOHANTY, Amar K. The influence of chemical surface modification on the performance of sisal-polyester biocomposites. **Polymer Composites**, v. 23, n. 2, p. 164-170, 2002.

MISKALO, Eugênio Polistchuk. **Avaliação do potencial de utilização de bambu (Dendrocalamus giganteus) na produção de painéis de partículas orientadas.** 2009. 111 f. Dissertaçao (Mestrado em Engenharia de Materiais) – Programa de Pos-graduaçao em Engenharia Mecânica e de Materiais, Centro de Tecnologia, Universidade Tecnológica Federal do Paraná, 2009.

MOHD YUHAZRI, Y.; PHONGSAKORN, P. T.; SIHOMBING, Haeryip; JEEFFERIE, A. R.; PERUMAL, Puvanasvaran; KAMARUL, A. M.; RASSIAH, Kannan. Mechanical properties of kenaf/polyester composites. **International Journal of Engineering & Technology,** v. 11, n. 1, p. 127-131, 2011.

MOHSENZADEH, Abas; ZAMANI, Akram; TAHERZADE, Mohammad J. Bioethylene production from ethanol: A review and techno-economical evaluation. **ChemBioEng Reviews,** v. 4, n. 2, p. 75-91, 2017.

MONTEIRO, Sergio N.; PERISSÉ, F. D. L.; COSTA, Lucas Lopes da; BEVITORI, Alice Barreto; SILVA, Isabela Leao Amaral da; BARBOSA, A. P. Natural lignocellulosic fibers as engineering materials – An overview. **The Mineral, Metals & Material Society and ASM International**, v. 42A, 2011a.

MONTEIRO, Sergio N.; SATYANARAYANA, K. G.; FERREIRA, A. S.; NASCIMENTO, D. C. O.; LOPES, F. P. D.; SILVA, Isabela Leao Amaral da; BEVITORI, Alice Barreto; INACIO, W. P. BRAVA NETO, J.; PORTELA, T. G. Selection of high strength natural fibers.

Revista Matéria, v. 15, n. 4, p. 488-505, 2011b.

MORRISON III, Wiley Herbert; ARCHIBALD, Douglas Dean; SHARMA, H. Shekhar Sharma; AKIN, Danny E. Chemical and physical characterization of water- and dew-retted flax fibers. **Industrial Crops and Products**, v. 12, n. 1, p. 39-46, 2000.

MOTA, Izabel de Oliveira da; PEREIRA, Michel de Azevedo; DAMACENA, Pedro Coelho; SANTOS, Luis Claudio Belmonte dos. Estudo das propriedades físicas e mecânicas do bambu brasileiro (*Bambusa vulgaris vittata*) para aplicação na construção de sistemas hidráulicos alternativos de distribuição de agua à baixa pressão. **Revista de Estudos Ambientais**, v. 19, n. 1, p. 18-26, 2017.

MOURA, Maria José; FIGUEIREDO, Maria Margarida. Aplicação das técnicas de picnometria de gas e de porosimetria de mercúrio à caracterização da madeira de *E. globulus*. **Silva Lusitana**, v. 10, n. 2, p. 207-216, 2002.

MÜLHAUPT, Rolf. Green polymer chemistry and bio-based plastics: Dreams and reality. **Macromolecular Chemistry and Physics**, v. 214, n. 2, p. 159-174, 2013.

NABI SAHEB, D.; JOG, J. P. Natural fiber polymer composites: A review. **Advances in Polymer Technology**, v. 18, n. 4, p. 351-363, 1999.

NASCIMENTO, Denise Cristina de Oliveira. **Analise das propriedades de compósitos de fibras de piaçava e matriz de resina epoxi.** 2009. Tese (Doutorado em Engenharia de Materiais) – Universidade Estadual do Norte Fluminense, Rio de Janeiro, 2009.

NATIONAL CENTER FOR BIOTECHNOLOGY INFORMATION. Acetic anhydride. *In:* **PubChem Compound Database,** 201-?a. Available at: <http://pubchem.ncbi.nlm.nih.gov/compound/7918>. Acces on: 8 January 2019.

NATIONAL CENTER FOR BIOTECHNOLOGY INFORMATION. Acetic acid. *In:* **PubChem Compound Database,** 201-?b. Available at: <http://pubchem.ncbi.nlm.nih.gov/compound/176>. Acces on: 8 January 2019.

NBR 15448-1. **Embalagens plásticas degradáveis e/ou de fontes renováveis. Parte 1: Terminologia.** [S.l.].

NOHARA, Liliana B.; KAWAMOTO, Aparecida M.; NOHARA, Evandro L.; REZENDE, Mirabel C. Otimização da interface/interfase de compósitos termoplásticos de fibra de carbono/PPS pelo uso do poli(ácido âmico) do tipo BTDA/DDS. **Polímeros: Ciência e Tecnologia**, v. 17, n. 3, p. 180- 187, 2007.

NOVA CANA. **Unica aposta no papel do biometano e do biogas de vinhaça para a matriz energética**, 2017. Available at: <http://www.novacana.com/n/meio-ambiente/unica-aposta-biometano-biogas-vinhaca-matriz-energetica-190917/>. Access on: 17 October 2017.

OKHUYSEN, B.; COCHRAN, R. C.; ALLRED, R. E.; SPOSILI, R.; DONNELLAN, T. M. Interface/interphase studies in epoxy matrix composites. *In:* SHARPE, Louis H. **Adhesion International 1993:** Proceedings of the 16th Annual Meeting of the Adhesion Society, Gordon and Breach Science Publishers Ltd, 1993. 797 p.

OKUBO, Kazuya; FUJII, Toru; YAMAMOTO, Yuzo. Development of bamboo-based polymer composites and their mechanical properties. **Composities: Part A**, v. 35, n. 3, p. 337-383, 2004.

OLIVEIRA, Akidauana Dandara Brito de. **Desenvolvimento de blendas de biopolietilenos verdes PEAD/PELBD.** 2015. 78 f. Dissertaçao (Mestrado em Ciência e Engenharia de Materiais) – Pos-graduaçao em Ciência e Engenharia de Materiais, Centro de Tecnologia, Universidade Federal de Campina Grande, 2015.

OLIVIER, Nelson Cardenas. **Analise de falha da camada polimérica externa de cabos umbilicais.** 2007. 190 f. Tese (Doutorado em Engenharia Mecânica) – Escola Politécnica, Universidade de Sao Paulo, Sao Paulo, 2007.

ONYLKWERE, Okwuchi Smith; IGBOANUGO, A. C.; ADELEKE, Tunde B. Optimization of acetylation parameters for reduced moisture absorption of bamboo fibre using taguchi experimental design and genetic algorithm optimization tools. **Nigerian Journal of Technology**, v. 38, n. 1, p. 104-111, 2019.

OSAKA, Emmanuel C.; ONUKWULI, Okechukwu Dominic. A modified Halpin-Tsai model for estimating the modulus of natural fiber reinforced composites. **International Journal of Engineering Science Invention**, v. 7, n. 5, p. 63-70, 2018.

PACHECO, Livia Julio. **Efeito da temperatura e da taxa de deformaçao no comportamento mecânico do PEAD reciclado.** 2014. 111 f. Tese (Doutorado em Ciências em Engenharia Mecânica) – Universidade Federal Fluminense, Niterói, 2014.

PADILHA, Angelo Fernando. **Materiais de Engenharia:** Microestrutura e propriedades. Curitiba: Hemus Livraria, Distribuidora e Editora S.A., 2000. 343 p.

PALUCKA, T.; BENSAUDE-VINCENT, B. Composites Overview**.** *In:* **History of Recent Science & Technology**, 2002. Available at: <http://www.authors.library.caltech.edu/5456/1/hrst.mit.edu/hrs/materials/public/composites/Composites_Overview.htm>. Access on: 27 September 2017.

PANTHAPULAKKAL, Suhara; SAIN, Mohini. Studies on the water absorption properties of short hemp-glass fiber hybrid polypropylene composites. **Journal of Composite Materials**, v. 41, p. 1871-1883, 2007.

PARDINI, Luiz Claudio; MANHANI, Luiz Guilherme Borzani. Influence of the testing gage length on the strength, Young's modulus and Weibull modulus of carbon fibres and glass fibres. **Materials Research**, v. 5, n. 4, p. 411-420, 2002.

PARK, C. H.; LEE, W. I. Chapter 3 – Compression molding in polymer matrix composites. *In:* ADVANI, Suresh G.; HSIAO, Kuang-Ting. **Manufacturing Techniques for Polymer Matrix Composites (PMCs).** 1st ed., Woodhead Publishing, 2012. 512 p.

PEACOCK, Andrew J. **Handbook of Polyethylene – Structures, Properties and Applications.** 1st ed. New York: Marcel Dekker, 2000. 544 p.

PELAEZ-SAMANIEGO, Manuel Raul; YADAMA, Vikram; LOWELL, Eini; AMIDON,

Thomas E.; CHAFFEE, Timothy L. Hot water extracted wood fiber for production of wood plastic composites (WPCs). **Holzforschung**, v. 67, n. 2, p. 193-200, 2013.

PENNAFORT Jr., Luiz Carlos Gonçalves. **Aplicação da mecânica da danificação na analise do comportamento de materiais compósitos poliméricos reciclados reforçados por fibras de coco.** 2015. Tese (Engenharia e Ciência de Materiais) – Programa de Pos-graduaçao em Engenharia e Ciência de Materiais, Departamento de Engenharia Metalurgica e de Materiais, Universidade Federal do Ceara, Fortaleza, 2015.

PEREIRA, Marco Antonio dos Reis. **Projeto bambu: introduçao de espécies, caracterizaçoao e aplicações.** 2012. Tese (Livre-Docência) – Faculdade de Engenharia de Bauru, Universidade Estadual Paulista "Julio de Mesquita Filho", 2012.

PEREIRA, Marco Antonio dos Reis; BERALDO, Antonio L. **Bambu de corpo e alma**. Canal6, 2007. 352 p.

PERRY, Jonh H. **Chemical Engineers Handbook.** 3rd ed., New York: McGraw-Hill, 1999.

PLASTICS EUROPE. An analysis of European plastics production, demand and waste data. *In:* **Association of Plastics Manufactures.** Plastics Europe, 2015.

PLASTICOMP. Benefits of long fiber reinforced thermoplastic composites. *In:* **Long Fiber Reinforced Thermoplastic Composites**, 201-?a. Available at: <http://www.plasticomp.com/long-fiber-benefits/>. Access on: 30 April 2019.

PLASTICOMP. Design consideration for successfully using long fiber reinforced thermoplastic composites – White Paper. *In:* **Long Fiber Reinforced Thermoplastic Composites.** 201-?b. Available at: <https://www.appliancedesign.com/ext/resources/WhitePapers/2016/PlastiComp-Long-Fiber-Design.pdf/>. Access on: 30 April 2019.

PLASTICS DIVISION OF THE AMERICAN CHEMISTRY COUNCIL. **Plastics and polymer composites technology roadmap for automotive markets**, 2014. Available at: <https://plastics-car.com/Tomorrows-Automobiles/Plastics-and-Polymer-Composites-Technology-Roadmap/Plastics-and-Polymer-Composites-Technology-Roadmap-for-Automotive-Markets-Full_report.pdf>. Access on: 1 September 2019.

POLYMER SCIENCE LEARNING CENTER. **Polyethylene**, 2003 - 2017. Available at: <http://www.pslc.ws/macrog/pe.htm>. Access on: 4 October 2017.

QISHENG, Zhang; SHENXUE, Jiang; YONGEJU, Tang. **Industrial utilization on bamboo.** Beijing: International Network for Bamboo and Rattan - INBAR, Technical Report n°. 26, 2002.

RAJESH, Murugan; PITCHAIMANI, Jeyaraj. Mechanical properties of natural fiber braided yarn woven composite: Comparison with conventional yarn woven composite. **Journal of Bionic Engineering**, v. 14, n. 1, p. 141-150, 2017.

RASSIAH, Kannah; AHMAD, Megat Mohamad Hamdan Megat. A review on mechanical properties of bamboo fibers einforced polymer composite. **Australian Journal of Basic and**

Applied Sciences, v. 7, n. 8, p. 247-253, 2013.

RAY, Dipa; SARKAR, B. K.; RANA, A. K.; BOSE, N. R. Effect of alkali treated jute fibres on composite properties. **Bulletin of Materials Science**, v. 24, n. 2, p. 129-135, 2001.

RAY, P. K.; CHAKRAVARTY, A. C.; BANDYOPADHYAY, S. B. Fine structure and mechanical properties of jute differently dried after retting. **Journal of Applied Polymer Science**, v. 20, p. 1765-1767, 1976.

REIFSNIDER, K. L. **Damage in composite material: Basic mechanisms, accumulation, tolerance, and characterization**. Baltimore: ASTM Special Technical Publication 775, 1982. 280 p.

REIS, Joao M. L.; PACHECO, L. J.; MATTOS, Heraldo S. da Costa. Temperature and variable strain rate sensitivity in recycled HDPE. **Polymer Testing**, v. 39, p. 30-35, 2014.

RIOS, Alexandre de Souza. **Mechanical behavior of recycled polypropylene reinforced by coconut fibers using X-ray tomography and digital image correlation.** 2015. 178 f. Tese (Doutorado em Engenharia e Ciência de Materiais) – Programa de Pos-graduaçao em Engenharia e Ciência de Materiais, Departamento de Engenharia Metalurgica e de Materiais, Universidade Federal do Ceara, Fortaleza, 2015.

RODRIGUEZ, Exequiel S.; STEFANI, Pablo M.; VAZQUEZ, Analia. Effects of fibers' alkali treatment on the resin transfer molding processing and mechanical properties of jute-vinylester composites. **Journal of Composite Materials**, v. 41, n. 14, p. 1729-1741, 2007.

ROUISON, David; COUTURIER, M.; SAIN, Mohini; MACMILLAN, B.; BALCOM, B. J. Water absorption of hemp fiber/unsaturated polyester composites. **Polymer Composites**, v. 26, n. 4, p. 509-525, 2005.

ROY, M. M. Mechanical properties of jute II: The study of chemically treated fibers. **Journal of the Textile Institute Transactions**, v. 4, n.1, p. T44-T52, 1953.

ROYLANCE, David. **Stress-strain curves.** Massachusetts: Institute of Technology, 2001. Available at: <https://ocw.mit.edu/courses/materials-science-and-engineering/3-11-mechanics-of-materials-fall-1999/modules/MIT3_11F99_ss.pdf>. Access on: 13 June 2019.

SAKA, Shiro. Structure and chemical composition of wood as a natural composite material. **Recent Research on Wood and Wood-Based Materials**, p. 1-20, 1993.

SALAM, Kamesh; PONGEN, Zulu. **Handbook on Bamboo.** National Bamboo Mission Ministry of Agriculture, Government of India. Guwahati: Cane and Bamboo Technology Centre, 2008. 45 p.

SANTI, Thais. Bambu para toda obra. **Revista O Papel**, v. 4, p. 22-34, 2015.

SAPUAN, S. M.; ISMAIL, H.; ZAINUDIN, E. S. Chapter 3 – Recent Advances in Polyethylene-Based Biocomposites. *In:* **Natural Fiber Reinforced Vinyl Ester and Vinyl Polymer Composites:** Development, characterization and applications, Woodhead Publishing, 2018. 392 p.

SATYANARAYANA, Kestur Gundappa; GUIMARÃES, José Luis; WYPYCH, Fernando. Studies on lignocellulosic fibers of Brazil. Part I – Source, production, morphology and applications. **Composites: Part A**, v. 38, n. 7, p. 1694-1709, 2007.

SATYANARAYANA, Kestur Gundappa; SUKUMARAN, Kalathil; MUKHERJEE, P. S.; PAVITHRON, Chorappan; PILLAI, Saju Gopalakrishna K. Natural fiber-polymer composites. **Cement & Concrete Composites**, v. 12, n. 2, p. 117-136, 1990.

SCHANG, O.; BILLON, N.; MURACCIOLE, J. M.; FERNAGUT, F.Mechanical behavior of a ductile polyamide 12 during impact. **Polymer Engineering and Science**, v. 36, n. 4, p. 541-550, 1996.

SHARMA, H. S. S.; FRASER, T. W.; MCCALL, D.; SHIELDS, N.; LYONS, G. Fine structure of chemically modified flax fiber. **The Journal of the Textile Institute**, v. 86, n. 4, p. 539-548, 1995.

SHELAT, B. R.; RADHAKRISHNAN, T.; IYER, B. V. The relation between crystallite orientation and mechanical properties of mercerized cottons. **Textile Research Journal**, v. 30, n. 11, p. 836-842, 1960.

SHIMIZY, Felipe Lange. **Remoção de lignina e hemicelulose: Influência na acessibilidade à celulose e sacarificação enzimática.** 2018. 73 f. Dissertaçao (Mestrado em Microbiologia Aplicada) – Pos-graduaçao em Ciências Biologicas, Universidade Estadual Paulista "Julio de Mesquita Filho", 2018.

SIH, G. C.; HILTON, P. D.; BADALIANCE, R.; SHENBERGER, P. S.; VILLARREAL, G. Fracture mechanics for fibrous composites. **Analysis of the Test Method for High Modulus Fibers and Composites**, p. 98-132, 1973.

SILVA, Flavio de Andrade; CHAWLA, Nikhilesh; TOLEDO FILHO, Romildo Dias. Tensile behavior of high performance (sisal) fibers. **Composites Science and Technology**, v. 68, p. 3438-3443, 2008.

SILVA, Isaac Freitas da; PEREIRA, Daniel dos Santos; SILVA, Silvana Rocha Ferreira. Estudos morfológicos do bambu (*Bambus cf. Vulgaris L.*), uma espécie invasora em area de mata atlântica no parque municipal de Maceio-Alagoas. **Revista Semente**, v. 6, n. 6, p. 99-109, 2011.

SILVA, Janaina Teixeira da. **Caracterização citogenética de espécies e variedades de bambu com potencial econômico no Nordeste brasileiro.** 2007. 53 f. Dissertaçao (Mestrado em Ciências Florestais) - Universidade Federal Rural de Pernambuco, 2007.

SILVA, Ronaldo Vinicius da. **Merostachys spreng. (Poaceae: Bambusoideae: Bambuseae: Arthrostylidiinae) no leste do estado de Minas Gerais, Brasil.** 2015. 135 f. Dissertaçao (Mestrado em Botânica) – Programa de Pos-graduaçao em Botânica, Universidade Federal de Viçosa, 2015.

SOUSA, Francisco Kegenaldo Aalves; UJIKE, Isao; KADOTA, Akihiro. Effect of different fiber angles for composite material with fiberglass reinforced on mechanical properties.

International Journal of Mining, Metallurgy & Mechanical Engineering, v. 4, n. 1, p. 1-6, 2016.

SOUZA, Andressa Martinelli de. **Os diversos usos do bambu na construção civil**. 2014. 102 p. Monografia (Graduaçao em Engenharia Civil) – Departamento Acadêmico de Construçao Civil, Universidade Tecnológica Federal do Paraná, 2014.

SPIECKERMANN, Florian Constantin. **Investigation of deformation induced changes of the microstructure of semicrystalline polymers and their impact on mechanical properties.** 2010. 127 f. Thesis (PhD in Science) – Fakultät für Physik, Universität Wien, 2010.

SPILLER, André Luis. **Modelamento da propagação de trinca: Aplicado a compósito particulado de matriz termofixa empregado como guarnição de freio.** 2012. 92 f. Dissertaçao (Mestrado em Engenharia de Minas, Metalurgica e de Materiais) – Programa de Pos-graduaçao em Engenharia de Minas, Metalurgica e de Materiais, Escola de Engenharia, Universidade Federal do Rio Grande do Sul, Porto Alegre, 2012.

SPOLIDORO, Pedro Varajao. **Características dendrométricas e propriedades físicas dos colmos de *Bambus vulgaris e Bambusa tuldoides*.** 2008. 55 f. Monografia (Graduaçao em Engenharia Florestal) – Instituto de Florestas, Universidade Federal Rural do Rio de Janeiro, 2008.

SREEKALA, M. S.; KUMARAN, M. G.; JOSEPH, Seena; JACOB, Maya; THOMAS, Sabu. Oil palm fibre reinforced phenol formaldehyde composites: Influence of fibre surface modifications on the mechanical performance. **Applied Composite Materials**, v. 7, p. 295-329, 2000.

SREENIVASAN, S.; IYER, P. Bhama; IYER, K. R. Krishna. Influence of delignification and alkali treatment on the fine structure of coir fibres (*Cocos nucifera*). **Journal of Materials Science**, v. 31, p. 721-726, 1996.

STAAB, George H.. Chapter 1 – Introduction to Composite Materials. *In:* **Laminar Composites.** Butterworth-Heinemann, 1999. 466 p.

TARANU, Nicolae; OPRISAN, Gabriel; BUDESCU, Mihai; SECU, Alexandru; GOSAV, Ionel. The use of glass fibre reinforced polymer composites as reinforcement for tubular concrete poles. **Proceedings of the 11th WSEAS International Conference on Sustainability in Science Engineering**, p. 508-513, 2016.

THE ROYAL SOCIETY OF CHEMISTRY. **Advancing the Chemical Sciences Composite Materials.** p. 1-3, index 4.3.1, 201-?. Available at: <http://www.rsc.org/Education/Teachers/Resources/Inspirational/resources/4.3.1.pdf>. Access on: 27 September 2017.

THOMAS, Sabu; JOSEPH, Kuruvilla; MALHOTRA, S. K.; GODA, Koichi; SREEKALA, M. S. **Polymer composite:** Volume 1 – Macro- and Microcomposites**.** 1st ed., Wiley – VCH Verlag GmbH&Co, 2012. 814 p.

THOMASSON, James L. The interface region in glass fibre-reinforced epoxy resin

composites: 2. Water absorption, voids and the interface. **Composites**, v. 26, p. 477-485, 1995.

TITOW, W. V. **PVC Technology.** 4th ed., London: Elsevier Applied Science Publishers, 1984. 1260 p.

TODOR, Mihai-Paul.; KISS, Imre. Systematic approach on materials selection in the automotive industry for making vehicles lighter, safer and more fuel-efficient. **Applied Engineering Letters**, v. 1, n. 4, p. 91-97, 2016.

TRIPATHY, S. S.; LANDRO, L. Di; FONTANELLI, D.; MARCHETTI, A.; LEVITA, G. Mechanical properties of jute fibers and interfacial strength with an epoxy resin. **Journal of Applied Polymer Science**, v. 75, n. 13, p. 1585-1596, 2000.

TSAI, Stephen W.; HAHN, Hong T. **Introduction to Composite Materials.** Pennsylvania: Technomic Publishing Co., 1980. 457 p.

TSERKI, V.; ZAFEIROPOULOS, Nikolaos Evangelos; SIMON, Frank; PANAYIOTOU, Costas. A study of the effect of acetylation and propionylation surface treatments on natural fibers. **Composites: Part A**, v. 36, n. 8, p. 1110-1118, 2005.

VARMA, D. S.; VARMA, M.; VARMA, I. K. Coir fibers – Part I: Effect of physical and chemical treatments on properties. **Textile Research Journal**, v. 54, p. 827-832, 1984.

VENKATACHALAM, N.; NAVANEETHAKRISHNAN, P.; RAJSEKAR, R.; SHANKAR, S. Effect of pretreatment methods on properties of natural fiber composites: A review. **Polymers & Polymer Composites**, v. 24, n. 7, p. 555-566, 2016.

VERMA, Deepak; JAIN, Siddharth; ZHANG, Xiaolei; GOPE, Prakash Chandra. **Green Approaches to Biocomposite Materials Science and Engineering.** Advances in Chemical and Materials Engineering Book Series, 2016. 322 p.

WAHAB, Razak; MOHAMED, Azmy; MUSTAFA, Mohd Tamizi; HASSAN, Affendy. Physical characteristics and anatomical properties of cultivated bamboo (Bambus vulgaris Scrad.) culms. **Journal of Biological Sciences**, v. 9, n. 7, p. 753-759, 2009.

WAHAB, Razak; MUSTAFA, Mohd Tamizi; RAHMAN, Shafiqur; SALAM, Mohammed Abdus; SULAIMAN, Othman; SUDIN, Mahmud; RASAT, Mohd Sukhairi Mat. Relationship between physical, anatomical and strength properties of 3-year-old cultivated tropical bamboo Gigantochloa scortechinii. **Journal of Agricultural and Biological Science**, v. 7, n. 10, p. 782-791, 2012.

WAHAB, Razak; MUSTAFA, Mohd Tamizi; SULAIMAN, Othman; MOHAMED, Azmy; HASSAN, Affendy; KHALID, Izyan. Anatomical and physical properties of cultivated two- and four-year-old Bambus vulgaris. **Sains Malaysiana**, v. 39, n. 4, p. 571-579, 2010.

WAMBUA, Paul; IVENS, Jan; VERPOEST, Ignaas. Natural fibres: can they replace glass in fibre reinforced plastics? **Composites Science and Technology**, v. 63, n. 9, p. 1259-1264, 2003.

WANG, Ge; SHI, Sheldon Q.; WANG, Jinwu; YU, Yan; CAO, Shuangping; CHENG, Haitao. Tensile properties of four types of individual cellulosic fibers. **Wood and Fiber Science**, v. 43, n. 4, p. 353-364, 2011.

WELLS, John M.; PAYNE, James A. Mycoflora and market quality of chestnuts treated with hot water to control the chestnut weevil. **Plant Disease**, v. 64, n. 11, p. 999-1001, 1980.

WOO, M.; PIGGOTT, M. R. Water absorption of resins and composites: IV. Water transport in fiber reinforced plastics. **Journal of Composites, Technology and Research**, v. 10, n. 1, p. 20-24, 1988.

ZAKRZEWSKI, Sonia R.; SHORTLAND, Andrew J.; ROWLAND, Joanne. Chapter 3 – The Biography of People. *In:* **Routledge Studies in Egyptology:** Science in the Study of Ancient Egypt. New York: Taylor & Francis, 2016. 410 p.

ZHANG, Xiaoping; WANG, Fang; KEER, Leon M. Influence of surface modification on the microstructure and thermo-mechanical properties of bamboo fibers. **Materials,** v. 8, n. 10, p. 6597- 6608, 2015.

ZUMMERMANN, H.; WALZE, R. Ethylene. *In:* **Ullmann's Encyclopedia of Industrial Chemistry.** 7th ed., Wiley-VCH, v. 13, p. 465-529, 2012.

APPENDIX A – GREEN POLYETHYLENE CERTIFICATIONS

Table A.1 – Green polyethylene *I'm green*™ certifications

Certification	Description
Beta Analytic	The international laboratory Beta Analytic Inc. analyzed the C14 carbon content by using a method to detect fossil carbon in the sample. The result for the green polyethylene *I'm green*™ showed that it was 100% made from renewable resources.
Vinçotte	The Belgian company Vinçotte, a global reference in the renewable content assessment, evaluated samples from HDPE and LLDPE, resulting in the maximum rating of four starts for its proven renewable content.
ISCC/Bonsucro	The seal from ISCC plus – International Sustainability and Carbon Certification –, an international certification system for biomass and sustainable fuels, sets specific production standards and was developed in cooperation with producers from various countries, including Brazil and Argentina. Bonsucro™, a London-based international organization with a slogan that says "Better Sugar Cane Initiative", establishes exclusive social and environmental principles and criteria for the production of sugarcane and its byproducts. The seal attests to sustainable practices and allows the sugarcane byproducts export to countries in Europe and Asia.

Source: BRASKEM (201-?c).

APPENDIX B – DIMENSIONS OF THE UNTREATED AND TREATED BF

Table B.1 – Average dimensions of largest (D_L) and thinnest (D_T) cross-sections and circular and elliptical areas of untreated and treated BF0110 with 5 cm length

	BF0110WT				BF0110TA			
	D_L (mm)	D_T (mm)	A_C (mm^2)	A_E (mm^2)	D_L (mm)	D_T (mm)	A_C (mm^2)	A_E (mm^2)
1	0.76	0.49	0.45	0.29	0.78	0.58	0.48	0.36
2	1.02	0.49	0.82	0.39	0.66	0.54	0.34	0.28
3	0.84	0.58	0.55	0.38	1.20	0.62	1.13	0.58
4	0.79	0.69	0.49	0.43	0.90	0.83	0.64	0.58
5	0.93	0.29	0.67	0.21	1.09	0.94	0.94	0.80
6	0.51	0.40	0.21	0.16	0.88	0.67	0.61	0.46
7	0.57	0.41	0.26	0.18	1.05	0.87	0.86	0.72
8	0.82	0.64	0.53	0.41	1.25	0.67	1.23	0.66
9	0.68	0.58	0.36	0.31	0.85	0.60	0.57	0.40
10	0.73	0.51	0.42	0.29	0.69	0.70	0.37	0.38
11	0.89	0.64	0.63	0.45	0.97	0.68	0.73	0.52
12	0.81	0.66	0.52	0.42	0.87	0.46	0.60	0.31
13	0.94	0.52	0.69	0.38	0.97	0.54	0.74	0.41
14	1.08	0.73	0.92	0.62	0.77	0.38	0.46	0.23
15	0.68	0.31	0.36	0.17	0.62	0.41	0.30	0.20
16	0.88	0.43	0.61	0.30	0.55	0.50	0.24	0.22
17	0.74	0.46	0.44	0.27	1.16	0.54	1.06	0.49
18	0.52	0.31	0.21	0.13	0.64	0.43	0.32	0.22
19	0.58	0.26	0.27	0.12	0.61	0.36	0.29	0.17
20	0.49	0.33	0.19	0.13	0.75	0.46	0.44	0.27
21	0.99	0.47	0.77	0.37	1.05	0.64	0.86	0.53
22	0.78	0.34	0.48	0.21	0.76	0.62	0.45	0.37
23	0.81	0.45	0.51	0.28	0.89	0.48	0.62	0.34
24	0.45	0.44	0.16	0.16	1.10	0.73	0.95	0.63
25	0.64	0.50	0.32	0.25	0.83	0.51	0.54	0.33

26	0.51	0.28	0.21	0.11	0.66	0.58	0.34	0.30
27	0.45	0.40	0.16	0.14	0.84	0.83	0.55	0.55
28	0.51	0.32	0.21	0.13	0.70	0.67	0.39	0.37
29	0.65	0.39	0.34	0.20	0.76	0.60	0.46	0.36
30	0.63	0.33	0.31	0.16	0.72	0.45	0.41	0.25
31	0.59	0.34	0.27	0.16	0.67	0.67	0.36	0.35
32	0.78	0.49	0.48	0.30	0.73	0.64	0.42	0.37
33	0.64	0.67	0.32	0.34	0.85	0.75	0.57	0.50
34	0.91	0.38	0.65	0.28	0.76	0.61	0.46	0.37
35	0.47	0.28	0.18	0.10	1.12	1.01	0.98	0.89
36	0.64	0.50	0.32	0.25	0.60	0.27	0.28	0.13
37	0.68	0.60	0.37	0.32	0.65	0.56	0.33	0.29
38	0.83	0.50	0.54	0.32	0.81	0.60	0.52	0.38
39	0.85	0.70	0.56	0.46	0.88	0.47	0.62	0.32
40	0.59	0.43	0.27	0.20	0.64	0.43	0.33	0.22
41	0.78	0.55	0.48	0.34	0.72	0.69	0.41	0.39
42	0.72	0.31	0.41	0.18	0.80	0.60	0.50	0.37
43	0.84	0.70	0.55	0.46	0.61	0.31	0.30	0.15
44	0.66	0.41	0.34	0.21	0.57	0.67	0.26	0.30
45	0.67	0.44	0.35	0.23	0.58	0.48	0.26	0.22
46	0.62	0.25	0.30	0.12	0.81	0.46	0.51	0.29
47	0.63	0.36	0.31	0.18	0.49	0.40	0.19	0.15
48	0.35	0.36	0.10	0.10	0.58	0.37	0.26	0.17
49	0.46	0.22	0.17	0.08	0.53	0.38	0.22	0.16
50	0.72	0.36	0.41	0.20	0.43	0.36	0.15	0.12

Source: Author.

Table B.1 – Average dimensions of largest ($\underline{D_L}$) and thinnest ($\underline{D_T}$) cross-sections and circular and elliptical areas of untreated and treated BF0110 with 5 cm length (continuation)

	BF0110TB				**BF0110TC**		
	$\underline{D_L}$ (mm)	**$\underline{D_T}$ (mm)**	**A_C (mm^2)**	**A_E (mm^2)**	**$\underline{D_L}$ (mm)**	**$\underline{D_T}$ (mm)**	**A_C(mm^2)**
1	0.99	0.82	0.78	0.64	0.79	0.65	0.49
2	0.69	0.67	0.37	0.37	0.64	0.47	0.32
3	0.44	0.34	0.15	0.12	0.77	0.71	0.47
4	0.65	0.43	0.34	0.22	0.50	0.47	0.19
5	0.43	0.44	0.15	0.15	0.85	0.56	0.57
6	0.36	0.38	0.10	0.11	0.79	0.44	0.49
7	0.77	0.65	0.46	0.39	0.81	0.41	0.52
8	0.55	0.50	0.24	0.22	0.70	0.56	0.39
9	0.47	0.41	0.17	0.15	0.62	0.27	0.30
10	0.65	0.43	0.33	0.22	0.60	0.43	0.28
11	0.79	0.46	0.49	0.28	0.67	0.58	0.35
12	0.62	0.59	0.30	0.29	0.77	0.71	0.47
13	0.86	0.33	0.58	0.23	0.86	0.62	0.58
14	0.40	0.39	0.12	0.12	0.61	0.54	0.29
15	0.59	0.45	0.28	0.21	0.54	0.53	0.23
16	0.55	0.54	0.24	0.23	0.79	0.59	0.49
17	0.42	0.37	0.14	0.12	0.70	0.50	0.38
18	0.29	0.27	0.06	0.06	1.10	0.60	0.96
19	0.77	0.70	0.46	0.42	0.58	0.61	0.26
20	0.69	0.39	0.38	0.21	0.51	0.36	0.20
21	0.75	0.72	0.45	0.43	0.76	0.80	0.45
22	0.52	0.45	0.21	0.18	0.77	0.66	0.46
23	0.41	0.34	0.13	0.11	0.88	0.54	0.61
24	0.48	0.29	0.18	0.11	0.72	0.67	0.40
25	0.57	0.48	0.25	0.21	0.84	0.59	0.55
26	0.67	0.74	0.35	0.39	0.73	0.73	0.42

27	0.93	0.43	0.67	0.31	0.74	0.61	0.43
28	0.77	0.64	0.46	0.39	0.64	0.65	0.32
29	0.60	0.49	0.29	0.23	0.77	0.53	0.46
30	0.83	0.68	0.54	0.44	0.88	0.60	0.61
31	0.77	0.59	0.46	0.35	0.58	0.41	0.26
32	0.79	0.64	0.49	0.40	0.82	0.34	0.52
33	0.62	0.51	0.31	0.25	0.74	0.71	0.43
34	0.69	0.49	0.37	0.27	0.66	0.66	0.34
35	0.81	0.68	0.52	0.43	0.70	0.36	0.39
36	0.66	0.45	0.35	0.24	0.94	0.47	0.69
37	0.46	0.35	0.17	0.13	1.05	0.73	0.87
38	0.54	0.40	0.23	0.17	0.68	0.67	0.37
39	0.56	0.34	0.25	0.15	0.55	0.63	0.23
40	1.25	0.75	1.22	0.74	0.62	0.46	0.31
41	0.60	0.48	0.29	0.23	0.86	0.20	0.58
42	0.73	0.60	0.42	0.34	0.68	0.44	0.36
43	0.18	0.22	0.03	0.03	0.79	0.53	0.49
44	0.91	0.46	0.65	0.33	0.73	0.57	0.42
45	0.75	0.53	0.44	0.31	0.82	0.63	0.53
46	0.62	0.52	0.30	0.25	0.65	0.34	0.34
47	0.87	0.40	0.60	0.28	0.72	0.59	0.40
48	0.62	0.42	0.30	0.20	0.68	0.69	0.37
49	0.84	0.84	0.56	0.56	0.56	0.62	0.25
50	0.97	0.60	0.74	0.46	0.66	0.49	0.34

Source: Author.

Table B.1 – Average dimensions of largest ($\underline{D_L}$) and thinnest ($\underline{D_T}$) cross-sections and circular and elliptical areas of untreated and treated BF0110 with 5 cm length (continuation)

	BF0110TD			
	$\underline{D_L}$ (mm)	**$\underline{D_S}$ (mm)**	**A_C (mm^2)**	**A_E (mm^2)**
1	0.45	0.50	0.16	0.17
2	0.98	0.78	0.76	0.60
3	0.74	0.43	0.43	0.25
4	0.82	0.47	0.53	0.30
5	0.64	0.70	0.32	0.35
6	1.20	0.41	1.13	0.39
7	0.53	0.46	0.22	0.19
8	0.46	0.45	0.17	0.16
9	0.50	0.62	0.20	0.24
10	0.83	0.51	0.54	0.33
11	0.80	0.46	0.50	0.29
12	0.62	0.29	0.30	0.14
13	0.75	0.82	0.45	0.48
14	0.59	0.39	0.27	0.18
15	0.83	0.82	0.54	0.54
16	0.51	0.41	0.21	0.16
17	0.44	0.39	0.15	0.13
18	0.56	0.68	0.25	0.30
19	0.89	0.39	0.63	0.28
20	0.71	0.51	0.40	0.29
21	0.92	0.58	0.67	0.42
22	0.88	0.61	0.61	0.42
23	0.70	0.52	0.38	0.28
24	0.70	0.66	0.38	0.36
25	0.58	0.42	0.27	0.19
26	0.64	0.50	0.33	0.26

27	0.86	0.54	0.59	0.36
28	0.91	0.75	0.65	0.53
29	0.74	0.47	0.44	0.27
30	0.54	0.86	0.23	0.36
31	0.86	0.60	0.57	0.40
32	0.88	0.38	0.61	0.27
33	0.85	0.76	0.56	0.50
34	0.78	0.43	0.48	0.27
35	0.84	0.52	0.55	0.34
36	0.66	0.19	0.34	0.10
37	0.69	0.61	0.37	0.33
38	0.65	0.42	0.33	0.21
39	0.47	0.46	0.17	0.17
40	0.43	0.29	0.14	0.10
41	0.49	0.42	0.19	0.16
42	0.48	0.48	0.18	0.18
43	0.79	0.57	0.49	0.35
44	0.85	0.60	0.57	0.40
45	0.91	0.64	0.65	0.46
46	0.87	0.50	0.59	0.34
47	0.57	0.32	0.25	0.14
48	0.51	0.45	0.20	0.18
49	0.58	0.46	0.26	0.21
50	0.90	0.59	0.60	0.41

Source: Author.

APPENDIX C – MECHANICAL PROPERTIES OF PERFORMED COMPOSITES

Table C.1 – Mechanical properties of PEg/BF0310WT

Data	PEg/ BF0310WT - SP1	PEg/ BF0310WT - SP2	PEg/ BF0310WT - SP3	PEg/ BF0310WT - SP4	PEg/ BF0310WT - SP5
A_0 (mm^2)	43.52	54.36	53.30	54.66	38.58
A* (mm^2)	41.22	49.69	56.36	53.02	35.79
w_0 (mm)	18.7	18.2	18.0	19.9	19.0
w* (mm)	18.2	17.4	17.7	19.6	18.3
E (GPa)	1.25	0.90	1.02	1.02	1.11
ε_{lenght_max} (%)	2.13	1.80	1.90	1.44	2.46
σ_{max} (MPa)	26.74	15.93	19.45	14.51	28.90

* Maximum values.

Source: Author.

Table C.2 – Mechanical properties of PEg/BF0310TB

Data	PEg/ BF0310TB - SP1	PEg/ BF0310TB - SP2	PEg/ BF0310TB - SP3	PEg/ BF0310TB - SP4	PEg/ BF0310TB - SP5
A_0 (mm^2)	43.09	44.33	40.27	47.75	44.32
A* (mm^2)	40.42	42.94	38.96	44.28	40.67
w_0 (mm)	19.1	19.0	18.3	18.9	19.0
w* (mm)	18.5	18.7	18.0	18.2	18.2
E (GPa)	1.35	1.22	1.55	1.16	1.23
ε_{lenght_max} (%)	2.81	2.27	1.96	2.81	2.49
σ_{max} (MPa)	39.38	27.21	31.09	34.55	31.67

* Maximum values.

Source: Author.

Table C.3 – Mechanical properties of PEg/BF0310TC

Data	PEg/ BF0310TC - SP1	PEg/ BF0310TC - SP2	PEg/ BF0310TC - SP3	PEg/ BF0310TC - SP4	PEg/ BF0310TC - SP5
A_0 (mm^2)	40.20	42.21	44.32	44.54	47.03
A* (mm^2)	35.86	39.83	43.36	44.09	44.59
w_0 (mm)	18.0	17.5	18.4	19.5	19.0
w* (mm)	17.0	17.0	18.2	19.4	18.5
E (GPa)	1.26	1.29	1.33	1.25	1.07
ε_{lenght_max} (%)	3.08	2.40	2.33	2.22	2.87
σ_{max} (MPa)	40.43	31.93	30.94	30.19	31.98

* Maximum values.

Source: Author.

Table C.4 – Mechanical properties of PEg/BF0310TD

Data	PEg/ BF0310TD - SP1	PEg/ BF0310TD - SP2	PEg/ BF0310TD - SP3	PEg/ BF0310TD - SP4	PEg/ BF0310TD - SP1
A_0 (mm^2)	37.95	46.25	38.94	42.08	37.95
A* (mm^2)	40.08	45.26	36.82	39.79	40.08
w_0 (mm)	18.5	18.5	18.1	18.1	18.5
w* (mm)	18.0	18.3	17.6	17.6	18.0
E (GPa)	1.20	1.15	1.40	1.15	1.20
ε_{lenght_max} (%)	3.12	3.01	3.05	3.14	3.12
σ_{max} (MPa)	38.98	36.24	45.14	37.96	38.98

* Maximum values.

Source: Author.

Table C.5 – Mechanical properties of PEg/BF1015WT

Data	PEg/ BF1015WT - SP1	PEg/ BF1015WT - SP2	PEg/ BF1015WT - SP3
A_0 (mm^2)	43.20	38.93	47.71
A* (mm^2)	39.45	30.33	44.75
w_0 (mm)	18.0	19.0	19.0
w* (mm)	17.2	17.3	18.4
E (GPa)	0.93	1.59	1.27
ε_{lenght_max} (%)	1.28	1.27	1.27
σ_{max} (MPa)	12.01	20.26	17.21

* Maximum values.

Source: Author.

Table C.6 – Mechanical properties of PEg/BF1015TC

Data	PEg/ BF1015TC - SP1	PEg/ BF1015TC - SP2	PEg/ BF1015TC - SP3	PEg/ BF1015TC - SP4	PEg/ BF1015TC - SP5
A_0 (mm^2)	43.94	39.97	45.83	39.67	36.00
A* (mm^2)	39.44	37.35	42.98	34.31	34.42
w_0 (mm)	19.0	18.0	19.0	20.0	18.0
w* (mm)	18.0	17.4	18.4	18.6	17.6
E (GPa)	1.14	1.33	1.17	1.47	1.64
ε_{lenght_max} (%)	1.69	2.10	2.03	1.75	1.64
σ_{max} (MPa)	17.55	27.60	23.27	25.89	25.47

* Maximum values.

Source: Author.

Table C.7 – Mechanical properties of PEg/BF0310WT///

Data	PEg/ BF0310WT/// - SP1	PEg/ BF0310WT/// - SP2	PEg/ BF0310WT/// - SP3
A_0 (mm^2)	35.33	35.80	36.20
A* (mm^2)	32.64	34.62	33.23
w_0 (mm)	18.0	18.1	19.1
w* (mm)	17.3	17.8	18.3
E (GPa)	0.78	0.62	0.76
ε_{lenght_max} (%)	1.69	2.88	1.60
σ_{max} (MPa)	13.58	17.97	12.26

* Maximum values.

Source: Author.

Table C.8 – Mechanical properties of PEg/BF0310WTX

Data	PEg/ BF0310WTX - SP1	PEg/ BF0310WTX - SP2	PEg/ BF0310WTX - SP3	PEg/ BF0310WTX - SP4	PEg/ BF0310WTX - SP5
A_0 (mm^2)	38.93	36.06	38.63	35.67	37.67
A* (mm^2)	36.99	34.08	37.83	34.12	36.52
w_0 (mm)	19.8	18.0	19.1	18.2	19.5
w* (mm)	19.3	17.5	18.9	17.8	19.2
E (GPa)	1.53	1.30	1.64	1.20	1.65
ε_{lenght_max} (%)	2.49	1.86	1.38	2.20	1.17
σ_{max} (MPa)	39.54	23.76	21.08	26.41	17.23

* Maximum values.

Source: Author.

Table C.9 – Mechanical properties of PEg/BF0310WT%

Data	PEg/ BF0310WT %-SP1	PEg/ BF0310WT %-SP2	PEg/ BF0310WT %- SP3	PEg/ BF0310WT %- SP4	PEg/ BF0310WT %- SP5
A_0 (mm^2)	35.91	43.55	40.16	39.04	35.89
A* (mm^2)	34.68	42.27	36.59	35.25	33.91
w_0 (mm)	17.3	20.2	19.8	18.1	17.9
w* (mm)	17.0	19.9	18.9	17.2	17.4
E (GPa)	0.65	0.74	0.70	0.69	0.73
ε_{lenght_max} (%)	2.03	1.46	1.86	1.92	1.73
σ_{max} (MPa)	14.12	11.04	13.78	13.72	13.34

* Maximum values.

Source: Author.

Table C.10 – Mechanical properties of PEg/BF0310WT#

Data	PEg/ BF0310WT# - SP1	PEg/ BF0310WT# - SP2	PEg/ BF0310WT# - SP3	PEg/ BF0310WT# - SP4
A_0 (mm^2)	40.42	43.28	41.77	40.44
A* (mm^2)	39.58	41.89	37.80	39.18
w_0 (mm)	19.0	18.5	18.5	19.0
w* (mm)	18.8	18.2	17.6	18.7
E (GPa)	0.92	1.16	0.93	0.98
ε_{lenght_max} (%)	1.07	0.65	0.75	1.31
σ_{max} (MPa)	9.10	7.30	6.86	12.65

* Maximum values.

Source: Author.